Pharmacokinetic Studies of Enteric and Delayed Release Formulations of Locally Bioavailable Drugs (LBD) Targeting the Colon

by
Katherine Thuy Shatzer

A dissertation submitted to the Department of Pharmaceutical Sciences,
College of Pharmacy
in partial fulfillment of the requirements for the degree of

Doctor of Philosophy

in Pharmaceutical Sciences

Chair of Committee: Ming Hu, Ph.D.

Committee Member: Gregory Cuny, Ph.D.

Committee Member: Xinli Liu, Ph.D.

Committee Member: Noah Freeman Shroyer, Ph.D.

Committee Member: Robert O. Williams III, Ph.D.

University of Houston
October 2019

DEDICATION

I dedicate this work to Eva Marie Shatzer, John Shatzer, and my future babies.

ACKNOWLEDGMENTS

I would like to thank and offer my utmost gratitude to my advisor, Dr. Ming Hu, who has supported and motivated me with great patience and knowledge throughout my PhD. I am grateful to him for giving me the opportunity to work under his supervision, and for his care and guidance. Dr. Hu is an excellent mentor and supervisor; he has encouraged me greatly with his invaluable advice.

I would also like to express my sincere gratitude to Dr. Robert O. Williams III, Dr. Noah Shroyer, Dr. Gregory Cuny, and Dr. Xinli Liu for serving as my committee members. I would also like to extend my appreciation to Dr. David Brammer (University of Houston, ACO), Dr. James Meen (University of Houson, College of Physical Engineer), Dr. Bryan Knoll, and Dr. Douglas Eikenberg for always having open ears and serving as my sounding board and my go to source for feedback.

My special thanks and acknowledgments are directed towards the Department of Pharmacological and Pharmaceutical Sciences at the University of Houston for providing me financial support by awarding scholarships and hiring me as a Graduate Teaching Assistant and later as a Graduate Research Assistant that immensely helped me pursue my PhD. in pharmaceutical sciences.

My greatest appreciation is reserved for my best friends and admirers, George and Barbara, my parents, Eva and John Shatzer, my family, whom have never wavered in their support and love from the application process through to the completion of Ph.D program. They

have always been there from the late nights to the long weekends. Their unconditional love has sustained me and provided the critical support I needed.

Finally, enormous thanks are owed to all those who have so generously shared their knowledge, wisdom, and time. Thank you for providing the scientific insight that has culminated in this thesis.

ABSTRACT

STATEMENT OF PROBLEM: Familial Adenoma Polyposis (FAP) is a debilitating condition that has a severe impact on the physical and psychological health, independence, and quality of life of an affected patient. Celecoxib is a selective COX-2 inhibitor class of NSAIDs that is undeniably effective against FAP. On-target off-organ cardiovascular toxicity prevents the use of Celecoxib as a treatment for FAP. A new COX-2 inhibitor, 6A1, is less systemically bioavailable due to its ability to undergo enterohepatic recycling (EHR). EHR delivered a variable quantity of 6A1 to the target tissue, colon, subject to variation amongst individuals UGT enzyme expression and ß-glucuronidase expression within the bacteria microbiomes that inhabit the gut. The body of this work aims to lower the therapeutic dose and the total systemic exposure (AUC) while increasing 6A1 concentration in the colon by capitalizing upon the complementary interplay between the EHR, novel coating techniques, and biodegradable polymer formulations.

METHOD: Pack drug powder (6A1), formulated 6A1 microparticulate, and image tracers inside size 9 hard gelatin capsules (S9C), coated with an inner layer of polylactic glycolic acid (PLGA 8515) with optimum thickness to serve as delayed-release coating via erosion mechanism and an outer pH-sensitive Eudragit S100 (ES100) coat to serve as an enteric coating. The control group used the uncoated hard gelatin capsules. Novel vacuum spin coating technique and parameters, as well as new solvent systems, were also investigated. The S9C were administered via oral gavage (control vs. coated capsules) to F344 rats (n=5), fed ad libitum. The location of the control and coated capsules within the

gastrointestinal tract and 6A1 systemic concentration were monitored simultaneously using Perkin Elmer IVIS Lumina III XRMS and UPLC-MS/MS. 6A1 and its metabolites were also quantified from the ex vivo (liver and colonic mucosa) tissues collected at the endpoints of the study.

RESULTS: Pharmacokinetic study data of 6A1 and its metabolites (glucuronide and sulfate) proved the capsules release was delayed beyond 5 hours, released its contents within the colon, and had a dose-normalized AUC (ng*hr/mL*mg) indicating systemic exposure of 6A1 is 9.04% of the systemic exposure of Celecoxib. The colonic concentration results of a 4-day multiple dosing 6A1 coated capsule study (20 mg/ Kg BID, 2682 ng/g formulation 1 and 1916 ng/g formulation 2) was comparable to 4-day multiple dosing 6A1 powder suspension study (40 mg/Kg BID, 3300 ± 300 ng/g).

CONCLUSION: The study validated an innovative colonic drug system. A combined approach of both pH-dependent and time-dependent particulate systems is highly desirable for use in a colon-specific drug delivery system. The approach has proven to reduce systemic drug concentrations, thus may reduce the side effects of the drug. Ultimately, treatment for other gastrointestinal tract diseases may benefit from the knowledge gained through this research.

TABLE OF CONTENTS

LIST OF TABLES

LIST OF FIGURES

LIST OF ABBREVIATIONS

A

AA: Arachidonic acid

AL: Alabama

ANOVA: Analysis of variance

APC: Adenomatous polyposis coli

APC Trial (Pfizer): Adenoma Prevention Clinical Trial

APPROVe (Merck): Adenomatous polyp prevention on Vioxx

API: Active pharmaceutical ingredient

AUC: Area under the curve

B

BCRP: breast cancer resistance protein

C

CA: California

CE: Collision energy

COX-1: Cyclooxygenase -1

COX-2: Cyclooxygenase -2

COXIBs: Selective COX-2 inhibitors

CRC: Colorectal Cancer

CV: Cardiovascular

CDDS: Colonic drug delivery system

C_{max}: Maximum drug concentration

C_{min}: Minimum drug concentration

CXP: Collision cell exit potential

D

DE: Delaware

DI: Distilled Water

DL-PLGA: DL-polylactide-co-glycolic acid

DMC: Methylene Chloride

DNA: Deoxyribonucleic acid

DP: Declustering potential

DSC: Differenttial scanning calorimetry

E

EE %: Encapsulation efficiency %

EHR: Enterohepatic recycling

EP: Entrance potential

ES100: Evonik Eudragit S100

F

FAP: Familial adenomatous polyposis

FDA: Food and Drug Administration

F344-Pirc Rat: Fisher 344-polyposis in the rat colon species

G

g: Gravity

g/dL: Gram per deciliter

GI: Gastro intestinal

GRAS: Generally recognized as safe

H

HCL: Hydrochloric acid

I

i.e.: In other words

IACUC: Institutional animal use and care committee

IC_{50}: Half maximal inhibitory concentration

IPA: Isopropanol alcohol

IVIS lumina: Perkin Elmer IVIS Lumina III XRMS

J

JMP: Jump statistical discovery from SAS

K

kDA: kilodalton

kV: kilovolt

L

LBD: Local Bioavailable Drugs

LC-MS: Liquid chromatography-mass spectrometry

LLE: Liquid-liquid extraction

LLOQ: Lower limit of quantification

M

M.D. Anderson: Monroe Dunaway Anderson

mg: milligram

mg/kg: milligram per kilogram

min: Minute

mL: milliliter

mm: millimeter

MMX: Multimatrix system

MO: Missouri

MRM: Multiple reaction monitor

MRP2: Multidrug resistant protein 2

MS: Mass spectrometer

Mw: Molecular weight

N

NaOH: Sodium hydroxide

ng/mL: Nanogram per milliliter

NIH: National Institutes of Health

Nm: nanoparticle

NSAID: Non-steroidal anti-inflammatory drug

O

ODAC: Oncologic Drugs Advisory Committee

P

PBS: Phosphate buffered saline

PD: Pharmacodynamic

PGE-2: Prostaglandin E2

PGI2: Prostacyclin

pH: power of hydrogen

PK: Pharmacokinetics

PLGA: Poly-lactile-co-glycolic acid

PVA: Polyvinyl alcohol

Q

QC: Quality control

R

RPM: Revolutions per minute

S

SPE: Solid phase extraction

SEM: Scanning electron microscopy

T

T_g: Temperature of glass transition

TGA: Thermogravimetric analysis

T_{Lag}: Time lag before drug reaches maximum concentration

T_{max}: Time drug reach maximum concentration

U

µAmps: micro amperes

µg/mL: microgram per milliliter

UGT: uridine 5'-diphospho-glucuronosyl- transferase

µL: Microliter

UM: microparticle

UPLC: Ultra-performance liquid chromatography

USP: United States Pharmacopoeia and in the Agency's dissolution methods database

USA: United States of America

CHAPTER 1: LITERATURE REVIEW

1.1. Familial Adenomatous Polyposis (FAP)

FAP is a debilitating condition that has a long term, severe impact on the physical and psychological health, independence, and quality of life of an affected patient. The affected patient develops hundreds to thousands of intestinal polyps, many of which become cancerous unless surgically removed. Most patients are asymptomatic for years until the adenomas are large and numerous resulting in rectal bleeding or even anemia, or cancer develops. Nonspecific symptoms may include constipation or diarrhea, abdominal pain, palpable abdominal masses, and weight loss. FAP is broken down into two sub conditions based upon severity, classic and attenuated. Classic is the more severe form of FAP. FAP is inherited in an autosomal dominant manner and results from a germline mutation in the adenomatous polyposis (APC) gene. Most patients, approximately 70%, had a family history of colorectal polyps and cancer (1).

Patients suffering from FAP will present with some extraintestinal manifestations that can include the following: osteomas, dental abnormalities (unerupted teeth, congenital absence of one or more teeth, supernumerary teeth, dentigerous cysts and odontomas), congenital hypertrophy of the retinal pigment epithelium, desmoid tumors, and extracolonic cancers (duodenum, stomach, skin, thyroid, liver, bile ducts and central nervous system). The extracolonic cancers may be benign or malignant.

Desmoid tumors are of particular significance; these are fibrous tumors usually occurring in the tissue covering the intestines and may be provoked by surgery to remove the colon. Desmoid tumors are likely to recur after they have been surgically removed.

Mutations in the APC gene cause both classic and attenuated familial adenomatous polyposis (1). The mutations affect the cell's ability to maintain normal growth and function. Cell overgrowth resulting from mutations in the APC gene leads to the colon polyps seen in FAP. Although most people with mutations in the APC gene will develop colorectal cancer, the number of polyps and the time frame in which they become malignant depend on the location of the mutation in the gene (2-4).

1.1.1. Epidemiology of FAP

FAP is a rare, inherited condition with a reported incidence varying from 1 in 6,000 to 1 in 22,000 individuals. FAP manifests equally in both sexes and is the second most common genetic Colorectal Cancer (CRC) syndrome. CRC is the third leading cause of cancer deaths in the United States (5). Worldwide, CRC is a major cause of cancer associated morbidity and mortality. Its incidence varies considerably among different populations with the highest incidence reported from Western and industrialized countries. Worldwide, about 85% of CRCs are considered to be sporadic, while approximately 15% are familial with FAP accounting for less than 1% (1). Adenomatous polyps appear by about 15 years of age in 50% of people with FAP, and by 35 years of age in 95%. Seventy percent of these individuals have colorectal malignancy by the age of 36 years, the average age of

symptomatic diagnosis. Over the lifetime of this illness, there is a 100% cancer risk, typically in the fourth and fifth decades of life. The average age of colorectal cancer onset for attenuated familial adenomatous polyposis is 55 years. No true pharmacologic treatment is available for these patients. Clinically, FAP manifests equally in both sexes by the late teens and in the twenties age group. Individuals with FAP carry a 100% risk of CRC (1, 5, 6)

1.1.2. Current Treatment for Management of FAP

Colectomy is the most common treatment and is typically performed shortly after the time of diagnosis. Total proctocolectomy, either with ileostomy or mucosal proctectomy and ileoanal pouch, eliminates the risk of developing colon and rectal cancer. If subtotal colectomy (removal of most of the colon, leaving the rectum) with ileorectal anastomosis is done, the rectal remnant must be inspected frequently; new polyps must be excised or fulgurated. If new polyps appear too rapidly or prolifically to remove, excision of the rectum and permanent ileostomy are needed (2-4, 7).

After colectomy, patients should have upper endoscopic surveillance at periodic intervals. Protocols for postsurgical lower endoscopic surveillance depend on the type of surgery performed but include annual endoscopic surveillance of remnant anorectal tissue (2-4). Yearly checkups with a physician should be opportunities to screen for other, extra-intestinal complications. One previous study in the USA reported that slightly more than

half of participants who had an FAP diagnosis had recent colorectal screening; rates were lower for at-risk relatives, suggesting underscreening (2-4, 7, 8).

1.1.3. Cyclooxygenase-1 and Cyclooxygenase-2 (COX-2)

NSAIDs are the most versatile group of drugs prescribed for inflammation, analgesic/antipyretic, and auto-immune diseases (9). Non-selective NSAIDs inhibit the synthesis of prostaglandins, thromboxane, and levuloglandins by blocking arachidonic acid substrates from binding to cyclooxygenase isozymes (10, 11), COX-1 and COX-2. The discovery of COX-2 in the early nineties ignited a new frenzy of selective COX-2 inhibitor drugs. For the decades that followed, these drugs boasted of enhancing the pharmacological effects and safety. COX-2 is a variant of COX-1 except for one amino acid. Crystallography revealed that COX-1 and COX-2 crystal structures reside in amino acid number 523. COX-2 has valine in place of isoleucine at position number 523. The different allows COX-2 to form a deeper hydrophobic binding pocket that accounted for the substrate selectivity (Figure 1).

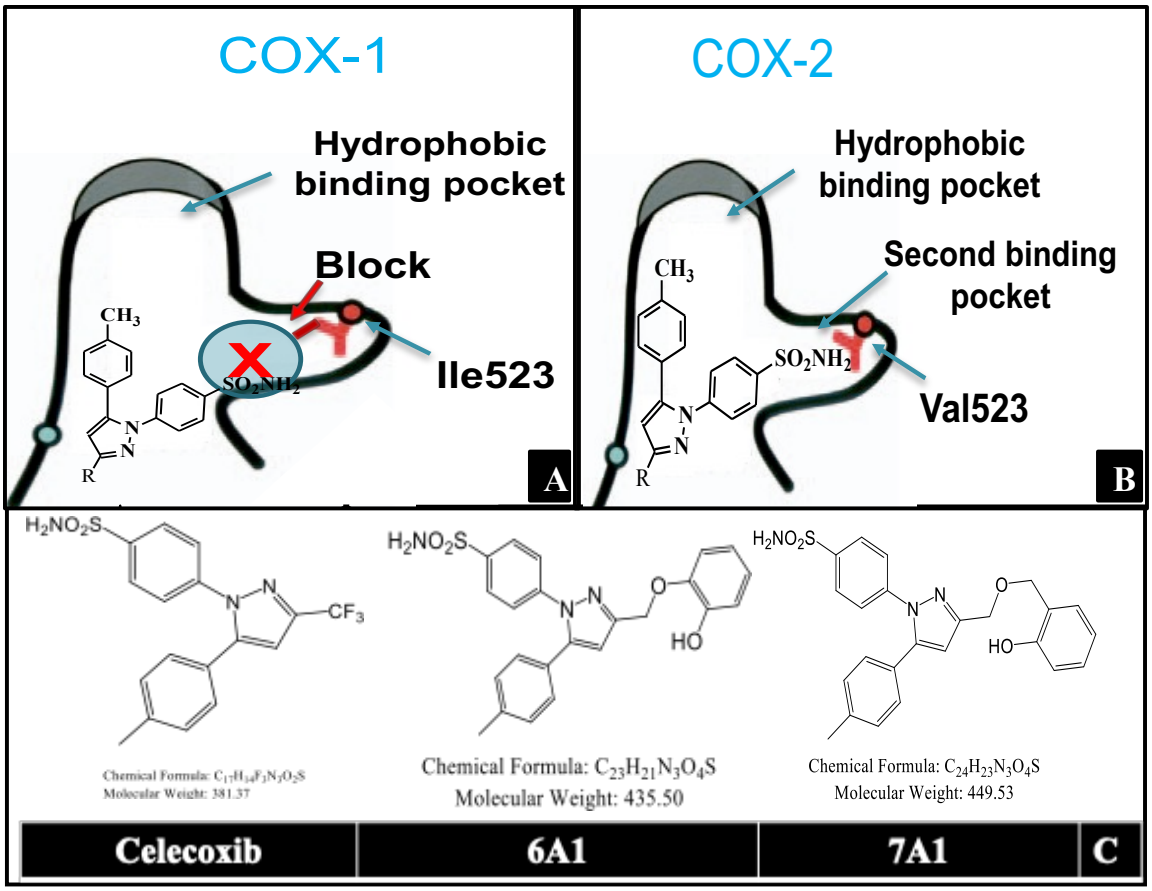

Figure 1: Schematic depiction of the structural differences between the substrate-binding channels of COX-1 and COX-2. Ile523 in the COX-1 (A) block the binding of celecoxib, while val523 in the COX-2 (B) form a second deeper binding pocket for celecoxib. This figure also illustrates the flexibility of the central pyrazole ring, which is in the gate side of the binding pocket. The structure of celecoxib, 6A1 and 7A1 (C) attaching an additional moiety did not affect the binding.

Additionally, crystallography showed the sulfamoylphenyl of the selective COX-2 inhibitor, celecoxib, is essential for the selective activity of celecoxib's COX-2 inhibition. Prostaglandins appear to play a vital role in the adenoma-carcinoma sequence by altering cell adhesion, inhibiting apoptosis, and promoting angiogenesis (12). COX-1 performs a distinct physiological homeostatic maintenance role within the systemic vascular and

gastrointestinal tract (13). The inhibition of COX-1 leads to gastrointestinal toxicity (14), cardiovascular toxicity, internal bleeding, and stomach ulcers. The COX-2 enzyme, the inducible, pro-inflammatory cyclooxygenase isoform is observed to be overexpressed and upregulated in FAP and CRC tissues. COX-2 overexpression is associated with poor survival outcome in colorectal cancer patients (6) and is used as a prominent predictive marker in inflammatory bowel diseases. Naturally, selective COX-2 inhibitors were designed to prevent the unwanted, adverse gastrointestinal events associated with NSAIDs.

A newly synthesized COX-2 inhibitor, 6A1 (Figure 1C) is comparable in its performance to that of celecoxibs, with a potential of lower on-target off-organ systemic toxicity. The trifluoromethyl moiety on the pyrazole backbone ring contributes little to the potency of celecoxib. Leverage on the above knowledge, 6A1 was designed to retain the sulfamoylphenyl group and central heterocycle of celecoxib, but with the addition of a phenolic group. The design promotes 6A1 to enter the EHR (Enterohepatic Recirculation) via liver enzyme glucuronidation. In vitro preliminary studies used celecoxib's IC_{50} value to screen the performance of leading compounds' ability to inhibit COX-2. The result identifies 6A1 as a potent COX-2 inhibitor. The novel locally bioavailable COX-2 inhibitor, 6A1 had been shown to rigorously enter the EHR, reduced systemic exposure and prolonged half-life in the colon, thereby potentially reducing the inhibitor's cardiovascular toxicities and increasing its efficacy in the colon. Usually, deconjugation of the metabolites into the parent drug molecules involves beneficial, symbiotic microbiomes in the colon. Localizing COXIBs in the colon could potentially solve the

aforementioned problem, but achieving this localization is currently not readily available on the market.

1.1.4. History of Celebrex ® (Celecoxib)

The FDA initially approved celecoxib for treating osteoarthritis and rheumatoid arthritis in April 1998. Pfizer later won FDA approval to use celecoxib as an oral adjunct to the usual care of endoscopic surveillance and surgery to reduce the number of adenomatous colorectal polyps in patients with familial adenomatous polyposis (FAP). The Oncologic Drugs Advisory Committee (ODAC) had recommended that the FDA grant accelerated approval for the new indication. Celecoxib inhibits cyclooxygenase-2 (COX-2), an enzyme whose overexpression had been linked to inflammation, FAP, and the development of colon and rectal tumors.

Pfizer conducted a randomized, double-blind, placebo-controlled study of 83 FAP patients at M.D. Anderson and St. Mark's Hospital, London, England. Two of the enrollees dropped out of the study for reasons unrelated to toxicity; 29 had colorectal polyps, 46 had both colorectal and duodenal polyps, and six had duodenal involvement only. Each had a minimum of five polyps of at least two mm in size. Patients received either a placebo, 100 mg celecoxib twice daily, or 400 mg celecoxib twice daily. Researchers performed endoscopic evaluations when patients entered the study and after 6 months of treatment. The primary efficacy endpoint was a mean percentage change in the colorectal polyp count in specific areas marked by tattoos.

In its analysis, the FDA review team accepted 78 patients and agreed completely with Pfizer in its interpretation of the mean percent of polyp decrease. Both found a 4.5% reduction in the number of polyps in the placebo group; a 14.5% reduction in the 100 mg celecoxib twice daily group; and a 28.0% reduction in the 400 mg celecoxib twice daily group.

In a review of rectal photos from 28 patients, Pfizer reported an 11% reduction in the placebo group and a 2.2% reduction in the 100 mg celecoxib twice daily group, while the FDA found a 15% and an 85.3% increase in the two, respectively. In the 400 mg celecoxib twice daily group, the Pfizer reported a 33.3% decrease in mean percent of polyps, and the FDA put the decrease at 32.6%.

Celecoxib 400 mg twice daily resulted in focal reduction and regression of colorectal polyps. Globally, there was an improvement in the endoscopic appearance of both the colorectal and duodenum.

Safety data for all 83 patients originally enrolled in the study showed that 65% of the placebo group and 47% of the patients in each of the celecoxib groups suffered grade two adverse events, largely gastrointestinal problems (35%, 29%, and 34%, respectively). Six percent of the placebo group, nine percent of the 100 mg twice daily group, and six percent of the 400 mg twice daily group suffered grade three events.

Pfizer only claimed that celecoxib reduced and resulted in the regression of polyps in FAP patients. Reducing the polyp burden may delay or even alleviate the need for surgery in FAP patients, resulting in increased lifetime survival.

Subsequently, in 2012, the FDA withdrew the Celecoxib indication for treatment of FAP due to its severe cardiovascular toxicity and other side effects (15). The risk of cardiovascular toxicity increases dramatically with the higher doses and longer durations required to treat FAP patients (16-19). Currently, marketed NSAIDs are not indicated for the treatment and prevention of FAP. Cardiovascular toxicity is a common side effect to all COXIB compounds. COX driven cardiovascular toxicity caused by the endogenous PGI_2 was originally proposed by G.A. Fitzgerald (14); additional evidence has emerged supporting this explanation (20, 21).

1.1.5. COXIBs as a Treatment for Management of FAP

COXIBs (e.g., celecoxib, rofecoxib), a subclass of nonsteroidal anti-inflammatory drug (NSAIDs) designed to selectively inhibit cyclooxygenase-2 (COX-2) for the treatment of arthritis, effectively reduced the incidence of colorectal cancer in FAP patients (5, 22-25). However, due to impending cardiovascular side effects (e.g., unstable angina, myocardial infarction, and cardiac thrombus) at the doses required for efficacy as a prophylactic (6, 17, 26-28), COXIBs cannot be used clinically to treat FAP. The inability to avoid or prevent these harsh side effects ultimately forced the withdrawal of the drug (i.e., rofecoxib) (29, 30) or drug indication (i.e., celecoxib) for FAP from the market (16), leaving many patients

at high risk for developing colon cancer without a safe and effective treatment other than colectomy (31, 32).

1.1.6. PGE2 Receptor and Its Tumor Genesis in the Context of Compound 6A1

COX-2 is an inducible form of the myeloperoxidases enzyme family that is located on chromosome 1 and found on the nuclear membrane or the luminal side of the endoplasmic reticulum (33). IL1ß, IL6, and TNFalpha are known to regulate the expression of COX-2 in response to growth and inflammations (34). Prostaglandin G2 is one of the downstream products catalyzed by COX-2 from plasma membrane arachidonic acid. The prostaglandins are responsible for vasodilation (PGD2, PGE2, PGI2), gastric, renal, platelet aggregation homeostasis (PGI2), mediating fever, pain, and inflammation (PGE2). In cancer cells, an increase of COX-2 expression positively correlates to an increase in PGE2 production. PGE2 modulates different functions via its binding ability to specific EP receptors. Binding of PGE2 to EP1 receptors led to the mobilization of intracellular calcium. Binding of PGE2 to EP2 and EP4 led to the deregulation of the cell proliferation pathway. EP2 and EP4 receptors are coupled to the G protein to activate adenylate cyclase, which increased the intracellular cAMP; intracellular cAMP activates PKA, PI3K, and GSK3 protein kinases that ultimately activate beta-catenin (35). The direct effect of PGE2 binding to EP3 receptors is still unclear. Through a concerted effort, the increasing concentration of PGE2 and its unclear binding pathway to different EP receptors

disequilibrates the intricate balance between program cell death and cell proliferation that gave rise to tumor genesis and progression (36).

The direct link between COX-2 and Wnt/ β-catenin remains unclear. However, the T-Cell factor/Lymphoid enhancer factor (TCF/LEF) family promotes COX-2 transcription also responsible for the transduction of Wnt/β-catenin (37). In both cancer patients and colon cancer derived cell lines, the overexpression of LEF-1 and Pontin52/TIP49a (proteins of the Wnt pathway), and COX2 enzyme are upregulated (38). A more direct link between Wnt/ β-catenin and COX-2 regulation was established using chondrocytes where the lymphoid enhancer factor 1 (LEF-1/β-catenin) binds to the 3′UTR region of the COX2 genomic locus complex and directly regulates COX2 expression (39) (Supplemental S1).

1.2. Current Practice for Colonic Drug Delivery System (CDDS)

Over the last four decades, colonic drug delivery research has yielded inconsistent results due to the variability between normal gastrointestinal physiology and pathophysiological disturbances during different disease stages. Notwithstanding, colonic drug delivery is still an attractive opportunity that offers many advantages, such as lowering the effective dose while achieving high drug concentration at the targeted local environments and reducing systemic side effects (40).

The two main routes of drug delivery to the colon are rectal and oral. The rectal route, mostly in the form of a suppository, has the most straightforward requirements for formulation and yields very consistent results. However, the rectal route is limited on where a drug can be delivered; the drug cannot be delivered to desired sites such as the cecum, ascending colon, or transverse colon. The oral route has been the primary alternative to deliver drugs targeting these proximal sites within the colon. Oral colonic drug delivery systems are effective in delivering acid label, narrow therapeutic index drugs targeted to various locations within the gastric tract, and low solubility drugs with high efficiency. The oral dosage form is aesthetic and convenient, thus has better patient compliance. The oral colonic delivery systems also had many challenges such as a transit time that is variable between individuals, a release mechanism that is effected by the type of diet and amount of food intake, the physiological and integrity differences of normal and disease stage, colonic pH fluctuation, as well as the microbiomes variability between individuals.

There are many methods to formulate drugs targeting the colon (Figure 2, (41); each has its advantages and disadvantages. Potential methods to target the colon include emulsion, nanoparticles, microparticles, and liposomes. Among these, nanoparticles and microparticles had the most studied techniques.

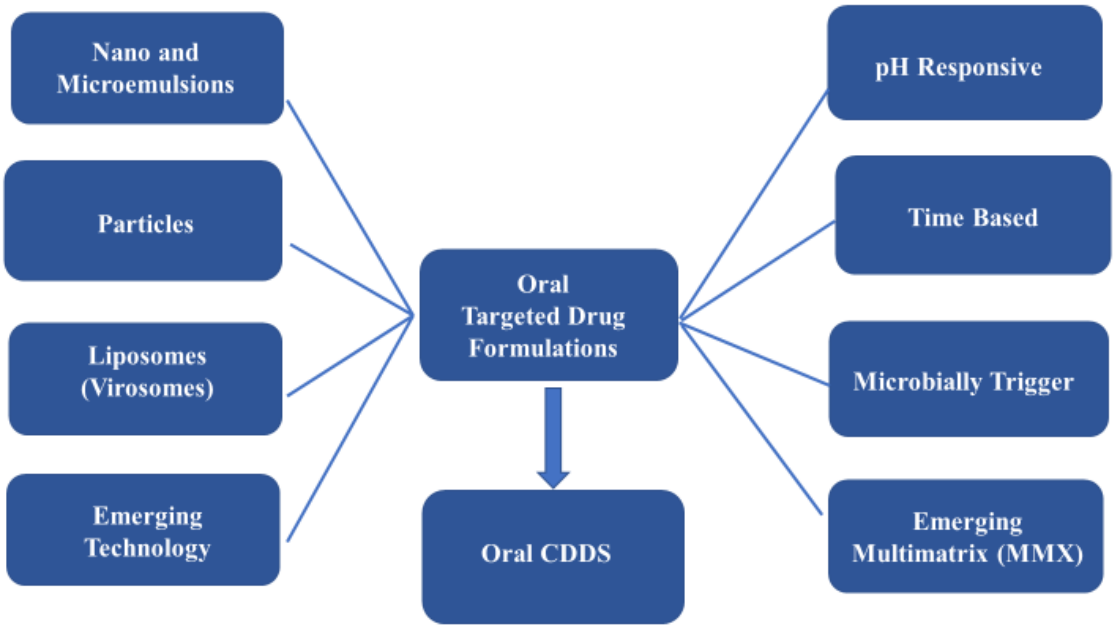

Figure 2: Current Practice for Colonic Drug Delivery Systems

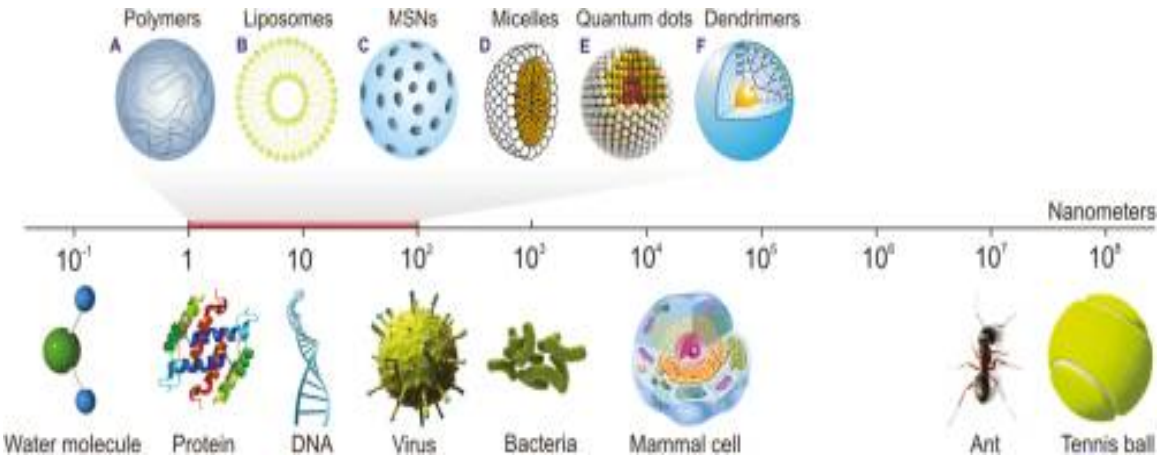

Figure 3: Respective size of different drug formulations (42)

Nanoemulsions and microemulsions (Figure 4, (43) are composed of droplets that contain drug particles and are then dispersed inside an oil medium and suspended in a water medium (o/w) or drug particles dispersed inside an aqueous liquid and suspended in an oil medium (w/o). Another type of emulsion is the bicontinuous emulsion which is composed of both o/w and w/o droplets, thus capable of capturing both hydrophobic and hydrophilic drugs. The nano and micro prefixes describe the droplet size, with the nano prefix ranging from 1 nm - 200 nm. The micro prefix represents a droplet size ranging from one micron and above. The liquid carrier that disperses the drug usually had the same hydrophobicity as the drug. The immiscibility between the water and oil needs to be stabilized by a surfactant (also known as an emulsifier). The surfactant serves as a thermodynamically isotropic interfacial membrane between the two liquid phases, lowers the surface tension, and creates a physical boundary that prevents the droplets from coalescence. Nanoemulsions and microemulsions are approaches used to improve drug bioavailability. A key component for emulsion systems is the drug release mechanism; the release mechanism is controlled through the skillful selection of surfactants and cosurfactants (44-46) that destabilize at the specific target thus allow the release of drugs.

Nanoemulsions (Figure 3) are popular for use with the nasal, dermal, and mucosa routes because of their large surface area that results in increased drug absorption and permeation. Nanoemulsions are also thermodynamically and kinetically stable, enabling easy sterilization. Submicron size droplets produce translucent nanoemulsions that are ideal for intravenous formulations. Emulsions require a large amount of surfactant and can

sometimes become unstable depending upon the temperature, pH, and ionic strength of the environment.

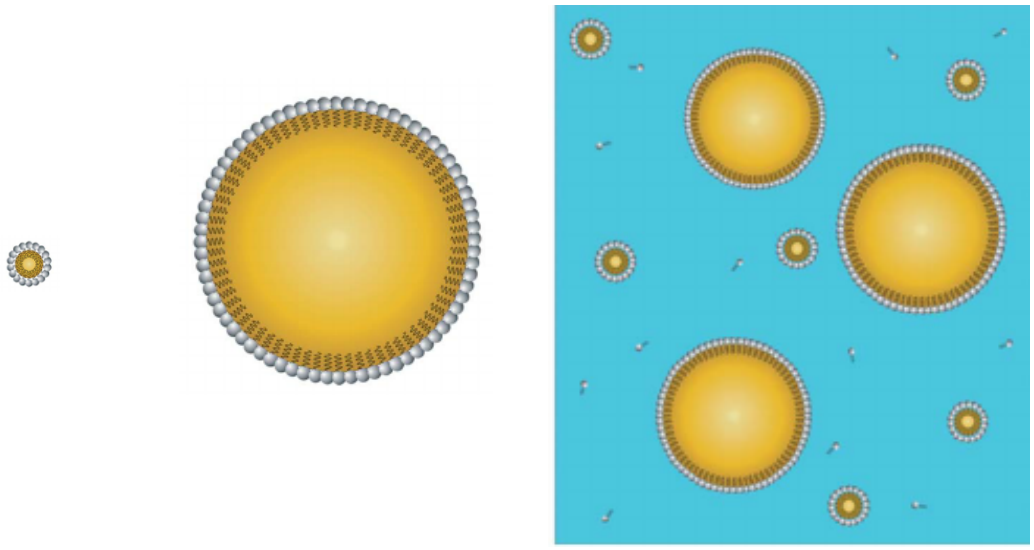

Figure 4: Comparison of nanoemulsion (A), microemulsion (B), and mixture of nanoemulsion and microemulsion(C) (46)

A group of researchers recently synthesized a dual mode imaging of ^{19}F magnetic resonance and near-infrared fluorescence capable nanoemulsion. The drug portion, Celecoxib, in this case, showed a strong signal within the cytoplasm of macrophages (45). The PGE2 reduction also inversely correlated with the drug's concentration. The result suggests that the contrasting agents formulated with the nanoemulsion method did not hinder drug permeation into the cell. The emulsion also was stable for more than two months. The approach established herein, targeted drug delivery and theragnostic, is promising.

The standard way of producing nanoparticles (nm) and microparticles (μm) is to include a lipid carrier or polymer matrix where the carrier encapsulates the drug. The two common types are solid and lipid particles. Various compositions and fabrication techniques are employed to increase the drug loading efficiency, achieve the desired pharmacokinetic profiles, and prevent dose dumping. An emerging trend observed is the use of a multi-particulate system where the raw drug and various sized particles are mixed in a controlled proportion as to achieve the desired drug release profile. Carrier materials also influence drug release from these particles (41, 47). The nanoparticles are usually formulated via some form of strong force such as high ultrasonication, wet-milling, or high-pressure homogenization. Microparticles are usually formulated via a coacervation method which consists of the emulsion solvent evaporation process, spray drying, and solvent extraction-evaporation method. Poly-lactic-co-glycolic acid (PLGA), pH-sensitive polymers (polymethracrylate i.e., Eudragit), cellulosic, and solid-phase anchored silica are examples of commonly used carriers for the formulation of particles (48). One disadvantage observed through recent clinical trials is the nonspecific extracellular release of the drug at the target site, the drug is released into the extracellular matrix thus the efficacy is also dependent upon the permeability of the drug (49). Figure 5 (42) below demonstrate a comparative size and surface area between nanoparticle and microsphere.

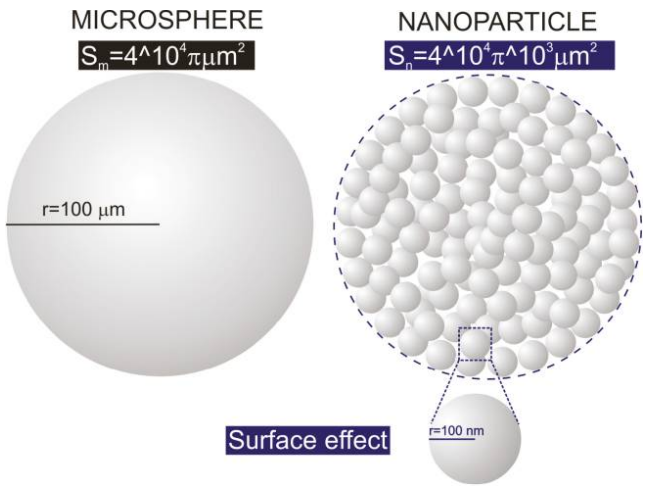

Figure 5: Respective size of a microparticle versus nanoparticle, surface area increases as size of spherical particle decreases (42)

Liposomes are lipid-based carriers that consist of a lipid bilayer that encapsulates an aqueous drug volume (hydrophilic drug) or hydrophobic drug within their lipid bilayer (50). Liposomes have amphoteric properties that enable them to be used as a carrier for both hydrophilic and hydrophobic drugs. Liposomes are shown to accumulate at inflamed tissues and can be enhanced via surface modification and addition of a targeting ligand (51). The surface modifications of liposomes are accomplished by physical anchoring and leveraging on the polarity of the chemical moieties or chemically treating the lipids and covalently bonding the moieties to the lipid (Figure 6, (52). Surface modified curcumin liposome in vitro study using colorectal cancer showed enhanced targeted delivery and drug concentration compared to a previously published curcumin liposome formulation (53).

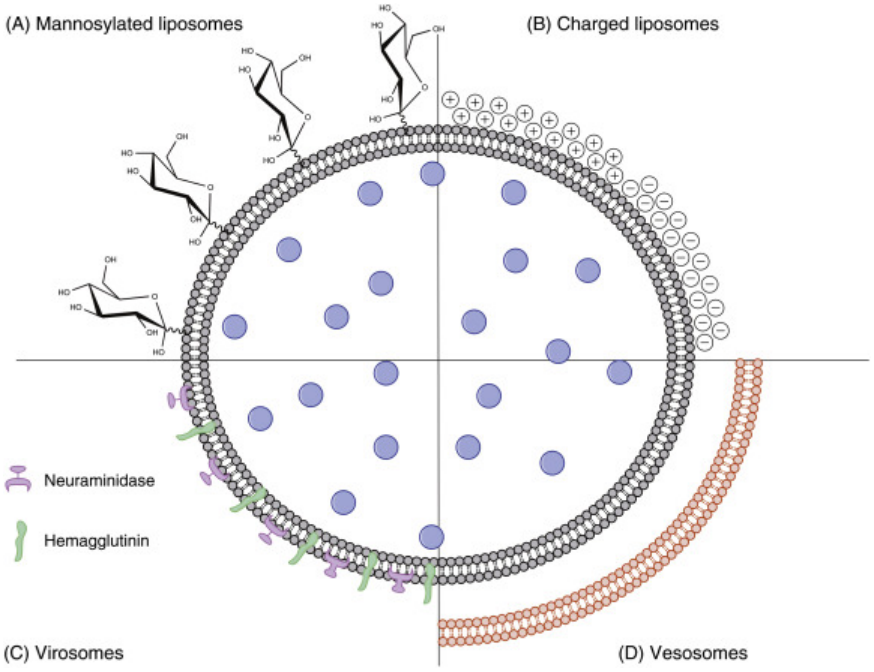

Figure 6: Various type of liposomes used for CDDS- A) Mannosylated, B)Ionic, C) Virosomes, D) Multilayered liposomes (Vesosomes) (51)

Since 2016, three completed clinical trials studying combination therapy for the treatment of colorectal cancers using liposomes as carriers had not had their results submitted. The lack of submitted results to the NIH clinical trials website is indicative of inconsistent or undesirable outcomes (54). In my opinion, liposomes targeting the colon lack a practical application due to the complicated pH terrain of the colonic environments that might have caused the instability and unspecific release of the liposomes.

Virosome is a small subset of liposomes which are made of a unilamellar phospholipid membrane but contain viral genetic materials (phospholipid and glycoprotein) that

facilitate a high amount of binding specificity. This formulation approach is one of a new emerging trend that leverage on the preexisting knowledge coming from the immunogenicity study accumulated over the years through the vaccine industry (55).

Other novel techniques for colon drug delivery system (CDDS) as therapy emerged during the last few years as more sophisticated analytical instruments became available (40). Of particular interested is the direct guidance of an external magnetic field to promote magnetic-nanoparticle accumulation and release at the targeted colon site. A group of researchers (56) combined such techniques with a monoclonal antibody (mAb198.3) to increase therapeutic specificity targeting of the FAT1 gene, and to reduce systemic toxicity. In the study, the researches adhered magnetic nanoparticles to anti-FAT1 mAb198.3. The formulation showed that mAb198.3, by targeting the FAT1 gene expression, recognized colonic cancer cells at different stages and locations (52).

Taking into consideration the complexity of the colon, each colonic drug delivery system needs to sufficiently address the differences of the gastric transit time, local microbial content, physiological pH, amount of inflamed tissues with altered drug absorption ability, and mucus thickness that changes the surface topography to achieve drug release at the intended site. The next few paragraphs will discuss the current colonic drug delivery systems together with their advantages and disadvantages.

1.2.1. pH-responsive release mechanism

The distal colon has a near neutral pH of 6.6 ± 0.5 compared to the proximal small intestine 4.5 ± 0.5; thus, targeting the distal colon via a pH-responsive release mechanism, in principle, is a straight forward solution, but in practice has proven challenging due to the inter-individual pH variations. A pH-sensitive drug delivery system must withstand the acidic environment of the stomach (1.2) and deliver a drug at the near neutral pH of the distal small intestine (7.5 ± 0.4) or the ileocecal junction. Interestingly, once in the colon, the pH turns slightly basic again due to the fatty acids produced by the resident microbiomes. The mean pH within a healthy colon has been reported to be 6.37 ± 0.58 in the right colon, 6.61 ± 0.83 in the mid-colon, and 7.04 ± 0.67 in the left colon (57). In the colon, the pH variations can be as high as two pH units (58). A methacrylic acid and methyl methacrylate copolymer are the primary polymers of choice when it comes to pH-sensitive formulations (59). Methracyclic-methacrylate copolymer is commercially known as the Eudragit series from Evonik. Eudragit is used in many coatings for particles, hard gelatin capsules, and tablets. A few commercially available Eudragit coated formulations are Asacol®, Ipocol, and Mesren MR (60). A pH-sensitive drug delivery system also faces the intra-individual variances resulting from differences in food intake (61). During disease stages, the right colon of ulcerative colitis patients is slightly acidic (4.7 ± 0.72) (62). In one extreme case, a patient with active ulcerative colitis has a pH of 2.3 in the proximal colonic. Another pH-sensitive pellet coated with Eudragit S failed to release the drug (63) suggesting that the failure of pH-sensitive dosage forms is influenced by more than just pH (64, 65) but also by residence time at the ileocaecal junction, by feeding status, and by

gastrointestinal fluid composition. Thus, commercial drug delivery systems leveraging on pH variation of the digestive tract is still underdeveloped (66, 67).

1.2.2. Time-based delivery to the colon

Time-dependent systems attempt to utilize the time delay between dosage form ingestion and colonic arrival to achieve colon-specific targeting. The drug release is generally achieved by erosion, diffusion, or swelling of different matrices over a predetermined period. Time-based approaches work on the assumption that a dosage form will spend approximately six hours in the stomach and small intestine during the fasted state. The time-dependent approach assumes that gastrointestinal transit time is solely influenced by the gastric emptying. Thus, a lag time can be added for the fed state. The erroneous part of this assumption is in the variability of the amount and type of food intake (68) When an individual is hungry, a phase III contraction wave in the stomach squeezes and flushes all material remains in the stomach to the small intestine include submicron particulates. When the stomach is full, food prevents the onset of phase III contraction wave. A study had shown that enteric coating tablets remained in the stomach for more than twelve hours (61). Thus, relying solely on the transit time to deliver the drug to the colon would not be sufficient.

The complexity of a time-based colonic drug delivery system intensifies as the CDSS is designed with the assumption that the small intestinal transit time is around three hours ± one hour. In reality, Davis, Hardy & Fara, 1986 and recently, Fara et al., 2009 demonstrated

the assumption of small intestinal transit time is inaccurate (69). The amount of time that food remains in the small intestine ranges from half an hour to nine hours, depending on the meal size and type of diet.

The order in which the medicine was taken also influences the amount of time taken to reach the colon. A study showed a tablet taken after a meal stayed in the small intestine significantly longer than the tablet ingested half an hour before a meal.

CDSS, in brief, are influenced by the small intestinal transit time, which in turn is influenced by the food intake, the time the meal was eaten in relative to the time the drug was taken, the shape and form of CDSS formulations, and the disease's stage of the patients. All these variables in total make it almost impossible to predict the individual's colonic arrival time which equates to an insurmountable task for the effort of designing a time-dependent colonic CDSS that would accurately deliver drugs for all patients(70).

1.2.3. Microbially Triggered Delivery Mechanism

Although much shorter than the small intestine, the colon has an overwhelming number of resident microbiota that exist sparsely in the upper gastrointestinal tract. The microbiota present serve as another approach for colonic site-specific drug release design.

Medicinal chemists exploited the large bacterial population in the colon to design their prodrugs. For example, sulfasalazine is a prodrug that successfully employs colonic microbiota to cleave the inactive precursor and release the active mesalazine. Other

enzymes produced by the colonic bacteria such as saccharolytic bacteroids and bifidobacterium to break down di-, tri-, and polysaccharides were successfully absorbed by the upper intestinal tract (71-73). Anaerobic bacteria are also known to be the main engine that produces polysaccharidases that break down short-chain fatty acids such as butyric, acetic, and propionic acids.

The high levels of polysaccharidase producing bacteria mean that attention has turned to polysaccharides as colonic delivery systems; these compounds are cheap, nontoxic, and biodegradable. A selection of polysaccharides can avoid degradation in the small intestine but are used as a substrate by the colonic microbiota. These polysaccharides can be used as coatings or matrix systems. The performance of polysaccharide based colonic delivery systems has been reviewed by many authors (74, 75) and will not be discussed in detail in this review. Although polysaccharide-based systems show great promise for colonic targeting, few have reached market. A system based on amylose mixed with the water-insoluble polymer ethylcellulose has demonstrated positive results in Phase I and II clinical trials. Amylose is a starch polysaccharide; starch polysaccharides come in many forms, several of which are indigestible by human pancreatic enzymes but act as a food source for colonic bacteria (76, 77) This combination of colon-specific polysaccharide and insoluble polymer (to prevent swelling and premature drug release) has achieved consistent colonic targeting with various drug molecules. McConnell et al., 2008d recently compared a pH-sensitive drug delivery system using Eudragit S to the polysaccharides prodrugs of amylose/ethyl-cellulose coated theophylline pellets that target colonic bacteria. The

targeted prodrug released in the colon is far more effective compared to the pH-coated pellets. The study was completed by utilizing gamma scintigraphy and pharmacokinetics data of theophylline (43). However, a phase III efficacious clinical trial studied eight UC patients using the above comparative approach. The authors noted that the prednisolone prodrug approach has fewer side effects compared to the pH-trigger method and proposed that such a prodrug approach may be useful for maintenance therapy.

A novel colon-targeted delivery system (CDDS) also relies on specific colonic bacteria to cleave prodrug into a drug (78). The microbiome-prodrug approach also incorporates pH sensitive elements for targeting the neutral colonic environment. The above dual mode often utilizes lactulose and acidic pH-responsive cores to help dissolve the tablets upon reaching the colon. The by-product of the prodrugs is usually some form of short-chain fatty acids that facilitates a burst release profile. The CDDS that relied on colonic bacteria has been successfully applied to theophylline, a drug that requires a narrow therapeutic index (43, 79, 80).

Given the success of bacterially triggered systems, a new concept in colonic drug targeting was introduced by combining pH-responsive and bacterially triggered mechanisms in a single layer matrix film (81). The technology comprises a mixture of pH-responsive polymer (Eudragit S) and biodegradable polysaccharide (resistant starch). The Eudragit S component in the coating has two functions - preventing the disintegration of the film in the upper gastrointestinal tract and controlling the swelling of polysaccharide. The

polysaccharide in the coating resists the digestion by mammalian pancreatic amylase enzymes and is digestible by colonic bacterial enzymes. Once entering the colon, both trigger mechanisms contribute to the dosage form disintegration, ensuring appropriate drug targeting. A gamma scintigraphy study showed that the system provides for colon specificity. Consistent disintegration of tablets coated with the single layer matrix film was observed at the ileocecal junction or colon.

The colonic environment in terms of pH, microbiomes, and disease stages is a highly dynamic environment, which is not adequately studied or understood. There is a great deal of variability in the colonic environment, affected by many factors that need to be considered; one of the most critical factors is the disease stage. There is no shortage of drug delivery applications for the colon; there are potential benefits for systemic delivery, and there is still scope for improved treatments for local conditions in the distal gut, such as inflammatory bowel disease and colonic cancer. These diseases are significant problems for the medical world, and there are new molecules, new strategies, and new technologies that can be exploited to improve patient care.

1.2.4. Emerging Combination Release Mechanisms

Recent advancements of CDSS tend to revolve around a combination of release mechanism technologies. Another successful example of this would be the multimatrix (MMX) system - in which both pH sensitive and diffusion release mechanisms were designed to achieve a burst drug release followed by a sustained drug release that targeted the colon. MMX's

most successful application was toward low molecular weight chemical entities such as mesalazine, budesonide, and low molecular heparins (82). The success with low molecular weight entities is understandable due to the inner core of water-insoluble gel that formed once the outer pH-sensitive coating had dissolved (83). Regardless, MMX is still not wholly site specific due to a pH burst release mechanism that has significant interindividual differences. A mesalazine release study via gamma scintigraphy images showed release started in the small intestine and ileum, then reached mean maximum plasma concentration in the ileocaecal junction. The budesonide MMX formulation performed the worst; the MMX tablet disintegration began in the mid-small intestine (79, 84).

1.3. Current Coating Techniques in the Pharmaceutical Field

Coating is the process of adding an outer layer of material to the surface of a substrate. There are many pharmaceutical coating techniques including conventional pan (involves coating capsules with a sprayed-on solution), fluid bed, dry powder (solvent-less) utilizing an electrostatically charged powder, magnetically assisted impaction, compression, hot melt extrusion, supercritical fluid, and supercell coating technology. These techniques function to mask taste and odor, protect from degradation, control the pharmacokinetic properties of drugs, or a combination of the aforementioned purposes. Fluid applied coated technique substrates sequentially transition through the following stages - fresh runny solution, semisolid, sticky, and dry film. Criteria for a successful coating technique would be to have little or no visual defects, no functionality defects, increase production, and

simplify operations. Unfortunately, not a single coating technique above meets all the criteria for all applications. Some coating techniques are more advantageous than others in some applications but less advantageous for other applications. An in-depth discussion regarding the conventional pan, fluid bed, and the dry powder coating techniques and their applications toward the coating of hard gelatin capsules follows in the next few paragraphs.

A conventional pan coater is one of the oldest coating technologies available — a thin film forms covering the capsules when a solution is sprayed into a temperature and pressure-controlled chamber. The pan continuously rotates tumbling the capsules; heated air is introduced evaporating the excess sprayed solution. A fluid bed coater (Figure 7, (85) is similar to the conventional pan with additional air injected below the capsules resulting in a suspended, fluidized bed. The design helps separate the capsules to prevent clumping while the coating solution is spraying. A critical disadvantage for conventional pan and fluid bed techniques is the prolonged processing time between successive applications of coats. The mass of the polymer dissolved in the spray solution is limited to 3% of the total capsule's weight to ensure even drying and prevent intense sustained attrition that leads to abrasion and chipping of the film. Other disadvantages to these techniques are the requirements of a large amount of bulk material, expensive equipment, and a trained technician. The technician must monitor critical parameters to ensure reproducibility between batches such as the spraying rate, dewpoint, mass solution flow, air flow, and temperatures.

Liquid solution coatings often include an aqueous or organic solvent to dissolve polymers. An aqueous solvent requires a large amount of energy and high temperatures to evaporate often resulting in an undesirable appearance of the film formed as well as degradation of the drugs. Organic solvents on the other hand are environmentally toxic. Liquid solution coating often requires lengthy processing and drying to altogether remove the solvents. This, in turn, increases manufacturing cost. The dry powder, solvent-less coating techniques such as the electrostatic dry coating relieve manufacturers of the above challenges (86). In general, the mixture of conductive particles and polymers are cast into a disk. An electric current is applied to an adjacent electrode thus ionizing the conductive particles, while an air jet is blown toward grounded capsules, the electrical field and the mechanical forces of the jetted air cause ionized particles to deposit onto the capsules. The voltage, air flow, and powder density together all work to control the thickness, performance, and the appearance of the depositing film. A critical challenge of this method is the precise parameters required to obtain desirable film as well as avoiding supercharging the substrate that would destroy the drug within the capsule. Finally, the cleanliness of the substrate, high impact force, heat generated within the chamber sometime led to uneven thickness, void space, and multilayers deposition of the films.

Fluidized Bed Coating

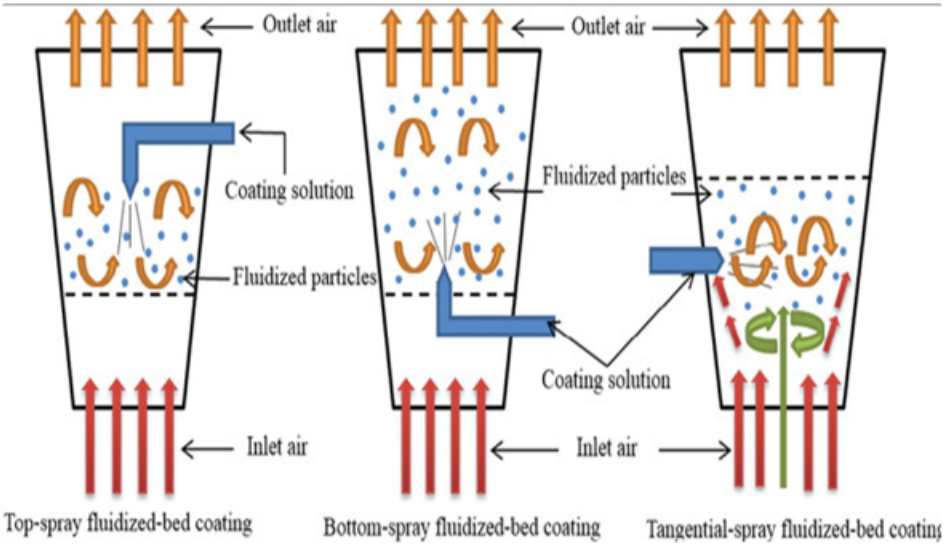

Electrostatic Dry Powder Coating

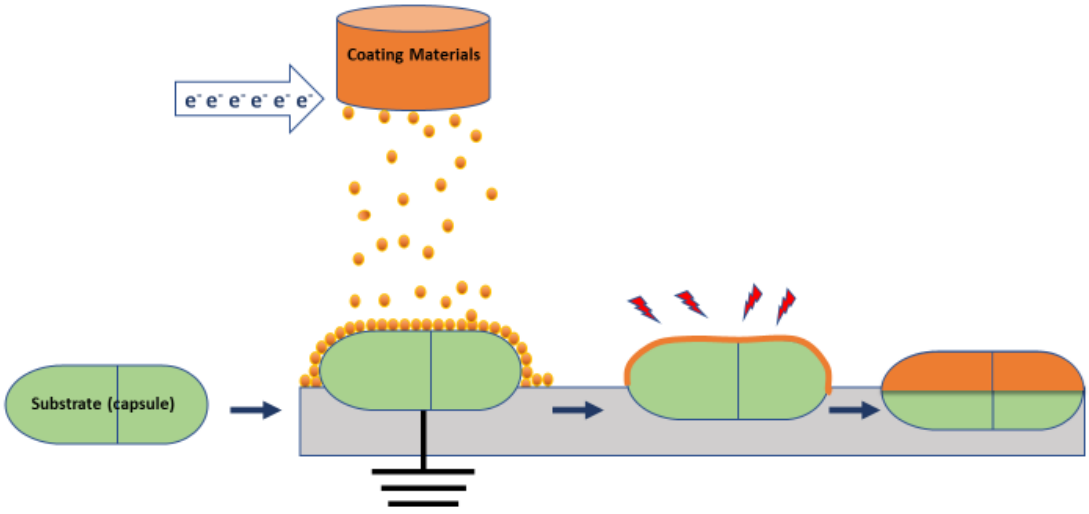

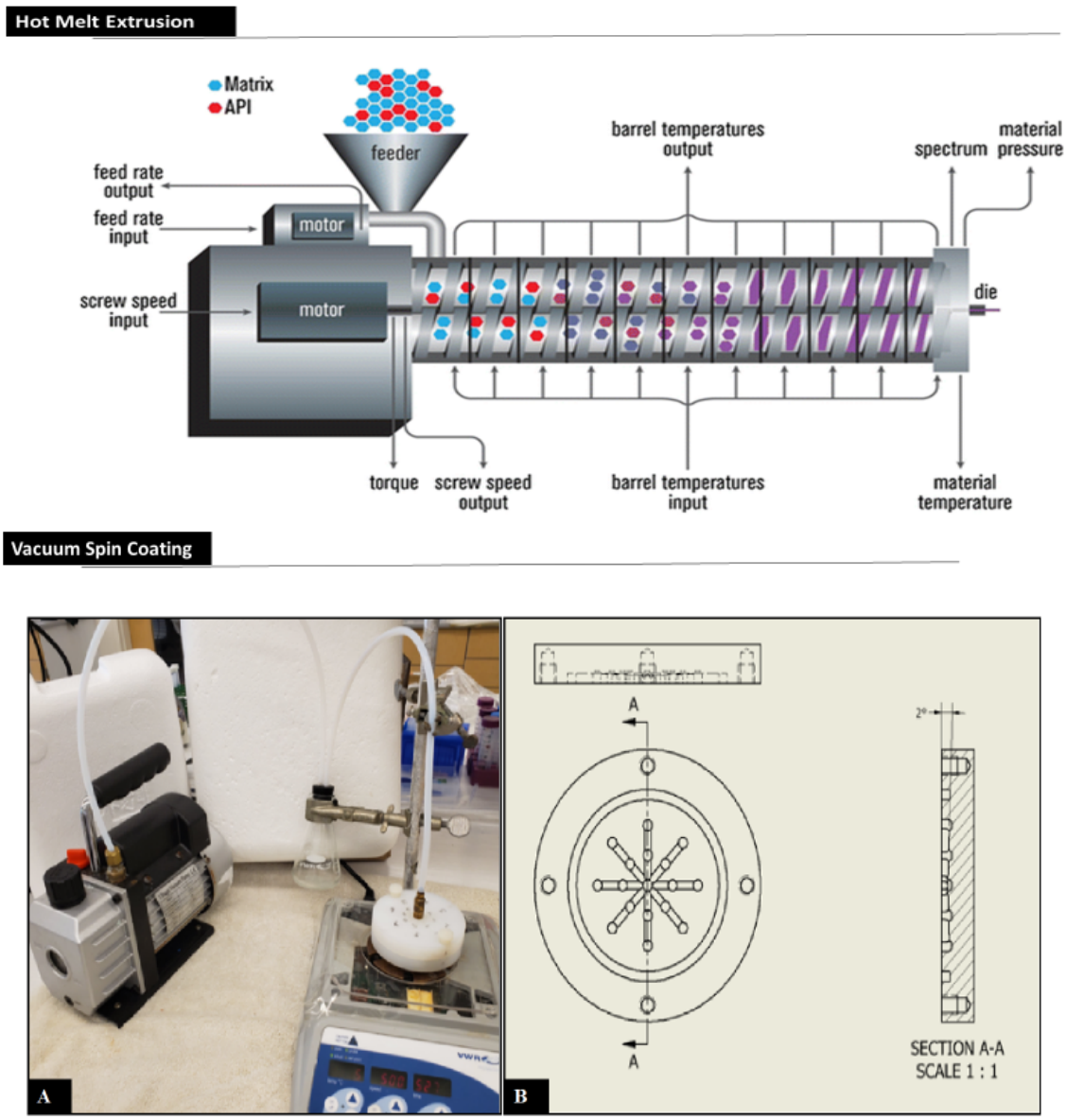

Figure 7: Current Coating Technology for (top panel) CDDS- Fluidized Bed (85), (second panel) Electronic dry powder (86), (third panel) Hot Melt Extrusion (87), and (bottom panel) Novel in house vacuum spin coating

1.4. Colon Bioavailable Drugs

1.4.1. Enterohepatic Recycling (EHR)

The concept of a “recyclable colonic drug” utilizing the enterohepatic recirculating loop to target and deliver drugs to the colon is a novel strategy. Bioavailability is a significant issue in drug development because sufficient drug concentration in the target organ is needed to elicit the desired therapeutic effects (88). Conventionally, most effort in drug development focuses on improving systemic bioavailability (i.e., increasing systemic exposure) since drugs with good systemic bioavailability means more drug circulating to the target organ (89, 90); however, the approach also increases toxicity across non-targeted organs. One of the major physiological barriers limiting systemic bioavailability is the first pass effect where drugs are absorbed from the intestine and metabolized in the liver, dramatically reducing the concentration of active drug reaching the systemic target organ. Medicinal chemists often try to avoid the first-pass effect as a means of improving bioavailability (91-93).

To achieve colon bioavailability, a modification in the current COXIBs structure by adding a desirable metabolic moiety (i.e., phenolic moiety) to enable the derivatives to undergo first pass effect. In other words, the engineered novel COXIBs will undergo rigorous first pass metabolism in the liver. Once administered orally, the desirable metabolic moiety of COXIBs derivatives is metabolites by hepatic uridine 5'-diphospho-glucuronosyl-transferase (UGTs), and efflux into the small intestine via transporters (e.g., BCRP, MRP2). For example, genistein, a soy-isoflavonoid with three hydroxyls, was rapidly metabolized by UGTs in the liver and extensively excreted through BCRP and MRP2 transporters via bile, resulting in a low systemic bioavailability (< 6%) (94-96).

1.4.2. Phase II Metabolism

Glucuronidation facilitates EHR. Glucuronidation is one of the most important phase II metabolic pathways of xenobiotics, and endogenous substances (97-99). Glucuronides of some phenolic compounds are good substrates of certain transporters (e.g., BCRP, MRP2), resulting in extensive hepatic secretion into the bile. The secreted glucuronides enter the intestine via the bile and often participate in recycling schemes after being hydrolyzed back to the parent drug by microflora. Adding a phenolic moiety to the structure of a COX-2 inhibitor thereby promoting it for glucuronidation could enable the inhibitors to undergo glucuronidation in the liver, efflux to the colon; thus, the locally bioavailable COX-2 inhibitors repeatedly enter into EHR, had low systemic exposure, and repeated colonic exposure.

Glucuronidation capability can be highly different in the liver than in the colon. Glucuronidation is catalyzed by UDP-glucuronosyltransferases (UGTs), which have approximately 24 known isoforms (97-99) with organ-specific distribution and expression levels (100). For example, UGT1A10 is exclusively expressed in the colon, whereas UGT1A9 and UGT1A1 are highly expressed in the liver but only poorly expressed in the colon (101). Furthermore, the colon's glucuronidation capability is low (by as much as 100x slower) compared to the small intestine and the liver (101). The glucuronidation rates of some flavonoids and drugs with phenolic moiety employed here are highly specified for the liver than in the colon (102, 103). The designed COX-2 inhibitors' phenolic moiety is

synthesized toward UGT1A1 enzymes and showed extensive glucuronidation in the liver and facilitate their biliary excretion.

EHR can prolong the drug's apparent half-life in the GI tract. Due to recycling, drug molecules are repeatedly present in the GI tract, resulting in a prolonged apparent drug half-life in the colon (104, 105). Bile salt molecule, an endogenous compound, is estimated to be recycled within the enterohepatic loops on average about 20 times due to EHR (106); although the number of recycling loops and repeated exposure of current locally bioavailable COX-2 inhibitors are still under investigation.

1.4.3. Microbial β-glucosidase

Due to the increase in hydrophilicity of the metabolites, the novel recyclable colonic targeted COX-2 inhibiting drugs are not expected to be reabsorbed by the epithelium enterocytes. There, once reaching the colon, the metabolites of locally bioavailable COX-2 inhibitors would get deconjugated and reverse back into active drugs via microbial β-glucosidase. The colon has approximately 100 billion to two trillion organisms per gram of luminal content. A variety of microbiomes are highly active in the glycosylation of phenolic glucuronides. A fraction of glucuronided candidates is observed to decouple from the glycolic acid and convert back into the parent compound. The above decoupling phenomenon is common in flavonoids. The recycled parent will be reabsorbed into the colon epithelial cells and resume the EHR cycle. EHR, deconjugation of metabolites, and reabsorption will repeat multiple times until all the drug molecules are eliminated through

the feces. Thereby, leveraging on the EHR will minimize the side effects associated with broad distribution of the drugs and the deconjugation of local colon microbiomes will help increase the concentration of drug delivery to the colon.

It has been accepted that for diseases such as FAP and CRC, the balance between the proliferation of pathogenic bacteria that incite inflammation and the probiotic bacteria that help to control the pathogenic microorganism population is disproportionate (107-109)). Studies showed that the pathogenic bacteria possess β-glucuronidase enzymes in CRC patients are many folds more active (80, 110). Shrewdly, locally bioavailable COX-2 inhibitors are optimized in our design to subjugate these microorganisms to reactivate the locally bioavailable COX-2 inhibitors metabolites into parent. Repeated drug exposure in the colon will be attained with minimal systemic exposure.

CHAPTER 2: CENTRAL HYPOTHESIS, STATEMENT OF PROBLEMS, AND SPECIFIC AIMS

2.1. Central hypothesis

In this application, we propose to delay and sustain the release of 6A1, a drug that is designed to be bioavailable in the colon (LBD), realizing low systemic drug exposure and avoiding off-organ toxicities. To achieve the proposed objectives, two different drug delivery systems were formulated. The first drug delivery system delays release via a novel coating technique in combination with a coating formulation that includes a pH-sensitive polymer and an erosion polymer for hard gelatin capsules. The second drug delivery system also uses hard gelatin capsules containing 6A1 enterically encapsulated microparticles aiming for a sustained release profile. The proposed novel coating formulation will achieve two objectives: the enteric biodegradable polymer coating will prevent early release of LBD COX-2 inhibitors (6A1) in the stomach that facilitate its absorption in the upper small intestine; the erosion mechanism makes the delayed release in the colon more precise, which could result in a smaller drug dose but higher colonic drug exposure. Delaying the release of 6A1 to the colon eliminates the impact of the inter-subject variability due to UGT expression in the liver, beta-glucuronidase activities expressed by colonic microflora, and colonic disease states. Additionally, delayed release delivery ensures a sufficient and consistent amount of 6A1 is present in the colon to saturate COX-2 enzymes. The proposed novel microparticle formulation will sustain the release of 6A1 via two mechanisms: slow

erosion of the microparticles and accumulation of the microparticles within the targeted site via its enhanced solubility and increased surface area. In combination with enterohepatic recycling (EHR), the new dosage forms will preclude or minimize systemic distribution of LBD COX-2 inhibitors and allow for rapid attainment and maintenance of adequate therapeutic concentrations in the colon. We hypothesize that the novel biodegradable polymer formulation and novel coating technique will synergistically function as a successful drug delivery system for treating diseases in the colon.

The approach used in this research is intended to fill a critical void in our understanding of how to create safe COX-2 inhibitors that prevent colonic cancer in FAP patients. If the concept is proven successful, the technology may be used with other novel drug candidates for colon cancer prevention and treatment of other colon diseases. The novel coating and formulation approaches for designing drugs tailored explicitly to the colon will be highly desirable and timely because they are fulfilling the unmet medical needs of not only FAP patients but patients suffering from other colonic diseases.

2.2. Statement of problems

FAP is a rare disease, but 100% of patients will develop colorectal cancer if they are not identified and treated at an early stage (1, 45); yet, no true pharmacologic treatment is available for these patients. COXIBs are the most versatile group of drugs prescribed for inflammation, analgesic/antipyretic, and auto-immune diseases and are undeniably effective in the treatment and prevention of polyposis formation. However, COXIBs that

circulate systemically inhibit COX-2 in on target off organs causing possible cardiovascular side effects (e.g., unstable angina, myocardial infarction, and cardiac thrombus) at the doses required for efficacy as a prophylactic (6, 16, 25-27), COXIBs cannot currently be used clinically to treat FAP. COXIBs are taken orally and absorbed through the stomach wall leading to systemic circulation. Additionally, COXIBs do not actively enter the EHR, thus large and frequent doses are required to reach a therapeutic level in the colon.

In the proposed research, utilizing EHR as a means to target drug delivery to the colon, is an unorthodox yet innovative approach. New chemical entities that undergo active glucuronidation via phase 2 metabolism are often eliminated early during the research and development phase due to an insufficient quantity of drug going to systemic circulation and ultimately inadequate therapeutic outcomes due to low exposure (39, 40). The current research focuses on a novel class of COX-2 inhibitors that are actively glucuronidated by the UGT1A1 enzyme, which is a subclass of phase II metabolic enzymes found in abundance in the livers. Because the glucuronides of 6A1 undergo EHR, gut microbiomes can successfully reconvert glucuronides back into aglycone, which becomes bioavailable again after absorption into the colon cells, thus reducing the systemic drug circulation while increasing their exposure in the colon. However, the concern of excessive inter-subject discrepancies (patient's intrinsic and extrinsic factors) have demonstrated the necessity to directly dose the drug to the colon after initial administration, as the regulatory agency mandated that safe and efficacious drugs should have consistent C_{max}, T_{max}, and AUC

across all populations (46). The variability might have been caused by the differences in the expression of UGTs in the liver and/or beta-glucuronidase activities expressed by colonic microflora, which may further be altered due to colonic diseases.

Furthermore, when exclusively relying on beta-glucuronidase to deconjugate the metabolites, an insufficient amount of the parent drug at the colon tissue exhibits its inhibitory efficacy. On the other hand, if we rely heavily on the UGT1A1 enzymes to metabolize 6A1, the result may be a low amount of bioavailability of metabolites effluxing to the colon or high systemic concentrations. Thus, the ability to deliver the right initial dose would be compromised. Formulation and coating of 6A1 packed inside the hard gelatin capsules ensures that the initial dose, at the correct concentration, will be delivered to the colon and sufficiently saturate the COX-2 enzymes, yielding a consistent C_{max} and T_{max} value across all populations.

2.3. Specific Aims

Aim 1: Use vacuum spin coating techniques and formulations to delay the release of 6A1 (& other locally bioavailable drugs) targeting the F344 rat colon. A controlled coating technique that results in an appropriate thickness, combined with an optimal formulation of biodegradable polymers that will protect and release 6A1 in a programmable manner (beyond 6 hours and pH 6.8). Compared to the small intestine, the colon is much shorter with a less absorptive surface; however, the colon has the longest transit time (1). The

optimal coating will be pH-sensitive to a basic environment and have an erosion mechanism that is uniquely tailored to the water content and microbiome within the colon.

Aim 2: Develop multi-modal oral delayed-release formulations to sustain 6A1 exposure in the colon (lower $AUC_{0\text{-}24Hours}$, increase local AUC_{colon}). Dual release mechanism with pH resistance, varying particle sizes ranging from 100-2000 nm should have the highest ratio of drug accumulation over given dose. The dual-release mechanism design aims to achieve maximum efficacy without subjecting the patients to a large dose and potentially reduce the dosing frequency (2). With the facilitation of JMP DoE 14 software, Eudragit S100 pH-sensitive polymer and PLGA 5050 is used to formulate the oral sustained release nano and microparticles of 6A1. The categorical outcome factors would be a sustained drug release above pH 6.0 and 6 hours after dosing. In vitro and vivo data have shown that both 6A1 microparticle formulations are highly stable, have a high encapsulation efficiency of 30.0 and 45, and exhibit a sustained release profile.

Aim 3: Evaluate the short-term efficacy of leading formulations of 6A1 with the F344 rat model. LBD (6A1) formulation and coating approach pharmacologic target in recessing the growth of adenomatous is reflective in their ability to accumulate at the colon and sufficiently inhibit COX-2 enzymes. The leading formulations from Aim 1 and Aim 2 will be used while aiming to lower systemic circulation and enhance the drug's efficacy by promoting accumulation only in the colon. A four-day BID of 20 mg/kg dose will determine: 1) maximum accumulation of 6A1 in the colon and 2) minimum blood

concentration-time profile of oral formulation at steady state. It is hypothesized that each additional dose will increase the C_{max} in colon especially for a compound that undergoes extensive glucuronidation such as 6A1.

If proven successful, the approach will result in overall reduced systemic drug concentrations ($AUC_{\_sytemic}$), thereby reducing the side effects and achieving high colonic drug accumulation ($AUC_{\_colon}$). A combined approach of both pH dependent and time-dependent particulate system may also be used for the treatment for other gastrointestinal tract disease.

CHAPTER 3: A SENSITIVE AND VALIDATED UPLC-MS/MS METHOD FOR QUANTIFYING A NEWLY SYNTHESIZED COX-2 INHIBITOR (6A1) AND ITS METABOLITES IN BLOOD, LIVER, AND COLONIC MUCOSA OF F344 RATS

3.1. Abstract

Studies have shown cyclooxygenase-2 (COX-2) enzyme is elevated in colorectal polyps. Marketed selective COX-2 inhibitors can successfully reduce polyp formation in the colon via inhibition of PGE_2 production by COX-2 (111, 112), but its prolonged administration as preventive care is not feasible due to on-target off-organ cardiac toxicity. A new COX-2 inhibitor (4-[3-(2-hydroxy-phenoxymethyl)-5-p-tolyl-pyrazol-1-yl-]-benzenesulfonamide (6A1)) with less systemic bioavailability, was synthesized and shown to be active in inhibiting COX-2 (113). A sensitive and robust ultra-performance liquid chromatography and tandem mass spectrometry (UPLC-MS/MS) method was developed and validated to simultaneously quantify 6A1, and its phase-II metabolites (glucuronide and sulfate) in rat's blood, liver, and colonic mucosa matrices. The Water's ACQUITY UPLC HSS T3 (2.1 x 100 mm I.D., 1.8 μm) column with gradient elution achieved the best peak separations. Both negative ESI and positive ESI were used to quantify 6A1 and its conjugated metabolites. The method's LLOQ of all three analytes were 2 ng/mL (or per gram) in blood, liver, and colonic. Good linearity ranges from 2 – 1,400 ng/mL for blood and 2 – 1,400 ng/g for tissue homogenates. The method was validated as per the Food and Drug Administration guidance with the intra- and inter-day precision of 5 - 14%, accuracy of 96.1 - 111.5%. The matrix effect for blood, colonic mucosa, and liver homogenates were

within the acceptable range (0.85 - 1.15). The established method was used to study the compound's pharmacokinetic behavior in the F344 rats.

Keywords: COX-2 enzyme, UPLC-MS/MS, Pharmacokinetic, Celecoxib, Enterohepatic recycling, NSAIDs

Abbreviations: UPLC, ultra-performance liquid chromatography; MS, Mass spectrometry; IS, internal standard; MRM, multiple reaction monitoring; LLOQ, lower limit of quantification; ULOQ, upper limit of quantification; 6A1, 4-[3-(2-hydroxy-phenoxymethyl)-5-p-tolyl-pyrazol-1-yl-] benzenesulfonamide; LLE, liquid-liquid extraction; SPE, solid phase extraction; QC, quality control; C_{max}, maximum concentration; T_{max}, time of occurrence of C_{max}; AUC, area under the curve; NSAIDs, nonsteroidal anti-inflammatory drugs; cyclooxygenase, COX; COXIBs, selective COX-2 inhibitors.

3.2. Introduction

Nonsteroidal anti-inflammatory drugs (NSAIDs) is perhaps the most versatile group of drugs prescribed for inflammation, analgesic/antipyretic, and auto-immune diseases (114). NSAIDs inhibit the synthesis of prostaglandins, thromboxane, and levuloglandins by blocking arachidonic acid substrates from binding to cyclooxygenase isozymes, COX-1 and COX-2. Certain prostaglandins appear to play a vital role in the carcinogenesis by altering cell adhesion, inhibiting apoptosis, and promoting angiogenesis (107, 115). Among these COS enzymes, COX-1 performs a distinct physiological homeostatic maintenance role within the vascular system and gastrointestinal tract. Inhibition of COX-1 may lead to gastrointestinal toxicity, cardiovascular toxicity, internal bleeding, and stomach ulcers. The COX-2 enzyme, the inducible, pro-inflammatory cyclooxygenase isoform is overexpressed and upregulated in many cancer tissues (116). COX-2 overexpression is associated with poor survival outcome in colorectal cancer patients (117) and is used as a prominent predictive marker in inflammatory bowel diseases (118). Naturally, selective COX-2 inhibitors (COXIBs) were designed to prevent the unwanted, adverse gastrointestinal events associated with NSAIDs.

Celecoxib (4-[5-(4-methylphenyl)-3-(trifluoromethyl)-1H-pyrazol- 1-yl]-benzenesulfonamide) is a potent selective inhibitor of the COX-2 enzyme (119, 120). Celecoxib is primarily indicated for the management of osteoarthritis, rheumatoid arthritis, ankylosing spondylitis, acute pain, and primary dysmenorrhea. Once absorbed, Celecoxib is

transported to the liver via the portal vein, metabolized into 4-hydroxyl-celecoxib by cytochrome P450 2C9 and 3A4 enzymes at the 4-methylphenyl functional group (121, 122), finally undergoing a phase-II metabolism, where the glucuronic acid is conjugated to the compound by UDP glucuronosyltransferases (123, 124). Ultimately, celecoxib is transformed into metabolites, reducing its availability in the targeted tissues (12, 80, 108, 125-129). Thus, the attainment of therapeutic levels of celecoxib at the lower gastrointestinal tract requires a high prescription dose (130-135) which results in dangerous cardiac side effects due to a high systemic drug concentration. Consequently, Pfizer withdrew Celebrex's indications for the treatment and prevention of colonic polyps in 2012 due to "on target off organ" cardiac toxicity (136-138).

A newly synthesized COX-2 inhibitor, 6A1 (4-[3-(2-hydroxy-phenoxymethyl)-5-p-tolyl-pyrazol-1-yl-] benzenesulfonamide), is comparable in its performance to that of celecoxib, with a potential of lower on-target off-organ systemic toxicity due to low systemic exposure (113). The objective of this study is to validate a sensitive, and specific method that could simultaneously quantify 6A1, and its metabolites in all three crucial matrices: blood, liver, and colonic mucosa using high performance liquid chromatography-mass spectrometry (UPLC-MS/MS). The development of this method is critical for the preclinical pharmacokinetic and efficacy studies of 6A1.

3.3. Materials and Methods

3.3.1. Chemicals and Materials

LC-MS grade acetonitrile, methanol, ethanol, dichloromethane, ammonium acetate, polyethylene glycol 300 bio-ultra, and Baohuoside I (IS) of 99.99% purity were purchased from Sigma-Aldrich Corp. (St. Louise, MO, USA). Acrodisc syringe filter with a PTFE membrane pore size of 0.2 um and diameter of 25 mm were purchased from Pall Corp. (Port Washington, NY). Oasis SPE 5 cc cassette were purchased from Water Corp. (Milford, MA). The parent compound, 6A1 was synthesized in house and quantified at 98% pure using the UPLC and NMR. 6A1 sulfate and 6A1 glucuronide are biosynthesized using F344 rat microsomes and MDCK II -UGT1A1-MRP2- overexpressed cells.

3.3.2. Biosynthesis and Purification of 6A1 Sulfate and Glucuronide

The biosynthesis of 6A1 glucuronide is done by F344 rat liver microsomes as previously published (121, 127, 131, 136). In brief, 10 μM of 6A1 were incubated in rat liver microsomes (~ 0.05 mg/mL protein concentration) for 8 hours at 37°C in a shaking-water bath (@ 60 rpm) resulting in the formation of 63% 6A1 glucuronide. The residual 6A1 from the incubated mixture's supernatant was removed via liquid-liquid extraction utilizing dichloromethane. The samples were run through the Oasis HybridSPE 5 cc cassette, washed with DI water three time the volume, and the eluents were washed out using 50% methanol in water. The collected eluents were then lyophilized, and stored in a −80°C freezer. The lyophilized residual was reconstituted with 100 μL of 50% methanol in water as stock solution of 6A1 glucuronide.

MDCK II-UGT1A1-MRP2-overexpressed cells were used to generate the 6A1 sulfate following a previously established and published method (131). In brief, 10 μM of 6A1 in HBSS buffer (pH 7.4) were incubated with MDCK II-UGT1A1-MRP2 cells overnight at 37°C. The 6A1 sulfate was extracted from the buffer using the above described SPE process for glucuronide, except 70% methanol in water was used to wash out eluent.

3.3.3. Chromatographic Conditions

Different combinations of mobile and stationary phases were employed to enhance the sensitivity and resolution of detection of 6A1, 6A1 sulfate, and 6A1 glucuronide. Acetonitrile, methanol, 0.1-5% formic acid in acetonitrile, 0.1 - 5% formic acid in methanol as organic phase, 1 - 2.5 mM ammonium acetate in water, and 0.05 - 1% formic acid in water as aqueous phase were tested as potential mobile phases. We tested both the Restek Raptor biphenyl and the Aquity HSS T3 columns as stationary phases to resolve 6A1, 6A1 sulfate, and 6A1 glucuronide.

The gradient elution was as follows: 0.1-.5 min 100% B; 0.5-1.5 min, 65% B; 1.5-2.5 min, 30% B; 2.0-3.0 min 15% B; 3.0 - 4.0 min, 10% B; 4.0 – 6.0 min, 95% B. The column temperature of 45°C, sample temperature of 20℃, injection volume of 10 μL, and a flow rate of 0.20 mL/min achieved the best peak sharpness and symmetry. The peak resolution defined as the amount of separation between two adjacent peaks, calculated using the following equation:

Peak Resolution = (time $peak_2$ eluted – time $peak_1$ eluted) / (0.5)(width $peak_2$ + width $peak_1$)

3.3.4. Mass Spectrometry Conditions

For MS/MS analysis, both positive and negative scan modes were employed to analyze 6A1, 6A1 glucuronide, and 6A1 sulfate. The representative MRM spectra of 6A1, 6A1 sulfate, and 6A1 glucuronide are shown in Figure 8. The analytes' intensity in positive scan mode is more sensitive for 6A1 and 6A1 glucuronide compared to the negative scan mode. However, the opposite is true for the 6A1 sulfate metabolite. To improve specificity, the multiple reactions monitoring (MRM) scan type was used. The MRM^+ transitions from precursor ions to product ions were optimized as m/z 436.3 → 326.2 for 6A1, 612.10 → 435.8 for 6A1 glucuronide and 515.3 → 369.1 for IS, based on their protonated molecules and corresponding product ions (Figure 9A, 9C, 9D). The MRM^- transition for 6A1 sulfate is optimized as m/z 513.3 → 434.1 and 513.1 → 369.1 for IS based on the deprotonated molecules and corresponding product ions (Figure 9B and 9E). Compound-dependent parameters in MRM mode for 6A1, 6A1 glucuronide, 6A1 sulfate, and Baohuoside I (IS) are summarized in Table 1. The main parameters for mass spectrum were used in the QTRAP 5500 system as follows: ion-spray voltage, 5.5 kV; temperature, 500°C; curtain gas, 20 psi; gas 1, 20 psi; gas 2, 20 psi; and collision gas, medium.

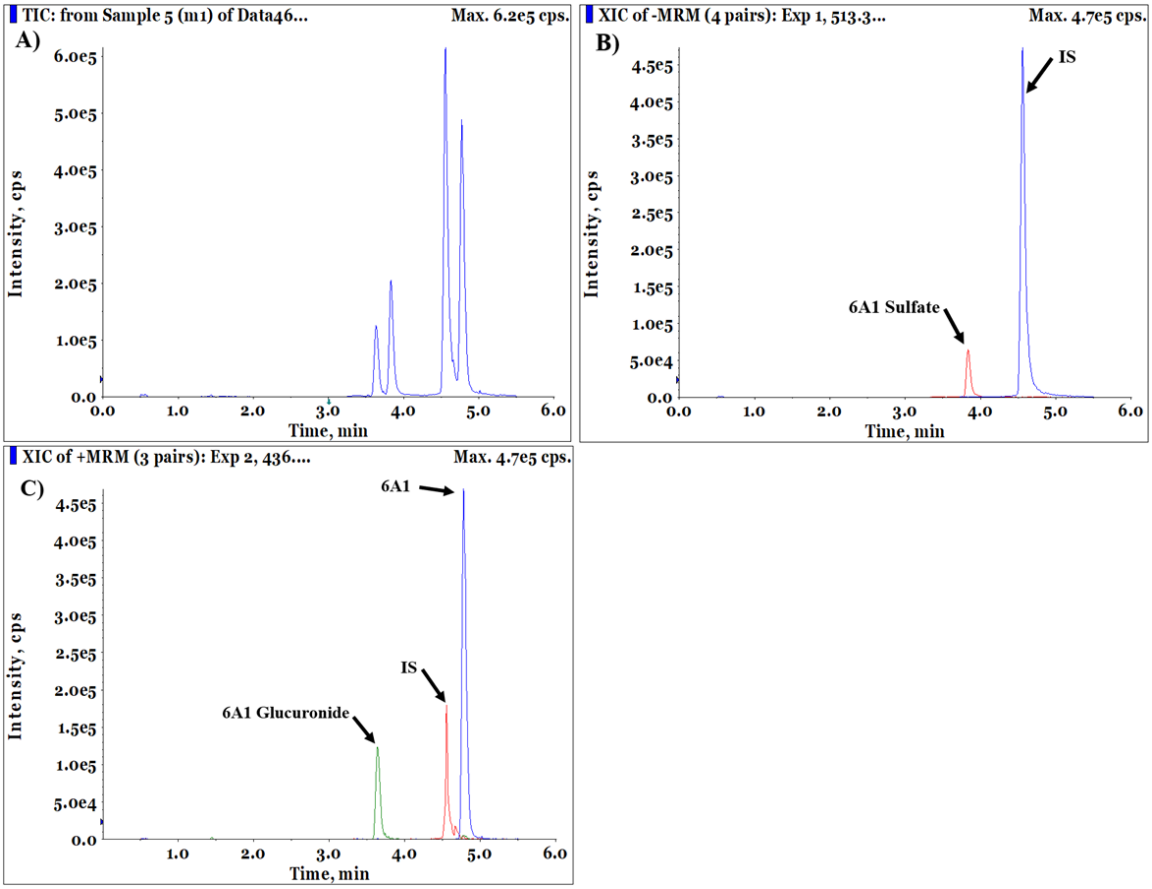

Figure 8: UPLC-MS/MS of validated method ran on a colonic mucosa sample. A) XIC of MRM of all four compounds eluting in the order of sulfate, glucuronide, IS, and 6A1; B) MRM- sulfate and IS; C) MRM+ glucuronide, IS, and 6A1

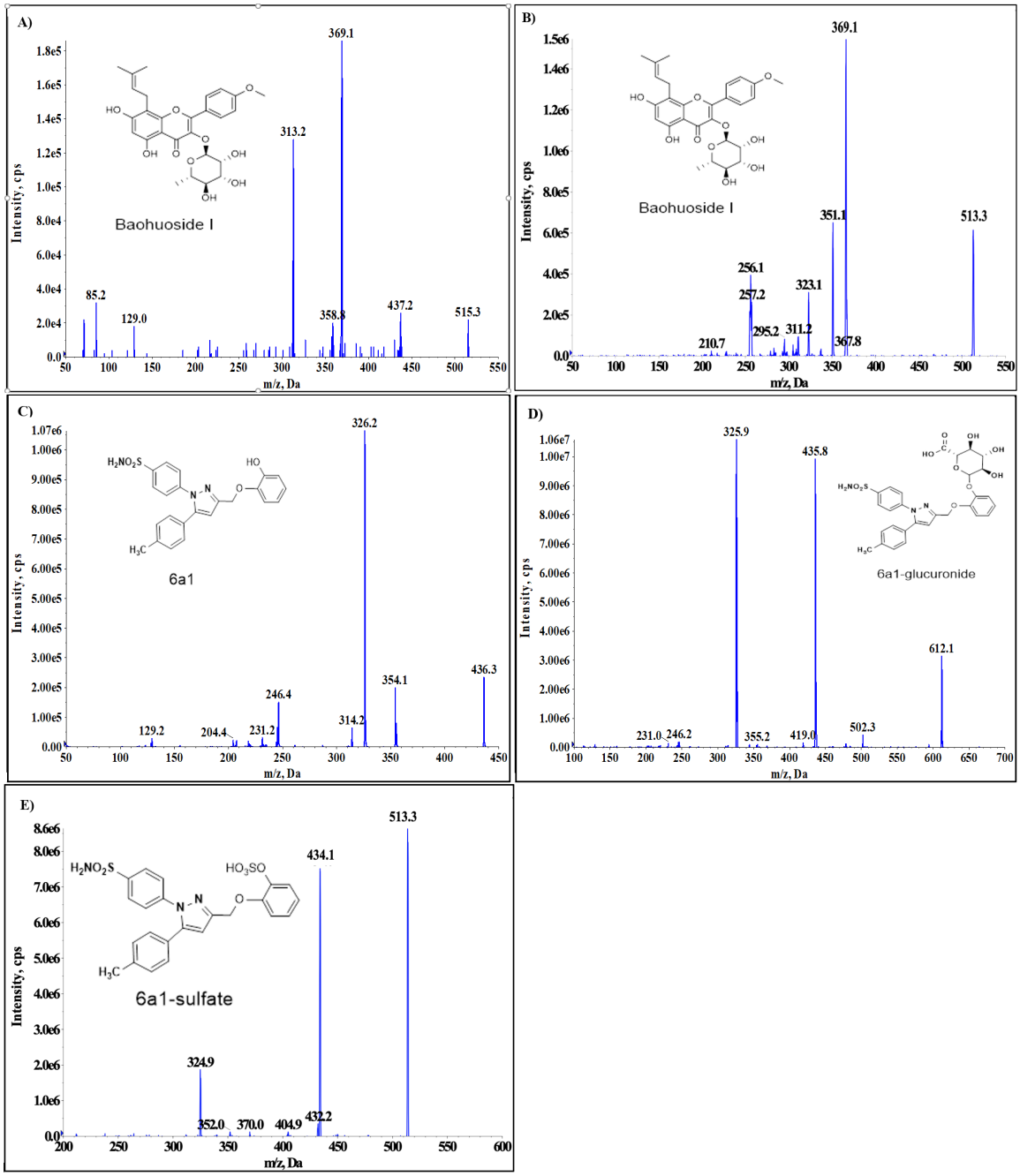

Figure 9: A) Product ion spectra of IS in negative mode; B) product ion spectra of IS in positive mode; C) product Ion Spectra of 6A1 in positive mode; D) Product Ion Spectra of 6A1 Glucuronide; E) Product Ion Spectra of 6A1 Sulfate

3.3.5. Preparation of Calibration Standards, Quality Control Samples, and Pharmacokinetic Study Samples of 6A1, 6A1 Glucuronide, and 6A1 Sulfate

Standard solution of 6A1, 6A1 glucuronide, 6A1 sulfate, and IS were prepared separately at 100 μg/mL in methanol. Each standard solution was then fractioned into multiple mini-Eppendorf tubes and stored at -80°C. Each standard solution was diluted with 1:2 water-methanol solution into the final working solution of 1 μg/mL on the same of day usage and discarded after each use. The calibration standard solution was prepared via serial dilution of working solution to achieve the following concentrations: 0.25, 0.5, 1, 2, 3.91, 7.81, 15.63, 31.25, 62.5, 125, 250, 500, 1,000, and 1,400 ng/mL.

3.3.5.1. Blood Samples

Blank blood samples (40 μL) were spiked with 10 μL of calibration standard solution at different concentrations of analytes and 10 μL IS solution (50 ng/ml in 50% methanol in water). Each sample was extracted with 1,500 μL of acetonitrile after vortexing for 3 minutes. All samples were centrifuged at 20,000 x g for 15 minutes at 5°C. The supernatant was then transferred to another tube and evaporated to dryness under a steady stream of air at room temperature. The residue was reconstituted with 40 μL of 66% methanol in water (2:1), vortexed, and centrifuged again at 20,000 x g for 5 minutes. After centrifugation, 10 μL of the supernatant was injected to UPLC-MS/MS system for analysis. For pharmacokinetic samples, spiking of the calibration standard solution was omitted.

3.3.5.2. Liver and Colonic Mucosa Samples

3.3.5.2.1. Tissue Homogenization

Liver tissue and colonic mucosa were excised from the sacrificed rats, washed with cold HBSS solution, and stored at −80°C in polypropylene tubes until homogenization. The frozen tissues were thawed, chopped and weighed. Exactly 50 mg of chopped tissue was homogenized in 500 µL of ice-cold homogenizing solution (pH 7.4) containing 10 mM potassium phosphate, 250 mM sucrose, and 1 mM EDTA dehydrate with a polytron tissue homogenizer. The homogenizer probe and test tubes were chilled at -4°C prior to use. Homogenization was paused for 20 seconds after every 30 seconds of homogenization at a medium speed. The homogenization was repeated 3 times until a visually uniform homogenate was obtained. Final tissue extract was stored at approximately −80°C prior to analysis. The homogenizer probe was washed sequentially with water, methanol, and water after every homogenization.

3.3.5.2.2. Extraction of 6A1, 6A1 Glucuronide, 6A1 Sulfate from Tissue Homogenate

Blank colonic mucosa or liver tissue samples (1 mg/µL) were spiked with 10 µL of calibration standard of different concentrations and 10 µL IS solution (Baohuoside 50 ng/mL of 1:1 methanolic water). An addition of 1,500 µL of cold acetonitrile and vortexing for 3 minutes to each sample precipitated out the protein. All samples were centrifuged at 20,000 x g for 15 minutes at 5°C. The supernatant then passed thorough the Oasis PRiME SPE 5cc cassette with applied vacuum. The eluents were collected and dried under a steady

stream of air at room temperature. The residue was reconstituted with 40 µL of methanol in water (2:1 v/v), vortexed, and centrifuged again at 20,000 x g for 5 min. After centrifugation, 10 µL of the supernatant was injected into the UPLC-MS/MS system for analysis.

Liver tissue and colonic mucosa at the conclusion of the pharmacokinetic study were collected, washed with cold HBSS buffer (pH 7.4), and stored at -80°C until homogenization. 50 mg of defrosted, chopped tissue was homogenized in 500 µL of ice-cold homogenization buffer (pH 7.4, containing 10 mM potassium phosphate, 250 mM sucrose, and 1 mM EDTA dehydrate) using a polytron tissue homogenizer with its probes and test tubes previously chilled at -4°C. Tissue homogenates are processed as mentioned in the paragraph above, omitting the addition of calibration standards.

3.3.5.3. Calculation of 6A1, 6A1 Glucuronide, 6A1 Sulfate Concentration in Tissue

Blood and tissue concentrations of 6A1, 6A1 glucuronide, and 6A1 sulfate were calculated using the slope and intercept of the linear regression line ($R^2 > 0.995$) generated from the standard curve of the same matrix. For example, a 392 ng /1000 µL nominal value of 6A1 has a count per second (CPS) raw read out of $5.56E^6$ with 50 ng of IS of $1.13E^6$. Back calculation gives the above read out of 378.49 ng/1000 µL, which has a 3.45% bias. The line generated range from 0 to 2000 ng/1000 µL of standard solution gives a slope of $1.3E^{-3}$ with $R^2 > 0.995$. For colonic mucosa of unknown concentration, the CPS readout of 10 µL

injection of the extracted tissue with 1 mg/μL tissue sample was $5.42E^6$ over the internal standard's CPS of $1.66E^6$ are normalized to give a ratio of 3.26. The normalized ratio is to avoid instrumental drift between each injection, thus 3.26 divided by the slope of the standard curve gives a concentration of 2,506.95 ng (1 mg/μL ÷ ng/1000 μL) of 6A1 per gram of colonic mucosa.

3.3.6. Method Validation

The linearity and stability, selectivity and specificity, sensitivity and carryover, accuracy and precision, as well as the extraction recovery and matrix effect studies followed US FDA guidance (139).

3.3.6.1. Calibration Curve and LLOQ

The least-square linear regression method ($1/x^2$ weight) was used to determine the slope and correlation coefficient of linear line. All linear regression lines were forced to go through origin at (0,0). Table 2 presents the linearity of calibration curves for 6A1, 6A1 glucuronide, and 6A1 sulfate of blood, liver, and colonic mucosa matrices. The LOD decided based on the 5:1 signal-to-noise ratio was 0.5 ng/mL, thus the lower limit of quantification (LLOQ) would be 2 ng/mL.

3.3.6.2. Sensitivity

The LLOQ samples at 2 ng/mL (n = 6) compared to blank matrix yielded peak/baseline ratio of five folds. No significant carryover was observed in the double blank samples after six high QC concentration injections (supplemental S1).

3.3.6.3. Specificity and Selectivity

The metabolites, sulfate and glucuronide were detected via negative and positive ion mode. Their respective peaks were not overlaps in the elution time. The base line separation between each analyte to the IS peak were set at equal or greater than 1.5-fold.

3.3.6.4. Accuracy and Precision

The "intra-day" and "inter-day" precision and accuracy of the method were determined with quality control (QC) samples at three different concentrations of 20, 200, and 1000 ng/mL (sextuplet per set) and the LLOQ of 2 ng/mL. Accuracy is to determine how close the empirical peak analyte normalized by internal standard peak ratios divided by standard curve slope and theoretical nominal value are to each other (Equation 1). This value is expressed in percentage with 100% being the same.

$$\%\ \text{accuracy} = 100\ \text{X}\ \frac{[extrapolated\ value]}{nominal\ value} \pm \%\ \text{standard deviation}$$ **(Equation 1)**

Precision is the percent of coefficient of variation within the group and within different group measured (Equation 2).

$$\%\text{CV} = 100\ \text{X}\ \frac{\text{standard deviation}}{mean\ value}$$ **(Equation 2)**

3.3.6.5. Extraction Recovery and Matrix Effect

Extraction recovery of 6A1, 6A1 sulfate, and 6A1 glucuronide in different bio-matrices (blood, liver, and colonic mucosa homogenate) were calculated by plotting the ratio of the peak areas of analyte (6A1, 6A1 glucuronide, and 6A1 sulfate) to IS (Baohuaside) in blank matrix spiked after the extraction procedure divided by the ratio of the peak areas of analyte to internal standard for the same matrix before the sample preparation step of LLE and SPE (Equation 3). Similarly, matrix effects were calculated by dividing the ratio of the peak area of the compound and internal standard spiked into extracted blank matrix by the ratio of the peak area of same compound and internal standard in neat solution at the same concentration (Equation 4). All these experiments and evaluations were performed according to the FDA recommended validation procedures (139).

$$\text{Extraction Recovery \%} = 100 \text{ X } \frac{Response\ of\ extracted\ analyte}{Response\ of\ Post\ Extracted - Extracted\ Spiked\ Analyte} \textbf{ (Equation 3)}$$

$$\text{Matrix Effect \%} = 100 \text{ X } \frac{Response\ of\ post\ extraction - Extracted\ spike\ analyte}{Response\ of\ non-extracted\ analyte} \textbf{ (Equation 4)}$$

Where:

Response of post-extracted spike analyte is the normalized respond of all 3 compounds (6A1, 6A1 glucuronide, and 6A1 sulfate) divided by IS (Baohuaside) that were added after the blank matrix has been processed via the LLE and SPE steps.

Response of non-extracted analyte is the normalized respond of all 3 compounds (6A1, 6A1 glucuronide, and 6A1 sulfate) divided by IS (Baohuaside) in neat solution.

3.3.6.6. Stability

Short-term, post-processing (25°C for 8 h), 3 freeze thaw cycles, and long-term (−80°C for 1 month) stabilities of 6A1, 6A1 sulfate, and 6A1 glucuronide were determined by analyzing three replicates of LLOQ and three QC samples at for all three matrices. The stability sample results were compared to the freshly prepared samples to determine the stability of each condition.

3.3.7. Preparation of the 6A1 Intravenous Injection Solution

0.25 w/v% solution of 6A1 was prepared in 40 v/v% of polyethylene glycol 300 and 60% v/v of ethanol. The solution was sonicated for five minutes until it became clear. The solution was further filtered using a 0.2 μm PTFE filter disc before injecting into the rats.

3.3.8. In Vivo Pharmacokinetic Study of 6A1

Male Fischer F344 rats (6–10 weeks, body weight between 250 to 280 g, n = 4) were purchased from Harlan Laboratory (Indianapolis, IN). Rats were kept in an environmentally controlled room (temperature: 25 ± 2°C, humidity: 50 ± 5%, and 12 h dark-light cycle) for at least 1 week before the experiments. The rats were fed ad libitum. The solution of 6A1 was administered via intravenous injection of the tail vein at a dose of 5.0 mg/Kg. Blood samples (about 20 –50 μL) collected into heparinized tubes at 0, 0.5, 1, 2, 4, 6, 8, 12, and 24 hours post dosing via tail snip with isoflurane as anesthetic. All collected pharmacokinetic blood samples were stored at − 80°C until analysis. After a

wash out period of 1 week, the rats were given a second dose via intravenous injection of 5 mg/Kg. Animals were sacrificed and tissues (colonic mucosa and liver tissues) were collected two hours post dosing. The procedures were approved by the University of Houston's Institutional Animal Care and Uses Committee (IACUC).

3.3.9. Pharmacokinetic Analyses

The primary pharmacokinetic parameters of interest were the maximum concentration (C_{max}), the area under the blood concentration–time curve (Figure 3) from baseline through 24 hours post-dose ($AUC_{0–24H}$), and duration of time after intravenously dosed until reaching maximum systemic concentration (T_{max}). The multiple C_{max}/T_{max} pairs that were observed are of special interest.

3.4. Results and Discussion

3.4.1. Solid stationary phase and column chemistry

A 1.8 um particle size Raptor Restek biphenyl column and a 1.8 um particle size Acquity HSS T3 column were used to separate 6A1, 6A1 glucuronide, and 6A1 sulfate analytes. The biphenyl column has the ability to retain polar aliphatic/aromatic solutes throughout a wide range of pH, making it the ideal choice (140). However, the peak resolution deteriorated as the pH of the aqueous buffer decreased (141, 142). Concurrently, the biphenyl column's pressure also increases; thus, ACN became the replacement organic phase in place of the MeOH (Supplemental S3). The HSS T3 column had better analytes

retention resulting in enhanced sensitivity using the same gradient elution method. The HSS T3 column also had a lower column pressure (6000 psi) compared to the biphenyl column (14,000 psi).

3.4.2. Selectivity, Specificity, and Sensitivity

Interference levels of endogenous compounds are determined via blank matrix injections (n=6). Glycoproteins, glycolipids, and phospholipids are known to interfere with the extraction and recovery of 6A1 and its metabolites from both colonic mucosa and liver tissue samples(143, 144). The addition of pass-through solid phase extraction using Oasis PRiME HLB cartridge after the liquid extraction step resolved low recovery due to endogenous matrix suppression of the ionization in the mass spectrometer. The chromatograms of blank matrix injections after each ULOQ sample exhibited a minor IS carryover peak at 4.15 minutes (Supplemental S2) equal to roughly about 5% of the LLOQ. However, the IS carry-over peak was negligible to the quantification of analytes in this method.

3.4.3. Linearity

Three different matrices- blood, liver, and colonic mucosa were used to validate the method. The calibration curves for 6A1, 6A1 glucuronide, and 6A1 sulfate of blood, liver, and colonic mucosa matrixes are linear in the range of 0.5-1,400 ng/mL for blood, 0.5-1,400 ng/g for liver, and 0.5-1,400 ng/g for colonic mucosa matrices (Table 2). Linear regression equations were calculated from the raw data of the Count Per Second (CPS)

response versus concentration graph with a weighting factor of $1/X^2$. The resulted coefficient of determination, R^2, for all regression lines were > 0.995 (Table 2).

3.4.4. Accuracy and Precision

The accuracy assay values for LLOQ and 3 QCs concentrations ranged from 96.1-111.5% for 6A1, 97.6-103.3% for 6A1 glucuronide, and 99.62-108.14% for 6A1 sulfate (Table 3). These ranges are within ± 15%, the acceptable limit recommended by the FDA. The intra-day and inter-day precision and accuracy were accessed by analyzing the sextuplet LLOQ and QC samples at low, medium, and high concentrations of analytes in blood matrix (Table 3). The precision values ranged from 5.33-13.12% for 6A1, 8.65-14.9% for 6A1 glucuronide, and 5.08-12.3% for 6A1 sulfate (Table 3).

3.4.5. Extraction Recovery

The mean extraction recovery for blood matrix analyzed from three replicates of LLOQ and three QC and LLOQ samples at 2, 20, 200, and 500 ng/mL were between 95.2-99.6% for 6A1, 94.3-100.1% for 6A1 glucuronide, and 96.1-101.3% for 6A1 sulfate (Table 4). The extraction recovery for liver tissue of LLOQ and three QC samples were between 93.6-95.9% for 6A1, 109-112% for 6A1 glucuronide, and 98-108.6% for 6A1 sulfate (Table 4). The colonic mucosa extraction recovery for the above LLOQ and QC samples were 99.4-103.8% for 6A1, 91.71-98.45% for 6A1 glucuronide, and 94.1-103.9% for 6A1 sulfate (Table 4). The extraction recovery of colonic mucosa had the highest %CV at low concentration (20 ng/g); however, all LLOQ and QC samples were reproducible judging

from the small %CV between groups and were within the recommendation of the FDA guidance (Table 4).

3.4.6. Matrix Effect

An ion enhancement (15.99%) in the response signal was observed for the LLOQ of colonic mucosa matrix. However, the effect was resolved after the additional application of 96-well Oasis HLB μ-elution plate. The overall matrix effect for blood samples ranged from 92-108%, 94.5-108.88% for colonic mucosa, and 88-113% for liver tissue (Table 5). The internal standard matrix effect is negligible thus comprehensive matrix effect was not evaluated.

3.4.7. Stability

Stabilities of 6A1, 6A1 glucuronide, and 6A1 sulfate of blood, colonic mucosa, and liver tissue were evaluated by analyzing triplicates of LLQC and QC samples at three different concentrations following 8 h at 25°C bench top (short term stability), 3 freeze thawing cycles, and at −80°C for 30 days (−80°C and 25°C). All the samples showed 95–105% recoveries after various stability tests (Table 6).

3.4.8. In Vivo Pharmacokinetic Study of 6A1

The established UPLC-MS/MS method was utilized to determine the concentration of 6A1, 6A1 glucuronide, and 6A1 sulfate in blood pharmacokinetic study and tissue samples collected from F344 rats (n=4). A single-dose intravenous administration of 6A1 was given

at 5 mg/Kg normalized by the rats' body weight. Figure 10 shows the mean blood concentration time profile of 6A1 and its metabolites. The validated method was able to detect all three compounds at and above the LLOQ of 2 ng/mL (or 2 ng/g of tissue samples).

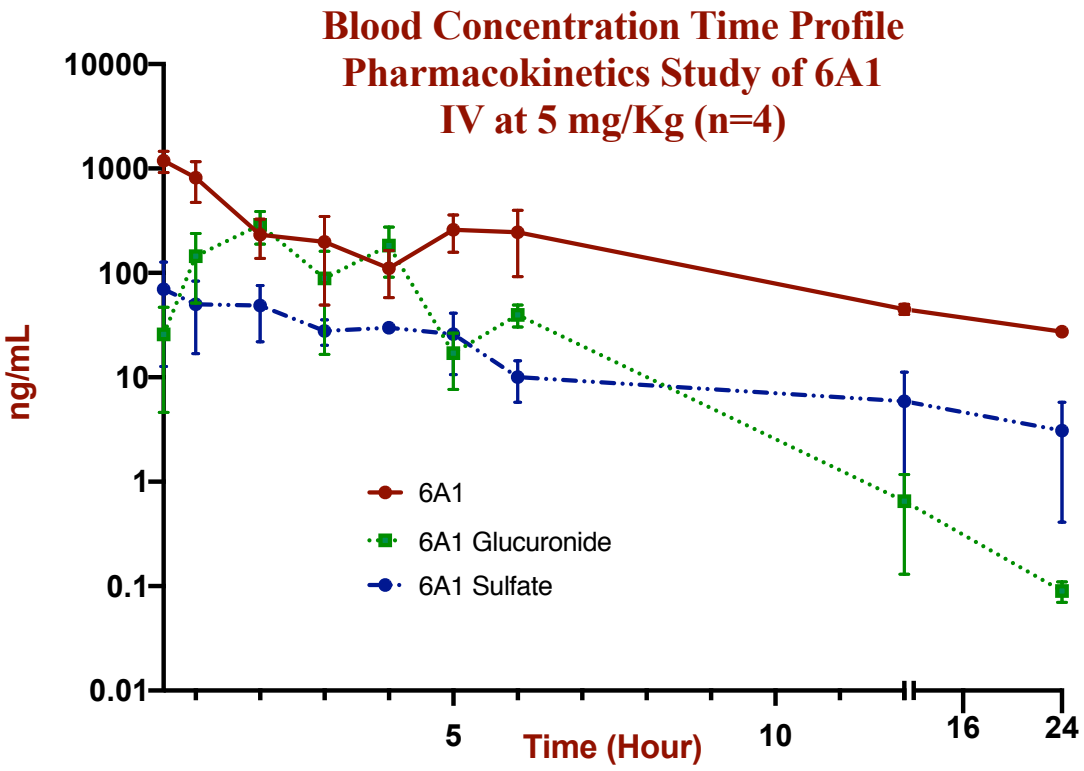

Figure 10: Blood concentration time profile pharmacokinetic study of 6A1 compound. Blood concentrations of 6A1 (Red Circles), 6A1Glucuronide (Green Squares), and 6A1 Sulfate (Blue Triangle) after i.v. administration of 5.0 mg/Kg in F344 rats (n = 3). Blood sample (10 µL) was spiked into acetonitrile (1000 µL), and IS (40 µL, Baohuaside in methanol, 1000 ng/mL). The mixture was vortexed and centrifuged for 15 min at 15,000 rpm. The supernatant was taken out, air dried, and reconstituted in 40 µL of 60% methanol and centrifuged for another 15 min at the same speed. Then 10 µL of supernatant was injected into the UPLC–MS/MS system. Each point is average of three determinations and the error bars are standard errors of the mean.

A double peak phenomenon was observed in the pharmacokinetic study of blood concentration-time profiles of 6A1 and 6A1 glucuronide. This indicated that the enterohepatic recirculation may be involved in the disposition of 6A1. A second peak of 6A1 at 258.47 ± 100.35 ng/mL was observed five hours after the dose was administered. The first 6A1 glucuronide peak (at 288.16 ± 94.88 ng/mL) was observed two hours post dose, whereas as a second 6A1 glucuronidation peak with concentration of 183.08 ± 52.71 ng/mL was observed at four hours after intravenous injection. Based on stability data established for 6A1 glucuronide, it is unlikely for the metabolite to deconjugate to 6A1 in the blood and tissues. Therefore, the double peak phenomenon is most likely the contribution of the enterohepatic recycling mechanism. It is believed that intravenous 6A1 is metabolized in the liver, secreted into the bile as 6A1 glucuronide and 6A1 sulfate. Once in the intestine, the colonic β-glucuronidase hydrolyzed the glucuronide metabolites into 6A1, which is then reabsorbed in the colon which give rise to the second peak of 6A1. The reabsorbed 6A1 again got glucuronidated and gave rise to a second peak of 6A1 glucuronide. The exact mechanism requires further investigation as to determine the recycling ratio and overall systemic exposure to 6A1. When compared to our previous study (145), a dose-normalized AUC (ng*hr/mL*mg) indicated that the systemic exposure of 6A1 is 9.04% that of the systemic exposure of celecoxib. The consistent 6A1 sulfate concentration of around 37.47 ± 17.22 ng/mL throughout the study suggested that metabolic disposition of 6A1 in F344 rats is primarily via glucuronidation. Colonic mucosa had an average ± SEM concentration of 225.94 ± 65.94 ng/g for 6A1, 26.78 ± 17.80 ng/g

for 6A1 glucuronide, and 5.12 ± 0.86 ng/g for 6A1 sulfate (Figure 11A). Liver tissues had an average concentration of 337.60 ± 100.27 ng/g for 6A1, 315.79 ± 81.55 ng/g for 6A1 glucuronide, and 218.14 ± 54.21 ng/g for 6A1 sulfate (Figure 11B).

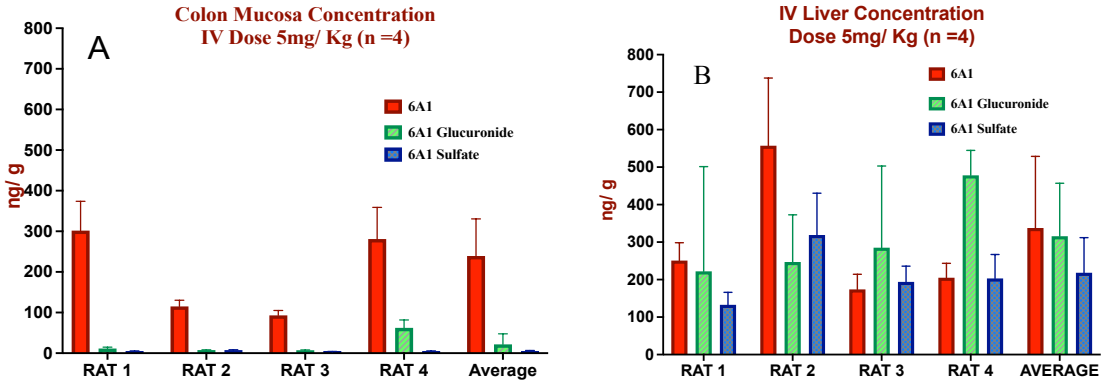

Figure 11: Colonic mucosa and liver tissue concentrations were collected two hours after given an intravenous dose of 5 mg/Kg. Liver and colonic mucosa concentrations were analyzed in triplicates. A) Colonic mucosa has an average ± SD concentration of 225.94 ± 65.94 ng/g for 6A1, 26.78 ± 17.80 ng/g for 6A1 glucuronide, and 5.12 ± 0.86 ng/g for 6A1 sulfate. B) Liver tissues, triplicate samples were also analyzed. Liver tissues had an average concentration of 337.60 ± 100.27 ng/g for 6A1, 315.79 ± 81.55 ng/g for 6A1 glucuronide, and 218.14 ± 54.21 ng/g for 6A1 sulfate

3.5. CONCLUSION

A robust, sensitive, and validated UPLC-MS/MS method was developed and successfully used to quantify 6A1, 6A1 glucuronide, and 6A1 sulfate in pharmacokinetic blood, colonic mucosa, and liver tissue samples. A larger sample size and additional routes of administration may be needed to strengthen the development of a pharmacokinetic model and its parameters' estimation. The method has a multitude of advantages, such as, high sensitivity (LLOQ 2 ng/mL), short analysis time (6 minutes), small sampling size (10 µL), good recovery with negligible matrix effect, and simplistic sample processing methods.

Table 1: Compound dependent parameters 6A1, 6A1 glucuronide, IS, and 6A1 sulfate parameters in MRM mode for LC-MS/MS

Analyte	Mode	Dwell Time (ms)	DP (V)	EP (V)	CE (V)	CXP (V)
6A1	Positive	50	47	10	23	19
6A1 Glucuronide	Positive	50	47	10	23	19
IS	Positive	50	71	10	31	10
IS	Negative	100	-8	-10	-34	-16
6A1 Sulfate	Negative	100	-30	-6	-31	-17

DP: declustering potential; EP: entrance potential; CE: collision energy; CXP: Collision cell exit potential

Table 2: Linearity of the standard calibration curve of 6A1, 6A1 glucuronide, 6A1 sulfate in blood, colonic mucosa, and liver tissue (Mean ± SD (%CV))

	Blood (n=6)		**Mucosa** (n=6)		**Liver** (n=6)	
	Slope ± SD (%CV)	R^2 ± SD (%CV)	Slope ± SD (%CV)	R^2 ± SD (%CV)	Slope ± SD (%CV)	R^2 ± SD (%CV)
6A1	0.00845 ± 0.000212 (2.51%)	0.999 ± 0.00354 (0.4%)	0.0074 ± 0.00021 (2.87%)	0.995 ± 0.00035 (0.04%)	0.0077 ± 0.0005 (6.38%)	0.998 ± 0.0005 (0.4%)
6A1 Glucuronide	0.0084 ± 0.00042 (5.05%)	0.998 ± 0.04 (4%)	0.0087 ± 0.0001 (2.70%)	0.998 ± 0.0004 (0.4%)	0.0087 ± 0.0007 (9.4%)	0.994 ± 0.003 (0.3%)
6A1 Sulfate	0.0023 ± 0.0003 (12.3%)	0.996 ± 0.0004 (0.04%)	0.0027 ± 0.000153 (2.97%)	0.994 ± 0.003 (0.3%)	0.0021 ± 0.00029 (13.72%)	0.996 ± 0.003 (0.4%)

Table 3: Intraday and Inter-day accuracy (Mean ± SD) and precision (%CV) data of 6A1, 6A1 glucuronide, and 6A1 sulfate for blood matrix using MRM method at three QC concentrations

Concentration (ng/mL)	Day 1 (n=6)		Day 2 (n=6)		Day 3 (n=6)		Inter-day (n=18)	
	Accuracy (%) Mean ± SD	Precision (%)	Accuracy (%) Mean ± SD	Precision (%)	Accuracy (%) Mean ± SD	Precision (%)	Accuracy (%) Mean ± SD	Precision (%)
6A1								
2	96.9 ± 2.58	2.66	108.11 ± 8.53	7.90	107 ± 8.32	7.22	107.08 ± 14.0	13.12
20	108.1 ± 8.55	7.91	106.9 ± 8.32	7.78	112.79 ± 8.02	7.11	109.26 ± 8.22	7.53
200	114.38 ± 4.75	4.15	108.3 ± 3.8	3.51	111.83 ± 7.78	6.96	111.5 ± 5.94	5.33
1000	89.26 ± 9.81	10.99	99.43 ± 6.28	6.31	99.61 ± 6.33	6.36	96.1 ± 8.74	9.10
6A1 Glucuronide								
2	97.98 ± 14.10	14.4	109.23 ±	9.31	102.76 ±	18.5	103.32 ± 14.43	14.07
20	89.97 ± 2.87	3.19	108.43 ± 5.71	5.27	102.47 ± 1.41	1.38	100.29 ± 8.67	8.65
200	91.42 ± 4.3	4.72	104.53 ± 4.45	4.26	107.54 ± 7.08	6.59	97.59 ± 13.7	14.00
1000	86.52 ± 3.64	4.20	105.97 ± 5.44	5.13	105.78 ± 7.68	7.26	98.33 ± 13.06	13.28
6A1 Sulfate								
2	101.10 ±	12.2	88.28 ± 10.70	12.1	105.71 ±	12.75	99.62 ± 12.33	12.35
20	90.89 ± 1.49	1.64	110.92 ± 4.94	4.46	110.92 ± 6.52	5.88	104.24 ± 10.71	10.27
200	97.71 ± 1.35	1.38	105.97 ± 1.0	0.94	114.45 ± 3.04	2.66	106.04 ± 7.28	6.87
1000	101.58 ± 1.21	1.19	109.43 ± 2.68	2.45	113.41 ± 2.68	2.37	108.14 ± 5.5	5.08

Table 4: The extraction and recovery (Mean ± SD (%CV)) of 6A1, 6A1 glucuronide, and 6A1 sulfate compounds for blood, colonic mucosa and liver tissue at LLOQ and three QC concentrations

		Blood	
Concentration ng/mL	6A1 Mean ± SD (%CV)	6A1 Glucuronide Mean ± SD (%CV)	6A1 Sulfate Mean ± SD (%CV)
2	97.6 ± 5.78 (2.99)	94.31 ± 1.98 (2.08)	98.97 ± 5.00 (2.39)
20	95.02 ± 1.02 (5.00)	96.70 ± 2.22 (2.3)	96.17 ± 2.12 (2.5)
200	99.59 ± 2.81 (2.82)	96.55 ± 2.15 (2.23)	101.32 ± 2.73 (2.67)
500	99.29 ± 1.87 (1.88)	100.16 ± 2.26 (2.26)	96.30 ± 3.65 (4.11)
1000	102.4 ± 4.13 (4.03)	108.41 ± 4.11 (3.79)	93.29 ± 1.65 (1.77)
		Mucosa	
ng/g	6A1	6A1 Glucuronide	6A1 Sulfate
2	103.85 ± 2.40 (2.31)	92.48 ± 2.58 (2.79)	94.07 ± 2.36 (2.51)
20	102.9 ± 7.99 (7.77)	91.71 ± 2.71 (2.96)	97.21 ± 11.2 (11.52)
200	102.02 ± 3.61 (3.54)	96.63 ± 6.32 (6.54)	97.56 ± 4.09 (4.19)
500	99.41 ± 1.04 (1.05)	98.45 ± 4.08 (4.14)	103.94 ± 3.08 (2.97)
1000	100.28 ± 6.40 (6.39)	96.87 ± 3.42 (3.53)	95.24 ± 6.03 (6.62)
		Liver	
ng/g	6A1	6A1 Glucuronide	6A1 Sulfate
2	93.67 ± 2.59 (2.77)	111.96 ± 6.04 (5.4)	108.62 ± 1.40 (2.77)
20	95.93 ± 1.47 (1.53)	109.01 ± 5.36 (4.91)	104.82 ± 3.00 (1.53)
200	95.91 ± .79 (.82)	110.39 ± 3.11 (2.82)	102.00 ± 2.23 (0.82)
1000	94.26 ± 1.27 (1.35)	110.72 ± 3.97 (3.59)	98.28 ± 1.89 (1.35)

Table 5: Matrix Effect (Mean ± SD (%CV)) of 6A1, 6A1 glucuronide, and 6A1 sulfate compounds for blood, colonic mucosa, and liver tissue at LLOQ and three QC concentrations

		Blood	
ng/mL	6A1	6A1 Glucuronide	6A1 Sulfate
2	108.10 ± 2.83 (2.63)	80.30 ± 4.62 (5.75)	105.80 ± 6.12 (5.78)
20	101.99 ± 2.63 (2.58)	108.73 ± 2.53 (2.33)	92.69 ± 2.63 (2.84)
200	103.99 ± 0.76 (0.75)	104.83 ± 4.77 (4.55)	103.90 ± 2.71 (2.61)
500	100.66 ± 2.27 (2.26)	95.64 ± 2.54 (2.69)	103.00 ± 4.20 (4.08)
1000	103.97 ± 2.81 (2.71)	99.93 ± 12 (12.01)	108.11 ± 8.54 (7.9)
		Mucosa	
ng/g	6A1	6A1 Glucuronide	6A1 Sulfate
2	108.43 ± 16.17 (14.91)	108.88 ± 17.41 (15.99)	96.70 ± 6.1 (6.31)
20	101.35 ± 12.52 (12.36)	102.93 ± 5.61 (5.45)	100.94 ± 10.08 (9.99)
200	98.96 ± 10.84 (10.97)	102.85 ± 6.90 (6.71)	97.57 ± 5.22 (5.36)
500	95.29 ± 10.9 (11.44)	94.54 ± 8.00 (8.46)	94.5 ± 5.88 (6.22)
1000	98.22 ± 1.65 (1.68)	99.43 ± 6.31 (6.35)	102.50 ± 2.83 (2.
		Liver	
ng/g	6A1	6A1 Glucuronide	6A1 Sulfate
2	88.23 ± 4.61 (5.22)	112.69 ± 9.4 (8.34)	112.75 ± 13.72 (5.22)
20	97.61 ± 8.99 (9.21)	105.28 ± 9.19 (8.73)	108.88 ± 5.4 (9.21)
200	99.56 ± 3.20 (3.21)	99.7 ± 7.38 (7.40)	100.25 ± 4.54 (3.21)
1000	104.54 ± 4.88 (4.67)	100.07 ± 4.44 (4.43)	98.25 ± 6.75 (6.87)

Table 6: Stabilities of 6A1, 6A1 glucuronide, and 6A1 sulfate of blood, colonic mucosa, and liver tissue were evaluated by analyzing triplicates of LLQC and QC samples at three different concentrations following A) 8 h at 25°C bench top (short term stability), B) 3 freeze thawing cycles, C) stored at −80°C for 30 days (−80°C and 25°C), and D) processed sample, autosampler, 20°C for 24 h

A) 8 h at 25°C bench top (short term stability)

		Blood	
ng/mL	6A1	6A1 Glucuronide	6A1 Sulfate
2	98.1 ± 5.63	89.3 ± 5.75	95.0 ± 6.7
20	100.7 ± 3.58	98.7 ± 2.43	92.9 ± 6.4
200	103.9 ± 4.75	100.8 ± 4.55	103.9 ± 5.2
500	100.6 ± 4.26	96.6 ± 4.69	105.0 ± 4.8
1000	101.9 ± 6.71	99.9 ± 11.0	101.1 ± 8.9
		Mucosa	
ng/g	6A1	6A1 Glucuronide	6A1 Sulfate
2	105.43 ± 13	104.88 ± 11	105.70 ± 10
20	102.5 ± 10.3	100.93 ± 6.6	100.94 ± 9.9
200	98.9 ± 6.4	99.2 ± 5.5	97.57 ± 5.4
500	95.9 ± 5.8	94.5 ± 8.0	94.5 ± 5.8
1000	92.2 ± 4.6	94.3 ± 5.3	92.50 ± 3.8
		Liver	
ng/g	6A1	6A1 Glucuronide	6A1 Sulfate
2	87.2 ± 11	110 ± 9.9	89.5 ± 11.2
20	90.2 ± 10.1	104 ± 7.6	98.3 ± 9.2
200	98.6 ± 9.8	97. 4 ± 5.4	102.5 ± 3.2
1000	102 ± 6.5	102. 2 ± 4.3	99.8 ± 3.1

B) 3 freeze thawing cycles

		Blood	
ng/mL	6A1	6A1 Glucuronide	6A1 Sulfate
2	98.10 ± 2.63	89.30 ± 5.75	104.80 ± 6.7
20	102.0 ± 3.2	95. 3 ± 3.7	96.3 ± 4.1
200	99.3 ± 0.8	98.7 ± 0.5	101.4 ± 0.8
500	100.1 ± 2.3	99.7 ± 1.8	104 ± 2.1
1000	105. 1 ± 2.8	98.9 ± 3.5	102.5 ± 3.2
		Mucosa	
ng/g	6A1	6A1 Glucuronide	6A1 Sulfate
2	88.4 ± 5.5	106. 8 ± 6	92.0 ± 9.1
20	98.5 ± 11	102.4 ± 4.3	94.4 ± 6.3
200	99.4 ± 6.3	102. 7± 0.90	97.57 ± 3.2
500	100.5 ± 5.6	98.5 ± 4.4	96.5 ± 4.8
1000	99.9 ± 6.3	97.6 ± 3.2	101.50 ± 3.8
		Liver	
ng/g	6A1	6A1 Glucuronide	6A1 Sulfate
2	87.3 ± 4.5	92.69 ± 7.4	102.5 ± 11.2
20	87.6 ± 3.9	95.28 ± 5.1	101.8 ± 4.9
200	89.5 ± 2.3	99.7 ± 2.8	100.5 ± 2.5
1000	94.3 ± 1.8	99.5 ± 2.4	99.25 ± 2.1

C) Stored at −80°C for 30 days (−80°C and 25°C while thawing)

Blood			
ng/mL	6A1	6A1 Glucuronide	6A1 Sulfate
2	98.10 ± 5.6	88.1 ± 6.6	98.5 ± 5.6
20	99.9 ± 4.6	89.3 ± 5.3	99.3 ± 5.5
200	98.1 ± 0.9	100.83 ± 3.7	101.4 ± 4.5
500	100.66 ± 1.25	98.4 ± 2.6	100.4 ± 3.9
1000	100.97 ± 3.1	99.3 ± 1.2	102.8 ± 4.0
Mucosa			
ng/g	6A1	6A1 Glucuronide	6A1 Sulfate
2	98.4 ± 12	88.8 ± 9.0	96.70 ± 6.7
20	101.5 ± 11	92.3 ± 7.3	100.94 ± 4.5
200	99.9 ± 6.8	102.5 ± 6.3	97.57 ± 3.6
500	97.3 ± 4.3	99.5 ± 5.1	94.5 ± 5.1
1000	98.2 ± 1.9	99.43 ± 4.0	102.0 ± 2.2
Liver			
ng/g	6A1	6A1 Glucuronide	6A1 Sulfate
2	88.3 ± 9.0	92.2 ± 8.1	89.9 ± 7.9
20	98.1 ± 7.1	98.9 ± 5.9	103.8 ± 6.1
200	99.6 ± 4.5	99.8 ± 3.8	101.1 ± 3.7
1000	105.4 ± 3.9	102.7 ± 3.1	98.9 ± 4.9

D) Processed sample, autosampler, 20°C for 24 h

		Blood	
ng/mL	6A1	6A1 Glucuronide	6A1 Sulfate
2	85.5 ± 4.0	87.1 ± 6.5	87.5 ± 5.6
20	89.2 ± 2.9	85.3 ± 3.5	89.3 ± 4.5
200	92.1 ± 3.1	98.83 ± 2.7	86.9 ± 2.5
500	100.6 ± 2.7	99.4 ± 1.6	98.5± 1.9
1000	101.4 ± 1.3	100.3 ± 1.4	91.9 ± 2.1
		Mucosa	
ng/g	6A1	6A1 Glucuronide	6A1 Sulfate
2	86.4 ± 9	87.8 ± 9.0	97.0 ± 6.7
20	91.5 ± 7	90.3 ± 7.3	98.3 ± 4.5
200	96.9 ± 5.9	100.5 ± 6.3	97.7 ± 3.6
500	97.3 ± 5.3	98.5 ± 5.1	96.5 ± 5.1
1000	97.2 ± 3.9	100.3 ± 4.0	101.9 ± 2.2
		Liver	
ng/g	6A1	6A1 Glucuronide	6A1 Sulfate
2	88.3 ± 9.0	94.2 ± 6.1	98.5 ± 9.1
20	98.1 ± 7.1	98.9 ± 2.9	93.8 ± 3.1
200	99.6 ± 4.5	97.4 ± 2.8	99.7 ± 5.7
1000	105.4 ± 3.9	99.7 ± 4.1	96.4 ± 4.6

CHAPTER 4: NOVEL BIODEGRADABLE COATING FORMULATION AND VACUUM SPINNING TECHNIQUE APPLIED TO SIZE 9 HARD GELATIN CAPSULES TO DELIVER A SELECTIVE COX-2 INHIBITOR TO THE COLON OF F344 RATS

4.1. Abstract

The purpose of this chapter was to use a newly-designed selective COX-2 inhibitor (6A1) in combination with a novel coating formulation and technique to deliver a high drug concentration to the colon. Drug powder and image tracers were packed inside size nine hard gelatin capsules (S9C), coated with an inner layer of polylactic glycolic acid (PLGA 8515) with optimum thickness of 115 ± 35 nm for PLGA 8515 and 50 ± 15 nm for ES100 to serve as delayed-release coating via erosion mechanism and an outer pH-sensitive Eudragit S100 (ES100) layer to serve as an enteric coating. Novel vacuum spin coating technique and parameters, as well as new solvent systems, were also investigated. Leading locally bioavailable COX-2 inhibitor's (6A1) pharmacokinetic behavior of S9C were extensively studied in F344 rats. S9C were packed with 6A1 (90% w/w), barium sulfate (5% w/w), and methyl blue (5% w/w), coated and administered via oral gavage to F344 rats. In vivo pharmacokinetic study of coated capsules was performed in conjunction with in vivo imaging. The blood concentrations time profile of the enteric (ES100) and delayed-release (PLGA) coating formulation administered via oral gavage achieved a delayed release beyond 6 hours and above pH 6.8. The ex vivo tissue stain showed the capsule released its contents at the distal gastrointestinal tract, i.e., the colon. Live in vivo images obtained also further validated the S9C released in the colon.

4.2. Introduction

Hard gelatin capsules provide an advantage over other solid dosage forms, in that the raw drug can be packed inside the casing thereby reducing the need for excipients and extensive formulations (146, 147). Hard gelatin capsules are hydrogenated collagen made up of abundant proteins that are readily broken down into amino acids and become available for absorption within hours of ingestions (148).

However, the coating of gelatin capsules is challenging. The smooth gelatin surface causes poor adhesion. Extreme pH or organic solvent usage in the polymer film can cause structural deformity and compromise the integrity of the capsules (149, 150). The application process of enteric and erosion films for the size nine hard gelatin capsule (S9C, 2.71 mm x 8.4 mm with a surface area of 68 mm^2), specifically designed for rodents and guinea pigs, is especially challenging and cumbersome with the conventional pilot study and dip-coating technique. Conventional coating equipment and the specific parameters are also inapplicable to the S9C in small quantities for experimental use. The novel coating technique is crucial for preclinical research and pilot studies where the amount of the new chemical entity is usually limited.

Polylactic-co-glycolic acid (PLGA) and Eudragit S100 (ES100) are two commonly used pharmaceutical excipients that are generally recognized as safe (GRAS) by the United States FDA and the European Medicines Agency. Both excipients are commercially available with different grades of copolymer blends and have been extensively studied

(151, 152). Both PLGA and ES100 are biodegradable materials with abundant preclinical and clinical research that focuses on the drug delivery systems (153). ES100 and PLGA polymers were chosen for this experiment because of their general safety and well-studied use for formulating an enteric and time delayed coatings.

In many fields of science, polymer degradation has been defined as the amount of time the material takes to degrade over its useful life time and nondegradation has been defined as breakdown that occurs after its useful life. In another way, the ratio between the time the polymer takes to degrade and the duration of the application of the polymer is used to determine whether or not the material is degradable (154). PLGA and ES100 used for the coating of enteric and time release capsules undergoes chemical degradation; PLGA also undergoes erosion.

All biodegradable polymers contain hydrolysable bonds where the passive hydrolysis or enzyme-catalyzed hydrolysis breaks down the chemical bond between the copolymers. The hydrolysis degradation occurs via a random chain scission process to form oligomers and finally monomers (155). The enzyme-catalyzed hydrolysis also referred to as biodegradation is when a biological system is partially involved in the chemical bond cleavage.

Most synthetic biodegradable polymers, PLGA and ES100, mainly undergo passive hydrolysis (156). The degradation rate is determined by its chemical bond, composition, the pH of the environment, the water content, and the swelling rate. Degradation begins

with water uptake into the bulk of the polymer matrix, which leads to swelling. Next, hydrolysis occurs resulting in oligomers and monomers degrading from the polymer. Progressively, the degradation changes the microstructure of the bulk, forming pores, where the oligomers and monomers are released. Heterogenous degradation refers to the surface degradation of the polymers whereas homogenous degradation describes a uniform break down of the bulk material throughout its matrix.

Erosion is a more complicated process of polymer degradation in which additional parameters such as the swelling rate and material porosity are involved. Poly (D,L-lactic-co-glycolic acid) three dimensional objects have been shown to exhibit an inverse flux erosion throughout the inner bulk material (154); once degradation begins increases in the degradation rate due to the lactide monomer content serves as an autocatalytic hydrolysis resulting in erosion (155, 157, 158). The PLGA erosion rate can be optimized by adjusting the amount of porosity and the sizes of the micropores within PLGA matrix (159).

PLGA is an excellent biodegradable and biocompatible polymer (153, 160). Varying the ratios of lactic to glycolic acid controls the rate of water cleavage. Lactic acid contributes to the rigidity of the polymer backbone, thus increasing the duration that the polymer remains within a biological system (161). How it was degraded? The primary mechanism for degradation of PLGA is the hydrolysis of the ester bond between the lactic acid and glycolic acid.

The PLGA 85:15 grade was chosen based on its rapid ability to provide scaffolding support for the hard gelatin capsule after it has become wet in the coating process, thereby preventing collapse of the capsule. PLGA 85:15 also allows for successive coating applications.

Eudragit S100 (ES100) is an anionic copolymer composed of methacrylic acid (MAA)-methyl methacrylate (MMA) at a 1:2 ratio. ES100 pH dependent nature were finely tune by the number of negative charge on the MAA's COOH functional group at basic condition (162). The hydrophobicity MMA units were realized by synthesizing co-polymer libraries with a systematic variation. ES100 is soluble in alkaline digestive fluids by salt formation (163, 164). A clinical study shown that a 5% W/W gain of the coated Eudragit S100 tablets (84 ± 4 micron) (64) release its content in the colon in 67% of volunteered subject.

A disadvantage noticed when using ES100 is the brittleness of the film as the total polymer weight increased. As such, the manufacturer recommended as much as 25 % addition of plasticizer into the formulation to increase flexibility (supplemental S4). However, the addition of plasticizer changes the dissolution profile and takes longer for the film to dry (165). Therefore, there is a need to develop alternative coating techniques to limit drying time, maximize polymer mass loading to 10%, and limit the use of plasticizer while achieving uniformly smooth, defect free films.

Coating is the process of adding an outer layer of material to the surface of a substrate. There are many pharmaceutical coating techniques including conventional pan (involves coating capsules with a sprayed-on solution), fluid bed, dry powder (solvent-less) coating that utilizing an electrostatically charged powder, supercritical fluid, and supercell coating technology. Substrates in fluid-applied coating technique sequentially transition through the following stages - fresh running solution, semisolid, sticky film, and dry film. Criteria for a successful coating technique would be little or no visual defects, no functionality defects, ease of production, and simplified operations. Unfortunately, not a single coating technique above meets all the criteria for all applications. Some coating techniques are more advantageous than others in certain applications as described below.

A conventional pan coater and the fluid bed coater used a spraying nozzle in combination with air injection to suspended and coat the capsules in a large batch. One disadvantage in the techniques is its stringent parameters such as the mass of the polymer dissolved in the spray solution is limited to 3% of the total capsule's weight to ensure even drying and prevent intense, sustained attrition that leads to abrasion and chipping of the coated film. Liquid solution coatings require a large amount of energy and high temperatures to evaporate solvent used, often resulting in an undesirable appearance of the film formed as well as degradation of the thermos-labile drugs. Liquid solution coatings had lengthy processing and drying durations. The dry powder, solvent-less coating techniques such as the electrostatic dry coating relieve manufacturers of the above challenges. A critical challenge of this method is the precise parameters required to obtain a desirable film as

well as avoiding supercharging of the substrate that could destroy the drug within the capsule. Finally, the cleanliness of the substrate, high impact force, the heat generated within the chamber sometime led to uneven thickness, void space, and multilayers deposition of the films. Other disadvantages to these techniques are the requirements of a large amount of bulk material, expensive equipment, and a trained technician. Faced with the aforementioned challenges, conventional coating techniques are not applicable to the research settings.

This research investigated three different coating techniques- dip coating (control), fluidic coating (technique 1), and the novel vacuum spin coating (coating technique 2). The parameters used to judge each technique were: smoothness of the film, reproducibility, and ease of clean up. Of the three, vacuum spin coating yielded the most optimal results.

Vacuum spin coating is one of the most common methods for applying thin films to substrates (166). A wide variety of technology sectors and industries commonly use vacuum spin coating. Vacuum spin coating's advantage is its ability to rapidly and easily produce consistently uniform films, ranging from a few microns down to a nanometer of thickness. Organic electronics and nanotechnology heavily rely on spin coating, and they had advanced many of the techniques that are used in other semiconductor industries to a more advanced level.

The vacuum spin coater apparatus works based on two physical properties. The first was an application of a vacuum that creates a shear force to facilitate the spread of the non-

Newtonian polymers throughout the 3-dimensional capsules. Secondly, the capsules were spun. As the capsule accelerates in rotation, it expulses all the undissolved polymer. Once the spin coater's RPM reaches its desired speed and the polymer fluid was sufficiently thinned out, viscous shear drag exactly balances the rotational accelerations, drying begins. Next, the capsule was spun at a constant rate, 500 RPM, and solvent evaporation dominates the coating thinning behavior. At this point, the rate of evaporation depends on two factors (a) the difference in the partial pressure of solvent evaporation between the free surface of the liquid layer and the gas layer flowing nearby (surface tension) and (b) the capillary forces developing in the channels between the latex particles. During the evaporation stage, the dissolved polymers solidified at the liquid-air interface in a highly viscous, lowly diffusive layer forming an unbroken film on the skin of the capsule (151).

4.3. Materials and Methods

4.3.1. Materials

LC-MS grade acetone, ethanol, methanol, dichloromethane, isopropanol, DI water, barium sulfate of 99.99% purity were purchased from Sigma-Aldrich Corp. (St. Louise, MO, USA). Ester-terminated DL-PLGA of 85:15 (PLGA 8515) were purchased from (Lactel Absorbable Polymers, Birmingham, AL). Evonik RÖHM GmbH (Darmstadt, DE) generously donated Eudragit S100 (ES100). Methyl blue, certified by the biological stain commission, M5528-25G, was also obtained from Sigma-Aldrich Corp. Size 9 capsules (S9C) were purchased from Torpac Inc. (Torpac Custom capsules & capsule fillers, 333

Route 46, Fairfield, NJ 07004, USA). The parent compound, 6A1, and 6A1 sulfate were synthesized in house and quantified at 98% pure using the UPLC and NMR. 6A1 glucuronide was biosynthesized using Hela-UGT1A9 cells, purified, and quantified at 98% pure using the previously established methods.

4.3.2. Preparation of Capsules

The hard gelatin capsules were visually inspected for shape and coloration, then weighed and selected for use if their weights were within 2 - 5% of the expected range. The drug powder (with 5% w/w barium sulfate 5% w/w and methyl blue) was packed into the capsules using the funnel and pestle kit sold by the vendor. The total weight of capsules and drug blend was monitored within a 3% range of drug packing of 20 mg. A trace amount of pH nine water (~2 µl via a pipette tip) was used to seal the body and cap. The sealed capsules were allowed to dry for 24 hours before any coating materials were applied (Figure 12).

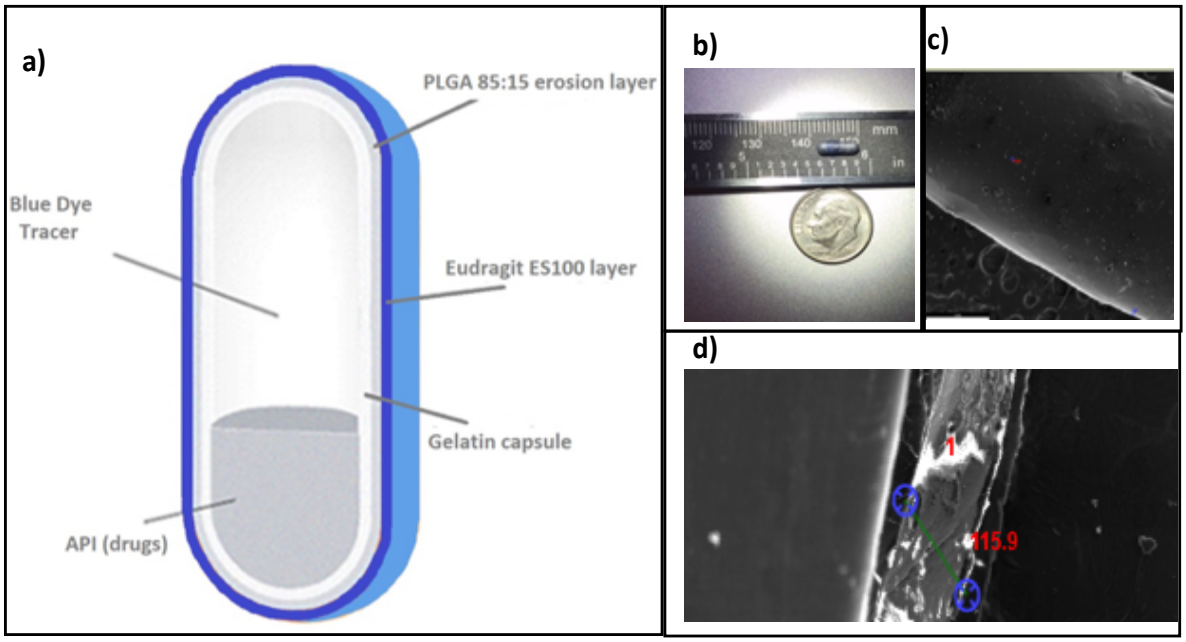

Figure 12: a) schematic of capsule coating layers, b) capsule's respective size compared to a dime; c) SEM topography view of coated capsules (40X magnification); d) thickness of coated capsule obtained from SEM side view given thickness of 115 ± 35 nm for PLGA 8515 and 50 ± 15 nm for ES100 (80K X magnification).

4.3.3. Factorial Solvent Design to Dissolve PLGA8515 and ES100

Full factorial designs were used to optimize the solvent systems used to incorporate PLGA 8515 and ES100 *(JMP 14 DOE, SAS Institute Inc. 100 SAS Campus Drive, Cary, NC 27513-2414, USA)*. The three continuous factors were: 50–80% for acetone, 5-15% for isopropanol, and 2-5% for deionized water. The responses were: minimal time takes for a single coat applicant to dry and the maximum optimal polymer weight dissolved in certain solvent systems. Such constraints allow for practical application (single polymer, single application) as well as efficient drying between successive coats (Figure 13).

A

SOLVENT SYSTEM

SOLVENT SYSTEM
Design Full Factorial
Screening
Model
Columns (6/0)
Pattern
ACETONE *
IPA *
WATER *
Rows
All rows 8
Selected 0
Excluded 0
Hidden 0
Labelled 0

	Pattern	ACETONE	IPA	WATER	TIME POLYMER DRY	MAXIMUM POLYMER ADDED
1	−−−	50	5	2	4	8
2	−++	50	15	5	17	10
3	++−	80	15	2	7	10
4	+++	80	15	5	10	13
5	+−−	80	5	2	3	10
6	−+−	50	15	2	15	10
7	−−+	50	5	5	8	13
8	+−+	80	5	5	6	14

B

Source	LogWorth	PValue
IPA(5,15)	1.343	0.04540
ACETONE(50,80)	1.152	0.07045
WATER(2,5)	0.978	0.10514
ACETONE*IPA	0.978	0.10514
IPA*WATER	0.427	0.37433
ACETONE*WATER	0.152	0.70483

Figure 13: Factorial screening design for ES100 solvent system with inputted empirical values (A). ES100 solvent system effect summary correlating the PValue set at 0.05 to logworth value (-log of PValue) of 1.30 (B).

4.3.4. Parameter Use for Coating of Capsules Vacuum Spin Coating

It was critical to clean and dry the vacuum spinning plates before coating each batch. The sealed capsules were then wetted with mild basic water (pH 9 NaOH 0.1 mM) and loaded into individual pods within the vacuum spinning plates. 50 µL of PLGA 8515 10 % solution was added into the individual pod, vacuum applied, and allowed the plate to spin for 30 seconds at low spinning speed (100 RPM). The pod spinning rate was increased to 500 RPM and spun for 15 minutes. A successive coat was applied by adding 50 µL of Eudragit

S100, applying vacuum, spinning for 30 seconds at a low spinning rate of 100 RPM, and followed by a spin rate of 500 RPM for 15 minutes. The capsule was sufficiently dried to be transferred into an individual micro-Eppendorf vial with a lid left open and allowed to stay in a desiccator for complete drying over 24 hours (Figure 14).

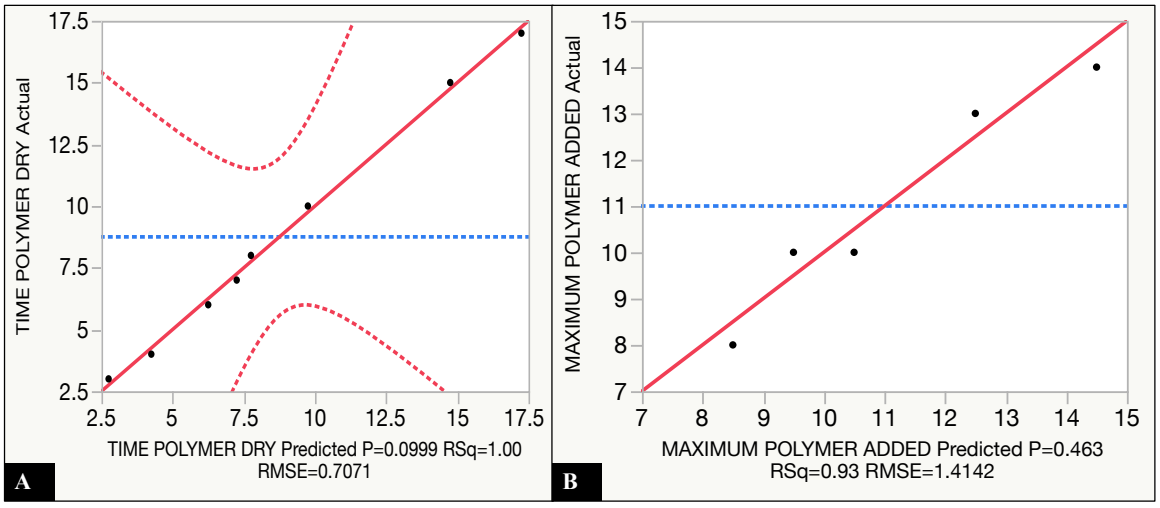

Figure 14: Predicted value and empirical data input generated models to predict ES100 polymer drying time and mass added with R^2 correlation value above 0.93. The ordinary least square model for predicting the polymer drying times is more powerful than the model used to predict the polymers' mass load based on the square root of the variance residuals observed RMSE values (0.7071 and 1.4142). RMSE was the square root of the observed variance residuals. The smaller the RMSE value, the closer the predicted value was to the real value.

4.3.5. Appearance and Quality Control Parameters of Coated Capsules

After each successive coating, a visual inspection of individual capsules was performed using a 3.5X-90X zoom trinocular microscope (AmScope, SM-1TSZ-V203); close observations were made to look for wrinkles, craters, and asymmetry (Figure 15). A

different sheen was observed comparing between the coated and uncoated S9C. The coated capsules were weighed, and the total mass gain was then used to calculate for the estimated thickness. The predicted thickness of the capsule was based on the below equation. The capsules were rejected if they were not within the ± 2.5% of the expected thickness (150 nm) based on mass gained.

$$\text{Thickness} = \sqrt[2]{\frac{total\ weight\ after\ 24\ hours\ dried - weight\ of\ drug\ and\ capsule}{68}} \quad \textbf{\textit{(Equation 5)}}$$

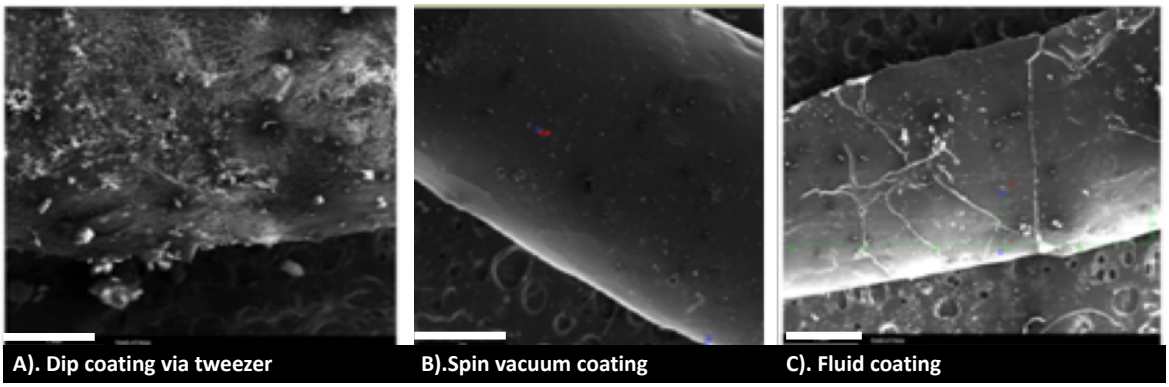

Figure 15: SEM topography images of dip coating (6A), vacuum spin (6B), and fluid coating technique (6C). All pictures had a 1 mm scale bar at 40X magnification.

4.3.6. Thermogravimetric Analysis (TGA)

Films of PLGA and DSC applied to capsules an hour prior were peeled and stamped to fit the aluminum pan. Approximately 10 ± 1 mg of each polymer film per sample was used. Randomized, triplicate films were tested. The TGA curves (Shimadzu, TGA50-H) acquired from temperature ramping rate were 10 °C min^{-1} from room temperature (~ 20°C),

held for 30 seconds at 30°C, and steady ramping till 500°C. Formulation consistency across all formulation batches was determined via the % weight loss curve.

4.3.7. Differential Scanning Calorimetry (DSC)

The DSC equipment (Shimadzu model DSC-60A) was programmed to heat the peeled films from coated samples within a range of room temperature (~ 20°C) to 500°C, at a heating rate of $10°C \cdot min^{-1}$. An aluminum, sealed sample holder was used. Reference sample contained an empty but crimped aluminum pan and lid. Nitrogen was utilized as the flowing gas, at a rate of $10\ mL \cdot min^{-1}$. The mass of the analyzed samples was 10 ± 1 mg (167).

4.3.8. Scanning Electron Microscopy (SEM)

The topography and thickness of randomized samples was inspected by using a scanning electron microscope (SEM, TM3000 tabletop microscope, Hitachi). Three (3) PLGA+ES coated capsules that passed the mass gain quality control step were chosen at random for every 24 coated capsules and dissected into two halves longitudinally. SEM images were obtained using the following operating parameters: 5.0 kV voltage, 4 mm working distance, and 10^{-6} millitorr vacuum. The side views of the capsule halves were captured at an 80,000x magnification and used to measure the coated films' thickness. Due to the excessive charging of the polymer substrate, the samples were coated with graphene prior to SEM imaging.

4.3.9. In Vitro Dissolution of Coated Capsules

The in vitro dissolution test for the coated capsules was performed, in accordance with the recommendation from UPS compendial dissolution, non-sink conditions (168). The simulated intestinal pH was adjusted via 2.5 µmol / L of HCl or NaOH from the 2.5 µmol / L of phosphate buffer. 1 mL of samples were collected every half hour, and the pH exposure and duration were as follows: 1.5 hours at pH 1.2 (stomach), 2.5 hours at pH 4.6 (small intestine), 2 hours at pH 6.8, 2.5 hours at pH 8, and 2.5 hour at pH 6.8. Each capsule was placed within a sinker housing, and the stirrer rate was set at 80 rpm (169) at 37 ± 2 °C. Samples at an extreme pH were air-dried, reconstituted, and neutralized before analysis. Drug concentration (6A1) was determined using the UPLC MS-MS method that was previously validated.

4.3.10. In Vivo, Ex Vivo, Live Imaging Study of Coated Capsules

Male Fisher F344 rats (6–10 weeks, body weight between 250 to 280 g, n = 12) were used. Rats were kept in an environmentally controlled room (temperature: 25 ± 2 °C, humidity: 50 ± 5%, 12 h dark-light cycle). Capsules were administered at a dose of 5 mg/kg via oral gavage. The study used two groups fed rats (administered control uncoated capsules vs. coated capsules) that were cage mates. Blood samples (about 20 –50 µL) were collected into heparinized tubes at 0, 0.5,1, 3, 5, 7, 10, and 24 hours post-dosing via tail snip with isoflurane as an anesthetic. All collected pharmacokinetic blood samples were stored at −80 °C until analysis.

The Perkin Elmer IVIS Lumina III XRMS in X-ray (40 kVp, 100 mAmps, 10 seconds) and photograph modes was used to image the capsules containing barium sulfate (specific settings and data acquisition can be found in greater details in Supplemental S5). The X-ray source was via the tungsten anode lamp. No hair removal was needed. The animals were anesthetized via the induction chamber with constant isoflurane feeding, weighed, manually transferred to the IVIS Lumina imaging system, and constantly fed isoflurane via the adaptor nose cone built within the imaging chamber. The animals were secured in individual pods. The pod could be rotated via a computer control interface. The position/sedation of animals was controlled via a live camera built-in within the chamber. At time: 0 (n=1), 2 (n=1), 4 (n=1), 6 (n=1), 8(n=1), 12 (n=3) hours, the IVIS Lumina III XRMS (170) was used to track the location of the capsules and the rats digestive tissues' were excised at the end of each time point to examine the intestinal tissue of methyl blue stains. The control group uses uncoated hard gelatin capsules. In vivo transit time and the capsules' release profiles were also monitored periodically during the pharmacokinetic study. The imaging group's (Group 1) animals were cage mates to the pharmacokinetic study group (Group 2) as to eliminate confounding factors (Figure 16).

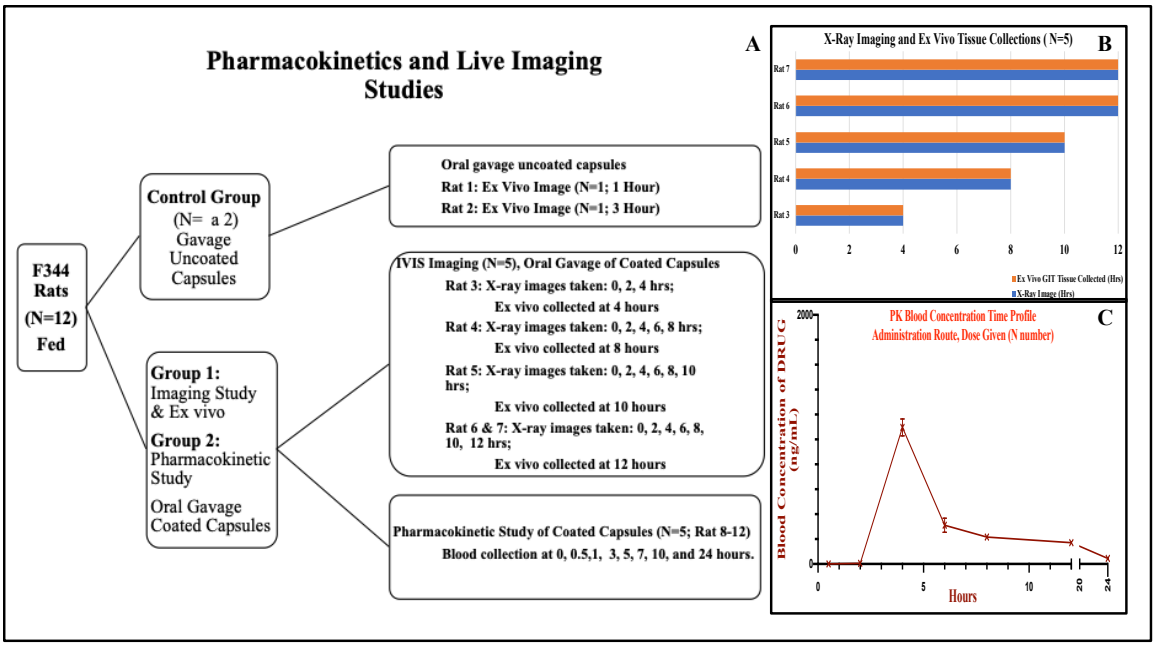

Figure 16: Study design for the pharmacokinetic, ex vivo, and live imaging study of enteric and delayed release coated capsules (dose = 5mg /Kg; n= 12). The control groups (n=2) were gavage uncoated size 9 capsules (S9C) and sacrificed at 1 and 3 hours post dose. Group 1 (n=5) were oral gavage coated S9C and the ex vivo tissues were collected at 4 (n=1), 8 (n=1), 10 (n=1), and 12 (n=2) hours post dose to examine the location and condition of the S9C. Group 2 (n=5 were cage-mates of Group 1 cohort) blood samples were collected at 0, 0.5, 1, 3, 5, 7, 10, and 24 hours post dose (purposefully off set the imaging time so as to reduce unnecessary stress to animals).

4.3.11. Statistical Analysis of Results

The blood concentration-time profiles of 6A1 of each subject (n=6) were analyzed by a noncompartmental method using WinNonlin® 6.1 (Pharsight Corporation, Mountain View, CA, USA). All statistical analyses were performed using the GraphPad Prism 8.0 program (GraphPad Software Inc., San Diego, CA, USA).

4.4. Results and Discussion

4.4.1. Design and Selection of Solvents for Capsule Coating Solution

A full factorial screening design with an extreme vertexes option was used (Figure 13A). The PValue, the likelihood that each solvent was significant, was set to 0.05 resulting in a Logworth of 1.30 (LogWorth is the -log (PValue)). The results indicated that the addition of isopropanol into the acetone:water mixture was significant and could not be omitted (PValue: 0.045; LogWorth: 1.34). There was no confounding factor between the solvents, namely the interaction between IPA:water, acetone:PA, and acetone:water (Figure 13B). However, the concentration ratio of IPA to acetone was more significant than IPA to water (Figure 16A). The R^2 linear fit of the theoretical predictive model to the empirical values was 1.0 for the time needed to dry using the redesigned solvent mixture (Figure 14A); the R^2 of the maximum amount of polymer added to the same solvent mixture was 0.93 (Figure 14B). Together, the predictive models indicate that the most desirable ratio of a solvent system for dissolving 11% of Eudragit S100, with a drying time of 8.75 minutes, was 60:10:3.5 (acetone: IPA: water, Figure 17). Because the water's PValue falls within the range of a significant 0.05 to an insignificant 0.1, its significance cannot be entirely ignored. The summary output showed no confounding factors between IPA to water and Acetone to Water. Again, the Logworth did not conclusively exclude confounding factors between acetone and water. Based on the cumulative results and the positive desirability simulated, water was included in all future formulations.

The prediction profiler was set and selected with maximum desirability of polymer mass loading (7.0 – 15%) and minimal time needed to dry (5.5 – 12 minutes) as constraints. The negative slope of polymer drying time to the increasing amount of acetone (Figure 17A) means that the addition of acetone to the formulation positively impacted the drying time of film; it took less time to dry the coated film. The positive slope of polymer drying time (Figure 17B) to the increasing IPA within the formulation suggested an increase in the amount of drying time to the film. Water had a negative effect on the formulation drying time but of lesser magnitude compared to IPA. The positive slopes of the profilers (Figure 16D and 16F) demonstrated that by increasing the ratio of acetone and water, an increased amount of polymer could be added to the system. Increasing the ratio of IPA decreased the amount of polymer that can be added (Figure 17E) implying that IPA has negative desirability to the amount of polymer dissolving within the system.

IPA was not excluded from the formulation even though it has an overall negative desirability based upon a visual inspection. A solvent system without IPA was observed to have excessive crater defects and be less smooth compared to the solvent system with 10 % IPA. Thus, IPA was incorporated into all future solvent systems.

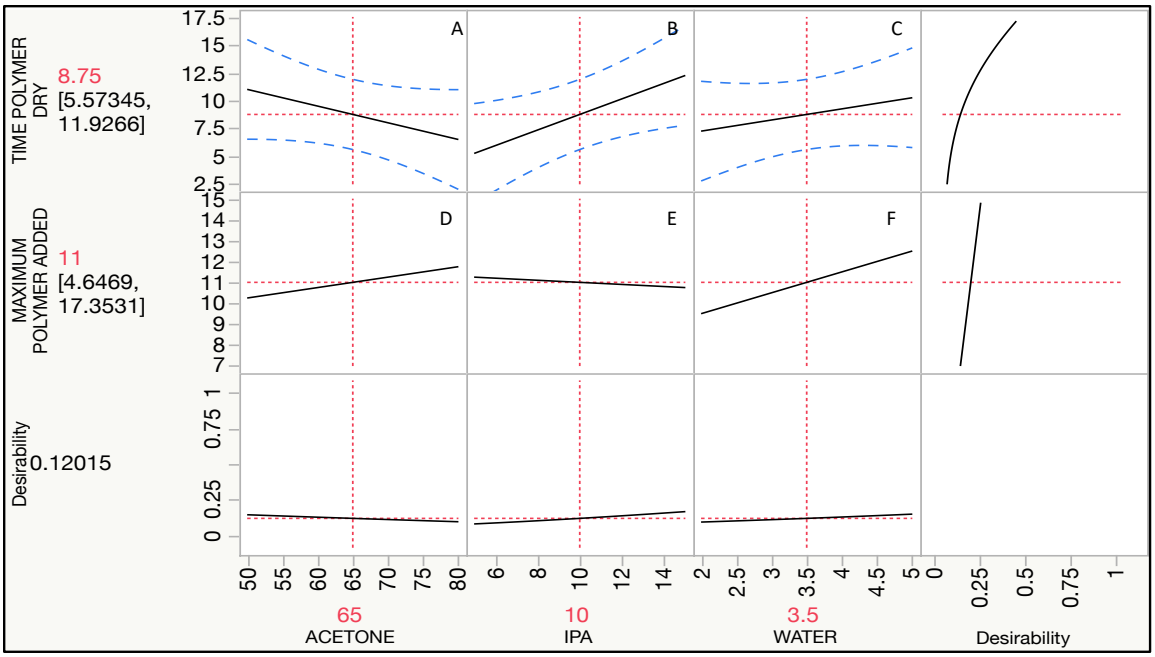

Figure 17: Factorial Screening Design via JMPDoe14 results show that the ES100 system was optimal at 65: 10: 3.5 acetone : IPA: DI water at 11% polymer weight, and 8.75 minutes drying time has the highest desirability.

4.4.2. Determination of Parameters Used for Vacuum Spin Coating of Capsules

Three different coating approaches were investigated. The dip-coating approach suffers from a serious drawback; the polymer becomes fuzzy at the holding and capsule contacting points (Figure 15A). The defective non-uniform coat surface contributed to a larger variability in the release of drug powder and tracers contained within the capsule. The vacuum spin coating approach successfully met the surface uniformity and apparent smoothness requirements (Figure 15B). The fluid coating approach also suffered from drawbacks such as excessive surface wrinkles (Figure 15C). A typical sample of the capsules that were coated by the fluidic coater can be seen in the right SEM image. The

cleaning steps, unclogging polymers, and the extended soaking of the capsules led to an excessive amount of wrinkle formation. Thus, the fluid coating approach was abandoned.

The new vacuum spin coating technique (Figure 18) achieved an 88% success rate, a total of 36 of the 40 capsules made via the novel technique passed the in-house quality assurance tests- smoothness of surface appearance, weight gained, thickness measurement, and in vitro dissolution. The approach proved vacuum spin coating was a superior choice for coating S9C (Figure 7A-D). The optimal PLGA 8515 inner erosion coat was made of 115 ± 35 nm PLGA 8515, and the optimal thickness of the pH-sensitive enteric coat was 50 ± 15 nm Eudragit S100. Different PLGA thicknesses were also investigated. PLGA 8515 layers that were thinner than 100 nm showed insufficient scaffolding support for S9C and had structurally deformed surface upon successive coating and drying. A PLGA 8515 film thicker than 150 nm failed to release its content at the targeted time. ES100 thickness also has some impact to the time taken the capsule to release its content; however, an imperfection in the coating layer of ES100 was not observed via the vacuum spin coating technique.

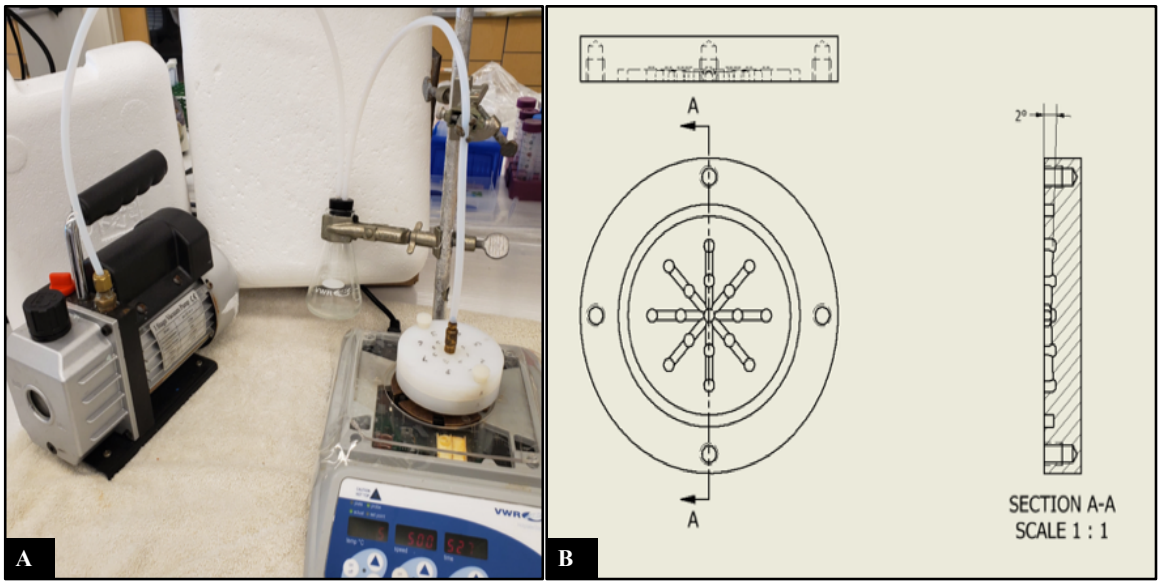

Figure 18: A) Novel vacuum spin coater (10 Pa vacuum, 500 RPM spin rate) capable of coating 8- 16 capsules in 30 minutes (with an 88% success rate); B) blueprint drawing of spinning plates.

4.4.3. Determination of Quality Control Parameters of Coated Capsules

4.4.3.1. Thermogravimetry Analysis (TGA)

Thermogravimetry analysis is the measurement of the weight loss curve with the response to temperature ramp. Here, the TGA was used to determine the total solid mass of the polymers' formulation and its consistency across each formulation batch used for each coating. The first steep drop in the weight loss occurred very early and at a relatively low temperature of 20 to 40 °C. The limited loss was accepted, as the weight loss occurs due to the dehydration of solvents. A second weight loss ~10% between 370 to 375°C was the final solid mass of the bulk polymers (Figure 19A-B). Compared to the solid materials, both PLGA 8515 and ES100 represented, on average, 9-10% of the formulation by weight.

The TGA also provided a general clarification regarding the nature of the polymer formulation decomposition's nature. The mass loss across each triplicate run for the materials remained consistent with respect to the onset temperature and duration, and the decomposition of both materials reflected in the total weight loss correlated with the decomposition of the materials' solid weights; thus, the results indicated that the solvents used to dissolve the polymers did not cause any physio-chemical reaction. Data acquired were consistent with published data (151) and in house historical data (Figure 19C-D).

4.4.3.2. Differential Scanning Calorimetry (DSC)

DSC was used to determine the integrity of dried polymer solutions for possible chemical oxidation and crystallization via inspection of the glass transition temperature (Tg)(167). Indium was used as the calibration standard for the DSC's temperature probe (Figure 19). ES100 had a small glass transition point at 175 °C. When overlaid with the ES100 dried film to that of solid power, the two curves (ran in triplicate) had the same pattern and was consistent with the published data (171). The DSC curves for both the PLGA 8515 solid and dried film presented a glass transition temperature (Tg) of 45°C, which agreed with the literature (161, 172). Both DSC and TGA confirmed that the solvents did not cause oxidation or phase changes to the polymers as to compromise its integrity (173).

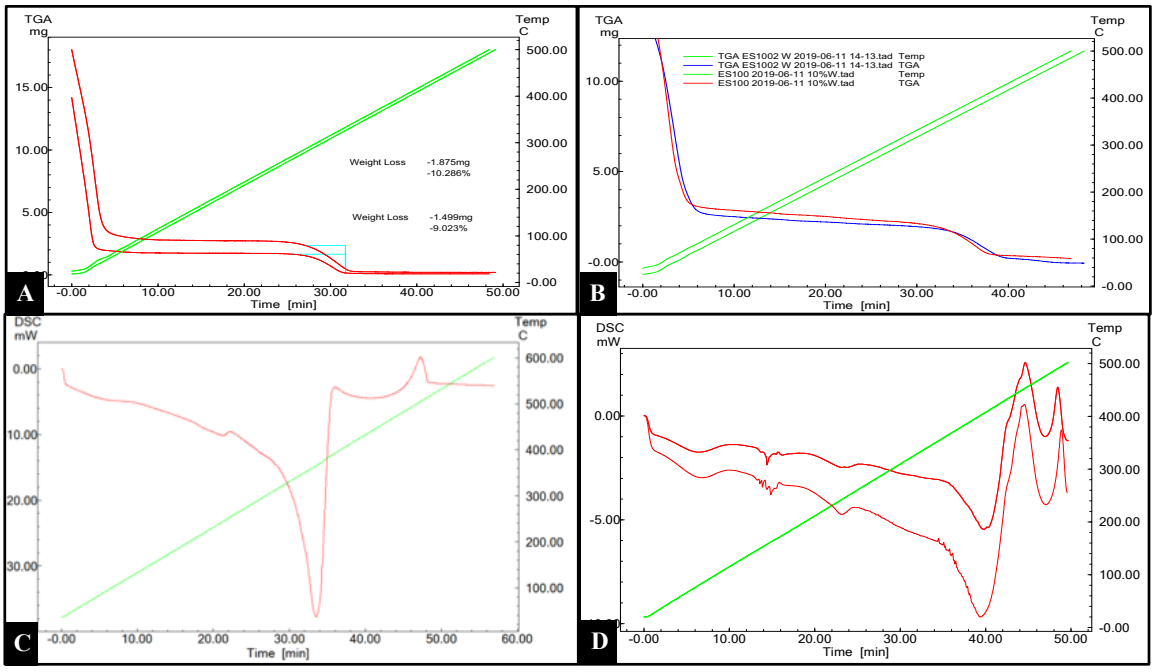

Figure 19: Thermogravimetry analysis and Differential Scanning Calorimetry Determination of Quality Control Parameters of Coated Capsules A) TGA of one month old PLGA versus newly formulated PLGA (9.023% vs 10.286%) ; B) TGA of 1 month old versus newly formulated ES100 with no substantial solvent loss displayed by the consistent mass loading and the ratio of solvent (first weight loss) to total solid mass (second weight loss) with respect to temperature compared between two samples (analyzed in triplicates); C) DSC curve for PLGA 8515; D) and DSC curve for ES100. Both DSC curves show a small glass transition, endothermic peak, and exothermic temperatures are consistent with historical data.

4.4.3.3. In Vitro Dissolution of Coated Size 9 Hard Gelatin Capsules (S9C)

The in vitro, pH-dependent dissolution profile of S9C containing 6A1 was investigated in a buffer with gradually changing pH to assess the ability of coated layers to protect the content from the acidity and accomplish an effective delayed-release delivery in neutral pH values (163). 6A1 was not released in the medium at pH 1.2 and 4.5 (<15% released) (Figure 20), suggesting that the capsules would not release their contents in the stomach.

Once the pH reached the value of 6.8, 6A1 was rapidly released within 21 minutes and completely emptied the drug content within two hours. One quality-control capsule that was rejected based on an in-house quality control criteria was also found (red curve, Figure 20). The dissolution test indicated the capsule failed to achieve acid resistance, and the delayed-release mechanism might have been caused by a thinner coating of material being deposited. Most of the coated capsules began the release of 6A1 at a pH of 6.8 and six and a half-hour after initial PBS exposure (Figure 20). The visual methyl blue stain results also confirmed the enteric and delayed-release mechanism of the coated S9C. Methyl blue packed inside coated S9C had spread into the medium beginning approximately 6 hours after initial PBS buffered exposure (Figure 20A). The methyl blue vortex tail was more apparent at 6 hours and 21 minutes (Figure 20B) and the capsule shell of completely emptied S9C were observed at 7 hours and 12 minutes (Figure 20C). Values from a student t test performed using the quantified amount of 6A1 samples collected during the dissolution test yielded insignificant differences within the seven S9C. The concentrations of 6A1 were determined using a previously established and validated UPLC-MS/MS method (174).

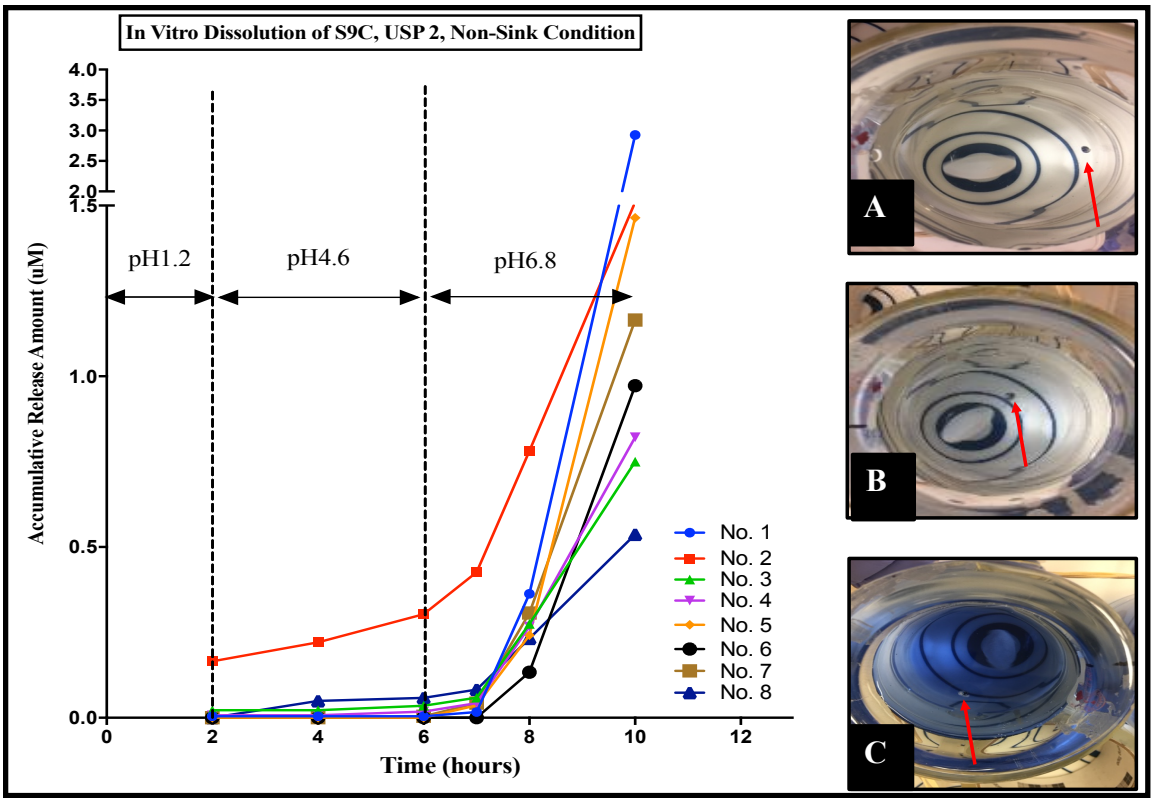

Figure 20: In vitro dissolution test performed for 7 coated S9C and one QC failed S9C (10% PLGA 8515 inner coat and 10% Eudragit S100 as pH-sensitive coat). Inset: A) Capsule showed indications of breakage 6 hours after initial PBS buffered exposure; B) Observed methyl blue trail leakage into medium 6 hours and 21 minutes after initial PBS buffer exposure; C) empty capsule shell remained 7 hours and 12 minutes after initial PBS buffer exposure at pH 6.8. The 6A1 concentrations were determined using previously established UPLC MSMS method.

4.4.4. In vivo and ex vivo imaging study of coated S9C

Coated S9C appeared as bright spots on the μ-CT IVIS images that were obtained by overlaying the X-ray and photograph modes; the coated material did not appear to interfere with the X-ray imaging agent, $BaSO_4$ (Figure 21A). For the first two hours, the coated S9C were visible in the stomach of group one and were not visible within the intestinal tract until four hours after gavage (Figure 21B-C). Many smaller bright spots were observed in the ceca and colons of the remaining animals in group one (Figure 21D). Eight hours post gavage, the S9C were not visible within the intestinal tract (Figure 21E-F). The disappearance of the image tracer can be explained by an insufficient amount of $BaSO_4$ density concentration at a location to provide positive X-ray contrast. In general, barium (atomic number 56) is an oral X-Ray contrasting agent specifically used to delineate the gastrointestinal tract in both preclinical and clinical settings (175, 176). Due to barium's toxicity, barium sulfate, an inert insoluble barium-complex given as an oral slurry is often formulated to a specific gravity of 1.5 density (mass/oral suspension concentration) for positive X-Ray capturing (177). Due to the depth of the tissue and air gap within the abdominal cavity, the disappearance of the capsule after 8 hours might have been caused by the S9C emptying its contents or becoming diluted with fecal matter thus lowering the barium density below the detectable concentration.

Upon examining the ex vivo tissue samples of the intestinal tract, the methyl blue stains were indicative of the S9C's location (178, 179). In the control group that were given uncoated S9C, one hour after oral gavage, the methyl blue mass was still in the stomach and mixed with chyme (Figure 21G). Three hours after oral gavage, the blue stains had passed the duodenum and were visible in the jejunum in the second control animal (Figure 10H). Contrarily, upon examining the ex vivo gastrointestinal tract of group one, which were given coated S9C four hours after oral gavage, no blue stains were visible from ruptured S9C (Figure 21I). The ex vivo ceca were extensively stained eight hours after oral gavage when examining the gastrointestinal tract (Figure 21J and supplemental S6). At 10 hours after oral gavage, ex vivo examination showed partial stains of the cecum and complete blue stains of the colon (Figure 21K). The remaining two animals from group one excreted blue-stained fecal pellets at ten hours, and the remnants of PLGA 8515's stringy material, as well as capsule shells, were visible at 12 hours after oral gavage (Figure 21L-N and Supplemental S3). The ex vivo tissues confirmed that the S9C had released most of its contents in the colon between six and eight hours after oral gavage.

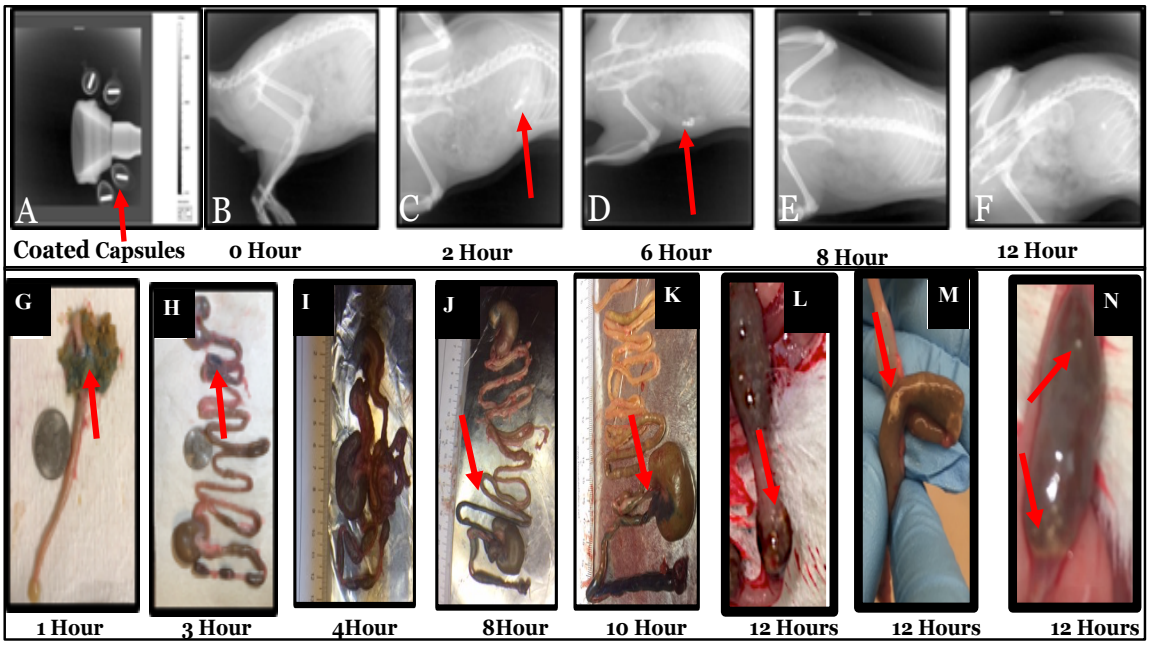

Figure 21: In vivo and ex vivo imaging study of coated S9C. Top panel: A) μ-CT IVIS image obtained of capsules packed with barium sulfate (bright spots). The coated capsules do not appear to interfere with the x-ray imaging agent, BaSO4. B) 0 hour after gavage, capsules are not visible within the intestinal tract; C) 2 hours after gavage, capsules visible (bright spot) within the stomach; D) 6 hours after gavage, smaller bright spots observed in colon; E) 8 hours, capsules are not visible within the intestinal tract; F) 12 hours (n = 3), capsules are untraceable within the intestinal tract. Bottom Panel: G) Ex vivo imaging of uncoated SC9 control animal's stomach showed methyl blue stains indicate the location of capsules 1 hour after oral gavage; H) 3 hours after oral gavage, the blue stain passed the duodenum and was visible in the jejunum; I) 4 hours after gavage, ex vivo intestine has no visible blue stain of the coated capsules group; J) At 8 hours after gavage, ex vivo cecum had extensive methyl blue staining; K) At 10 hours, ex vivo showed partial staining of the cecum and complete blue staining of colon; L, M, and N) are 12 hours after coated S9C were given, some remnants of undissolved polymer film fragments and capsule shells were visible and mangled in the forming fecal pellets. Some blue stained droppings were also observed (Supplemental S5).

4.4.5. Pharmacokinetic study of the coated S9C

The validated UPLC-MS/MS method was used to determine the blood and tissue concentrations of 6A1, 6A1 glucuronide, and 6A1 sulfate in a pharmacokinetic study

utilizing F344 rats (n=5). A single oral gavage S9C of 6A1 was given containing a 5 mg/Kg dose normalized by the rats' body weight (Figure 22). The mean blood concentration time profile of 6A1 and its metabolites detected at and above the LLOQ of 2 ng/mL (or 2 ng/g of tissue samples). Five of the blood concentration data points below the LLOQ, but above the LOD, were also quantified. The first C_{max}/T_{max} of coated S9C 6A1 observed five hours after oral gavage (1320.68 ± 141.20 ng/mL/ 5Hr) which has a T_{lag} time of four and a half hours compared to the intravenous route previously studied ((n=4) at 5 mg/ Kg dose, 1700 ± 859.5 ng/mL). The dose normalized C_{max} of oral S9C was 4.09% compared to the C_{max} of the 6A1 IV. The first 6A1 glucuronide peak was also observed at 687.08 ± 182.12 ng/mL five hours after oral gavage. The 6A1 sulfate concentration of 41.20 ± 5.29 ng/mL throughout the study suggested that metabolic disposition of 6A1 in F344 rats was primarily via glucuronidation.

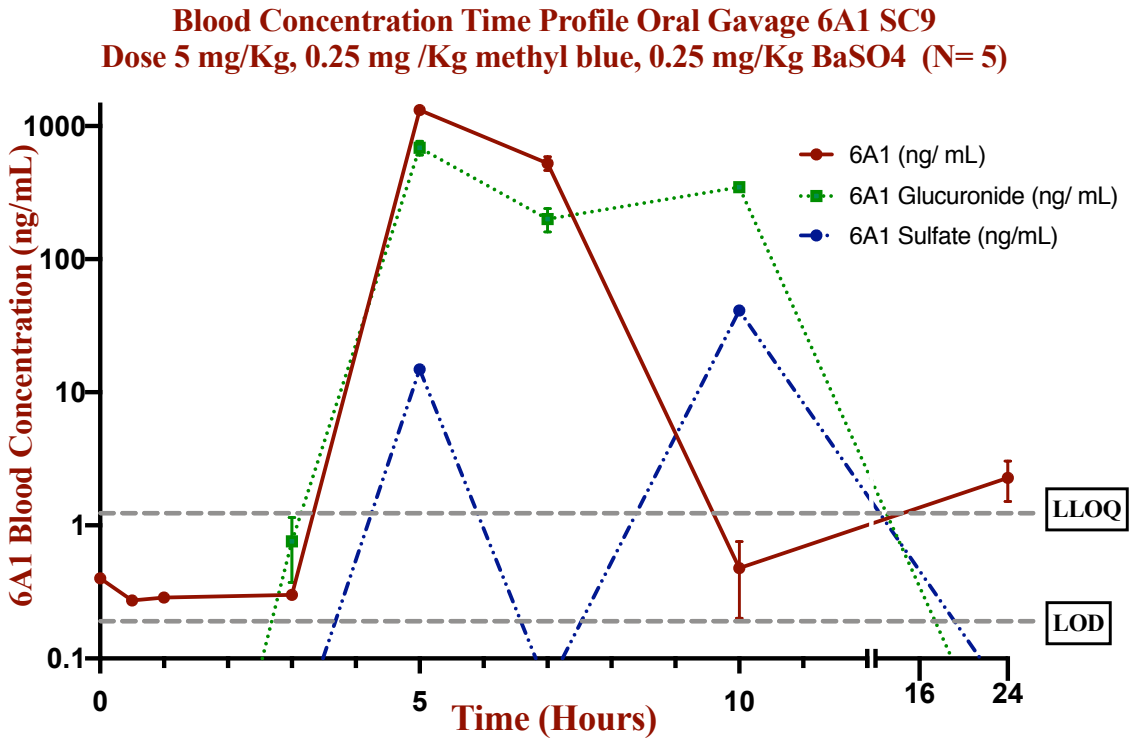

Figure 22: Blood concentration time profile from the pharmacokinetic study of coated S9C (n= 5). The 6A1 and its metabolites' concentrations were determined using previously established UPLC MSMS method (LLOQ of 2 ng/mL with instruments' LOD of 0.50 ng/mL).

The 6A1's dose normalized $AUC_{\_24Hour\_S9C}$ was 0.7942 ± 0.1731 nM/mL for S9C dosage form. Compared to IV $AUC_{\_24Hour\_IV}$ of 8.489 ± 1.291 nM/mL, the $AUC_{\_24Hour\_S9C\_Uncoat}$ was 12.00% and 9.35% for the enteric and delayed release coated capsules. In other words, the absolute bioavailability (F_{app}: $AUC_{\_24Hour\_S9C\ Coated}$ /$AUC_{\_24Hour\_IV}$) of 6A1 coated capsule was 9.30%, and the relative bioavailable (F_{Rel}: $AUC_{\_24Hour\_S9C\ Coated}$ / $AUC_{\_24Hour\_S9C\_Uncoated}$) between the uncoated and coated capsule dosage form was 78.0%. Thus, the total systemic exposure of the S9C coated dosage form reduced the total systemic

exposure to less than 10%. A 2-way ANOVA test was performed with the Tukey post hoc approach for dependent variables ($AUC_{\_24Hour}$ and time) of which the test yielded significant across all three dosage forms. The Tukey's multiple comparisons across rows (time of each blood samplings vs concentration) had significant different across three dosage up to 4 hours post dosed, which further support the T_{lag} time observed from the C_{max}/T_{max} of 6A1dose normalized blood concentration time profile. The 6A1 glucuronide $AUC_{\_24Hour\_S9C\_Coated}$ exhibited a similar pattern to that of the 6A1 parent compound but yielded statistically insignificant when a one-way ANOVA analysis were performed across the glucuronide metabolites of all three-dosage form (Figure 23).

Colonic mucosa tissue triplicate samples were also analyzed for three rats that were collected at 10 hours (n=1) and twelve hours after oral gavage of S9C; the average 6A1 tissue concentrations were 400.0 ± 65.94, 482.50 ± 35.86, and 525.0 ± 26.78 ng/g. Compared to the colon tissue concentration of rats via intravenous dosing (225.94 ± 65.94 ng/g), the S9C colonic tissue concentrations were 1.7 and 2.3 times higher. The 6A1 colon tissue concentration of S9C were 6 times higher than the oral suspension after adjusted for the different in dosage (Song Gao's R03 grant proposal data). A Holm-Sidak's multiple comparisons test was used to analyze the three dosage forms of colonic tissue 6A1 concentrations and the output suggested that IV and oral suspension tissue concentration was significant ($P = 0.0019$); there were also a significant difference between IV and coated S9C ($P = 0.0017$), but the most dramatic differences were observed between the coated S9C dosage and oral suspension ($P < 0.0001$).

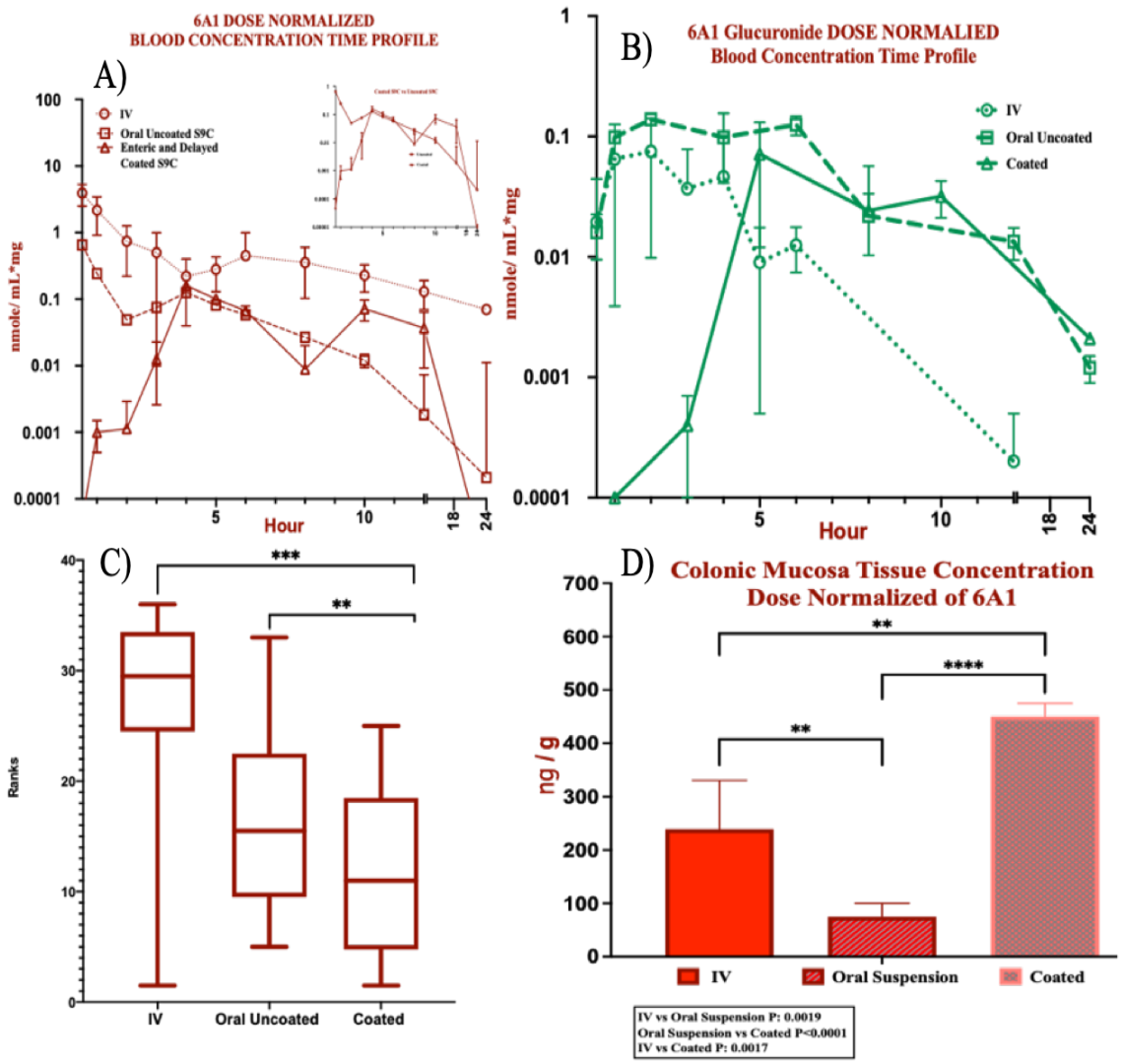

Figure 23: A) Dose normalized blood concentration time profile pharmacokinetic studies of 6A1 from intravenous dose (5mg / Kg, n=4), oral gavage of uncoated S9C (20mg / Kg, n=5), and oral gavage of coated S9C (20mg/ Kg, n=8). B) A dose normalized time point of 6A1-glucuronide between three routes of administration. C) The Kruskal-Wallis of the one-way ANOVA of 6A1 ranks suggested that there was a significant difference between IV/S9C_coated and S9C_uncoated/S9C_coated. Interestingly, the test did not find any substantial different between the IV and uncoated S9C (oral suspension formulation). D) The significant impact was also reflective in the statistical analysis when compared between the three routes of administration and the colonic tissue concentrations. An

ordinary one-way ANOVA statistical run of dose normalized 6A1 glucuronide did not yield any significant difference between the three groups.

4.5. Conclusion

A new solvent system was discovered and investigated for the polymers in this experiment. The solvent ratio of 65% acetone: 10% IPA: 3.5% water will dissolve up to 11% of Eudragit S100 and achieve the shortest amount of time needed to dry each coated film at 8.75 minutes. Utilizing the novel vacuum spin coating technique, the size 9 hard gelatin capsules (S9C) packed with the novel selective COX-2 inhibitor (6A1), resulted in consistent coatings that attained a uniform release mechanism targeting the colon.

When compared to our previous study (145), a dose-normalized AUC (ng*hr/mL*mg) indicated that the systemic exposure of 6A1 is 9.04% that of the systemic exposure of celecoxib given oral suspension (145). A separate oral suspension study with a 40mg/kg BID dose of Celebrex (dose equivalent to an 800mg/day in human) indicated all CV toxicity signs but also reduced the colonic tissue PGE_2 by 58%. The same study also showed the Celebrex concentration of about 556.67 ng/g of colonic tissues. Compared to the same treatment and dosage, 6A1 concentration was 138.75 ng/g in the colon (180).

The combination novel coating approach could overcome the exiting drawbacks associated with their conventional dosage form (i.e oral suspension). The pharmacokinetic study, the in vivo imaging, and the ex vivo tissue staining, and the colon drug concentration (525.0 ± 26.78 ng/g) showed that the cumulative approaches were able to deliver more than twice the amount of 6A1 to the colon compared to the intravenous route, three times the amount of 6A1 compared to oral suspension, and similar in magnitude to the concentration needed to have therapeutic effect compared to Celebrex.

CHAPTER 5: ZERO ORDER RELEASE OF ENTERIC AND DELAYED COATINGS OF S9C AS TO DELIVER A SELECTIVE COX-2 INHIBITOR (6A1) TO THE COLON OF F344 RATS

5.1. Abstract

Leading locally bioavailable COX-2 inhibitor (6A1) pharmacokinetic behaviors in a F344 rat were extensively studied. Raw drug powder and image tracers packed inside enteric and delayed release coated size 9 hard gelatin capsules (S9C) were given via oral gavage to the rats. The approach succeeded in delaying the release and deliver high concentration of 6A1 to the colon. The above colonic drug delivery system simulates a prophylactic treatment with a higher colon tissue accumulation when compared to intravenous injection (IV) or oral suspension dosage forms. In this research, enterically coated microparticles were formulated and packed inside the coated S9C in place of raw 6A1 powder. It was hypothesized that the combination approach will achieve a zero order sustained delay release of 6A1 in the colon (lower $AUC_{\_systemic}$, increase local $AUC_{\_colon}$). Previous data from a drug mixed into the rats' food indicated a steady state would be reached after four days of medication (180); as such, a single dose pharmacokinetic study in conjunction with a short term (4 days) efficacy study were done. F344 rats (n=12) were divided into two groups. Each group was administered 20 mg/Kg doses normalized by the rats' weight. Blood samples were collected periodically and the blood concentration time profile of normalized dose showed the total systemic exposure ($AUC_{\_systemic}$) remained constant

while the $AUC_{\_colon}$ increased by two folds upon analyzing the ex vivo colonic mucosa tissues samples.

5.2. Background

The COX-2 enzyme was observed to have up-regulation, overly express in the polyposis of FAP patients, and attenuate the progression of these polyposis lesions in the colon. If FAP lesions are treated at an early stage, not only can the FAP patients' morbidity and mortality rates decline, but their quality of life can be improved (1, 5, 7). Currently, marketed NSAIDs are not indicated for the treatment and prevention of FAP (2). However, Sulindac and Erlotinib are sometimes prescribed for FAP post-operatively to prevent polyposis formation and reduce the occurrence of frequent successive relapses (3, 4). Given the detrimental consequences of FAP as it relates to patient cancer risk and the need for repeated invasive surgical interventions, it was critically important to develop a systemic treatment with low toxicity that has the potential to reduce polyp burden as an adjunct or alternative to surgery.

Often orally administered drugs are broadly distributed via systemic circulation before accumulating at the intended target sites. Thus, accumulation of a therapeutic dose at the intended organs (i.e. colon) also requires a very high dose resulting in a dangerously high drug concentration in systemic circulation. In order to prescribe a COX-2 inhibitor as preventive care and treatment for FAP patients, achieving the desired colon tissue concentration requires a very high oral dose that can result in right COX-2 target but wrong

organs toxicity. The research aims to leverage a leading coating formulation and vacuum spin coating technique to reduce high systemic exposure (AUC_total) resulting in cardiovascular toxicity.

Recently, the development of a multi matrix approach (MMX) had gained some success in delivering a high concentration of drugs to the colon (181). The technology is a proprietary blend of liposome and hydrophilic excipients mixed with drug powders and pressed into a tablet. The tablets were then coated with an enteric coat to prevent upper gastrointestinal absorption. The approaches proved to be a successful drug delivery system to the colon in a few clinical trials (182).

The exact mechanism by which the pH microparticles in this study are uptaken and broken down in the enterocytes is unclear. However, there have been numerous studies that looked into the mechanism, and leading theory indicates that the ES100 microparticles follow the clathrin-mediated endocytosis pathway (183). The concentration of poly-methacrylic acid seems to influence the rate of cellular uptake (higher concentrations of polymethacrylic acid increases the negative surface charge and decreases the hydrophobicity contributed to the decreasing concentration of the copolymer) (184). The charge density of the microparticles may have resulted in lysosomal rupture due to osmotic swellings, thus resulting in the release of drugs into the cytosol (185)

When compared to the small intestine, the colon is much shorter, only about 1.5 meters. The absorptive surface is much less than the small intestine; however, the colon has the longest transit time. The average transit time for material from ingestion to the colon is about five hours. The minimum dwell time in the colon is three to four hours before defecation (43). The optimal COX inhibitor release target time is, therefore around six hours to ensure passage through the stomach yet allow for release prior to defecation. A successful pH-sensitive, biodegradable coating was expected not to dispense until the capsule reaches the colon where the pH is at least 6.8. The microbiomes on the surface of the wall of the colon were observed to produce a significant amount of bicarbonates, thus neutralizing the acidic content from the stomach and elevating the colon pH to 6.8 and above. There has been much research utilizing the pH-sensitive polymer or erosion rate of polymers to deliver drugs to the colon. The pH-sensitive method, however, has had limited success because the GI tract pH varies depending upon individuals and their diets. The erosion mechanism depends significantly on water content and the species of healthy microbiomes. Taking into account the pH differential, transit time within the GI tract, and the erosion mechanism, the specially fabricated hard gelatin coated capsules were formulated to dispense their payload in the colon. A combination of biodegradable polymer and a novel coating process may result in a new frontier of preventative care for many FAP patients, which currently have no effective treatment. In vivo data proved that a combination of pH-sensitive and time-release methods in conjunction with a unique coating technique was a more programmable mechanism to achieve a controlled release of

an oral drug in the colon (45-60). Celebrex and 6A1 coated capsules are anticipated to become significantly safer by applying the proposed capsule coating methods for the treatment of FAP. If proven successful, the design will qualify as a preventative treatment of colonic cancer in FAP patients conforming to FDA's stringent criteria for preventive chemotherapy.

5.3. Material and Methods

5.3.1. Chemicals and Materials

Chapter 3 established methods for the preparation and purification of 6A1, 6A1-Sulfate, and 6A1-glucuronide. Acetone, dichloromethane, isopropanol, DI water of 99.99% purity, and Polyvinyl alcohol (PVA, Mw ~ 31–50 kDa) were purchased from Sigma-Aldrich Corp. (St. Louise, MO, USA). Ester-terminated DL-PLGA of 50:50 and 85:15 were purchased from (Lactel Absorbable Polymers, Birmingham, AL). Evonik RÖHM GmbH (Darmstadt, DE) generously donated the ES100. Capsule sinkers, Catalog #3, item PSCAPWHT-XS were purchased from Dissolution Accessories (The Netherlands, De Kreek 12, 4906 BB Oosterhout).

5.3.2. Formulation of 6A1 Microparticles

Polymeric pH-sensitive ES100 microparticles loaded with 6A1 were prepared via the wet milling and spontaneous emulsification solvent evaporation methods; the final formulation was a combination of these previously published methods (162, 163, 186) with some

modifications. The powder 6A1 was first wet milled at 10 mg/mL in 35% methanol water at 1,600 rpm for an hour. Different volumes of 10 mg/mL of 6A1 ranging from 0 - 1.0 mL were added dropwise into different volumes of 5% (w/w) ES100 ranging from 0 – 1.0 mL (Table 7). The organic phase containing both 6A1 encapsulated by ES100 was emulsified in 20 mL of 2.5% PVA by microtip sonicator for 30 seconds at 10 µAmps, paused for 30 seconds in ice water, and repeated for thirty cycles. The slurry was left on gentle stirring for six hours. During the gentle stirring, the organic phase started to migrate into the greater stabilized aqueous solution and the organic solvent started to evaporate. The migration resulted in microspheres precipitated into the aqueous phase. Ultracentrifugation at 20,000 x g for ten minutes, at four degrees, was used to collect the suspended multi particulates. The collected microspheres were filtered via a paper filter and lyophilized after being washed three times with distilled water.

Table 7: Top: DoE of Nanoparticle formulations; Bottom: Leading Formulations from the DOE JMP 14 experiment.

Formulation	6A1 (10ug/ml)	PLGA 5050 (5% w/w)	Eudragit S100 (5% w/w)	PVA (2.5 % w/w)	Particle Size (nm)	Time Delayed Release	Conclusion
	Drug	Delayed Release	Enteric Coat	Surfactant	(200-500nm, 10X dilution)	4-10 Hours	
1	0.75	1.00	0.75	0.78	50000.00	33.33	Failed Both
2	0.25	0.75	1.00	0.25	218.00	33.33	Failed Both
3	0.75	0.00	0.25	0.00	50000.00	33.33	Failed Both
4	0.00	0.00	1.00	0.75	50000.00	33.33	Failed Both
5	1.00	0.25	0.25	1.00	433.00	0.00	Failed Time
6	0.25	0.76	0.25	0.81	219.00	6.67	Passed
7	0.77	0.00	0.81	0.25	50000.00	0.00	Failed Sized
8	0.00	1.00	0.00	0.00	50000.00	0.00	Failed All
9	0.25	0.25	0.75	1.00	50000.00	33.33	Failed Both
10	0.00	1.00	1.00	0.25	183.00	0.00	Failed Time
11	0.00	0.00	0.00	1.00	50000.00	33.33	Failed Both
12	1.00	0.25	1.00	0.00	50000.00	33.33	Failed Both
13	0.25	0.25	0.00	0.00	50000.00	16.33	Failed Topography
14	1.00	0.75	0.75	0.75	186.00	7.25	Passed
15	0.77	1.00	0.25	1.00	194.00	13.00	Passed
16	1.00	0.75	0.00	0.25	178.00	4.17	Failed PH

Forumulation	6A1 (10ug/ml)	PLGA 5050 (5% w/v)	Eudragit S100 (5% w/v)	PVA (2.5 % w/v)	Particle Size (nm)	Time Delayed Release (H	Conclusion
	Drug	Delayed Release	Enteric Coat	Surfactant	(200-500nm)	4-10 Hours	
6	0.25	0.76	0.25	0.81	219.00	6.67	Passed
14	1.00	0.75	0.75	0.75	186.00	13.00	Passed
15	0.77	1.00	0.25	1.00	194.00	4.17	Passed

5.3.3. In Vitro Dissolution Tests of microparticles packed inside coated S9C

The in vitro dissolution test for the microparticles packed inside coated S9C was performed, in accordance with the recommendation from UPS compendial dissolution, non-sink conditions (168). The simulated intestinal pH was adjusted via 2.5 µmol/L of HCl or NaOH from the 2.5 µmol/L of phosphate buffer. A 1.0 mL of samples were collected every half hour and the pH exposure/duration were as follows: 1.5 hours at pH 1.2 (stomach), 2.5 hours at pH 4.6 (small intestine), 2 hours at pH 6.8, 2.5 hours at pH 8, and 2.5 hour at pH 6.8. Each capsule was placed within a sinker housing and the stirrer rate was set at 80 rpm (169) at 37 ± 2°C. Samples at an extreme pH were air-dried, reconstituted, and neutralized before analysis. Drug concentration (6A1) was determined using the UPLC MS-MS method that was previously validated after the removal of ES100 via methylene chloride.

5.3.4. In vivo pharmacokinetic study food effect on the $AUC_{\_systemic}$ of 6A1 and time of capsule release (C_{max}/T_{max})

The raw 6A1 powder was packed inside coated S9C at a 20 mg/Kg dose normalized by the rat's weight. For the single dose pharmacokinetic study, blood samples were taken at 0, 0.5, 1, 2, 3, 4, 6, 8, 10, 12, and 24 hours after gavage. The fasted rats (n=8) were housed inside a special metabolic cage as to prevent coprophagy, food was withheld for twelve

hours, and free access was given to water. After the S9C were given, food was given to the fasted group. The fed rats were fed ad libitum and given water.

5.3.5. In vivo pharmacokinetic study of each successive coating's effect on the total systemic exposure of 6A1($AUC_{\_systemic}$) and time of capsule release (C_{max}/T_{max})

Similar to the previous in vivo studies, the raw 6A1 powder was packed inside coated S9C at a 20 mg/Kg dose normalized by the rat's weight. A single dose of uncoated capsule, enteric coated capsules, and enteric & delayed release coated capsules were given to F344 rats via oral gavage. The blood samples were taken at 0, 0.5, 1, 2, 3, 4, 6, 8, 10, 12, and 24 hours after gavage.

5.3.6. Single dose pharmacokinetic study of 6A1 microparticles formulated for sustained release using two leading microparticle formulation 1 (F1) and formulation 2 (F2)

The microparticles were packed inside coated S9C at a 20 mg/Kg dose normalized by the rat's weight. For the single dose pharmacokinetic study, the blood samples were taken at 0, 0.5, 1, 2, 3, 4, 6, 8, 10, 12, and 24 hours after gavage. A four day twice daily pharmacokinetic study was done where the rats were given, twice daily, the microparticles packed inside coated S9C at a 20 mg/Kg dose normalized by the rat's weight. The blood samples were taken at 12, 14, 16, 18, 24, 36, 48, 60, 62, 64, 66, 68, 72, 84, and 89 hours after gavage.

5.3.7. Multiple-Oral-Dose Regimen pharmacokinetic study of 6A1 microparticles formulated for sustained released packed inside the enteric and delayed release coated S9C

The dosing schedule for the multiple oral dose regimen for the four day efficacy study were twice daily (BID) at 12 hours apart. The given dose was 20 mg/Kg normalized per rat's weight.

Highly detailed dosing information can be found in Table 3. There are two different microparticle blends; Formulation 1 (Group 1) has 88.8 mg of 6A1 per gram of materials which correlated to an encapsulation efficiency (EE) of 30%. Thus, Group 1 multiple dose regimen group needed a total of three capsules per dose and a total of six capsules per rat each day. Formulation 2 has 56.3 mg of 6A1 per gram of particles, thus equating to an EE of 45%. Group 2 needed a total of four capsules per rat per day as the doses given were 20 mg/kg BID.

5.3.7. Statistical Analysis

The blood concentration-time profiles of 6A1 for each subject were analyzed by a noncompartmental method using WinNonlin® 6.1 (Pharsight Corporation, Mountain View, CA, USA). All statistical analyses were performed using the GraphPad Prism 8.0 program (GraphPad Software Inc., San Diego, CA, USA). T_{max} and T_{lag}, the nonparametric 95% CI was calculated for the difference in median values of each groups. The dose dependence of T_{max} and T_{lag}, rounded to the nearest scheduled time points, was investigated

by the Wilcoxon rank sum test to calculate a median and the difference in medians between dose groups.

5.4. Results and Discussion

5.4.1. Formulation of 6A1 Nanoparticles

Formulation development is a critical step in the process leading toward efficient, safe, and stable commercial products. Methods with high throughput capability provide a considerable advantage by expanding the conditions and parameters required. JMP 14 Software DoE facilitated the development of the pilot formulations.

Fifteen pilot formulations were completed to determine the optimal ratio of 6A1-PLGA 8515-ES particles. Of the fifteen, three leading formulations: number 6, 14, and 15 met both the particle size and delayed release criteria set forth (Table 7, Figure 24, and Figure 25). Noticeably, all three formulations had a high percentage, above 75%, of the surfactant PVA. Of the three, number 6 was the leading formulation for both the in vitro dissolution and the in vivo pharmacokinetic studies. Formulation 6 had the best performance of all the nanoparticle formulations and was used as a precursor for the preparation of 6A1 microspheres. Scale up 6A1 microparticles were generously made by collaborators (Dr. Gan Yong, Shanghai Tech University, Pudong, Shanghai, China).

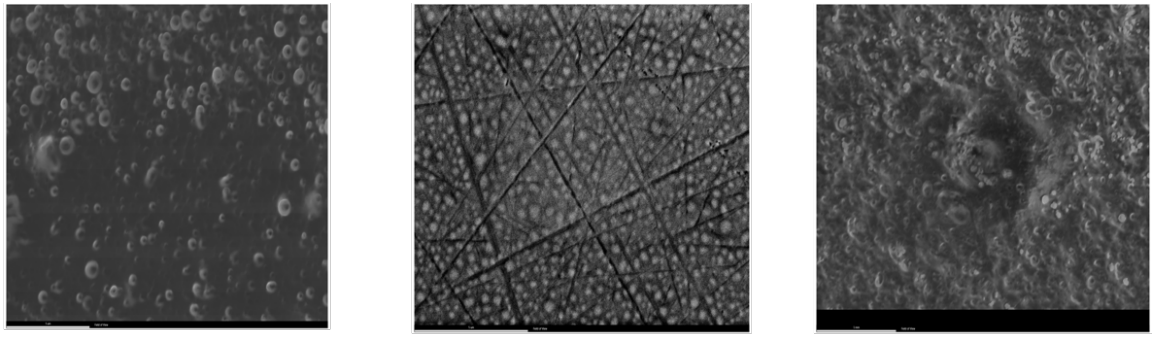

Figure 24: SEM images of leading formulations 6, 14, and 15. SEM images were obtained using the following operating parameters: 5.0 kV voltage, 4 mm working distance, and 10^{-6} millitorr vacuum. The side views of the capsule halves were captured at an 80,000x magnification

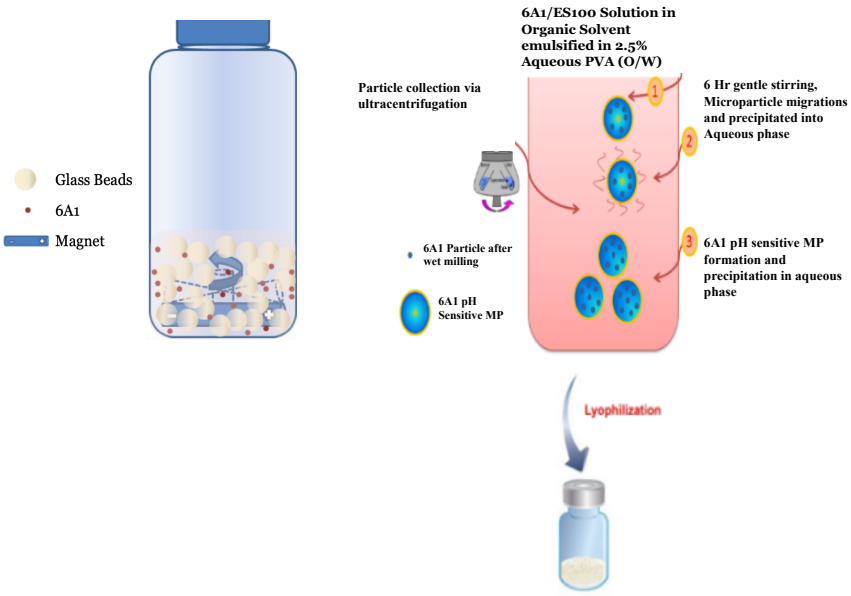

Figure 25: Wet milling and spontaneous emulsification solvent evaporation processes for fabrication of 6A1 microparticles. 10mg/ml of powder 6A1 in 35% methanol water was micronized with three different sized glassbeads at 1,600 rpm for an hour. Different slurry volumes (0 - 1.0 mL) were added dropwise into different volumes of 5% (w/w)

ES100 (Table 7). The organic phase containing both 6A1 encapsulated by ES100 was emulsified in 20 mL of 2.5% PVA by microtip sonicator for 30 seconds at 10 µAmps, paused for 30 seconds in ice water (30 cycles). The microparticle was gently stir for 6 hours, collect via ultracentrifugation (20,000 x g,10 minutes, 4 degree Celsius).

5.4.2. In Vitro Dissolution Tests

The drug loading (EE%) of pH sensitive microparticles was determined by dissolving the microparticles in an alkaline PBS buffer (187), and then using a liquid-liquid extraction method to remove the 6A1 compound using DMC. The in vitro, pH-dependent release profile of 6A1 from the pH-sensitive microparticles was investigated in a gradual pH-changing buffer to assess its ability to protect the content from the acidity and accomplish an effective delivery in neutral pH values (163). The 6A1 microparticles were rapidly released and emptied their content from the enteric and delayed release coated S9C. One under weighted capsule that had failed the quality assurance method was also tested. Most of the coated capsules released 6A1 microparticles at pH 6.8 (Figure 26). The result suggested the weight of a capsule was a reliable quality assurance method to qualify each coating batches.

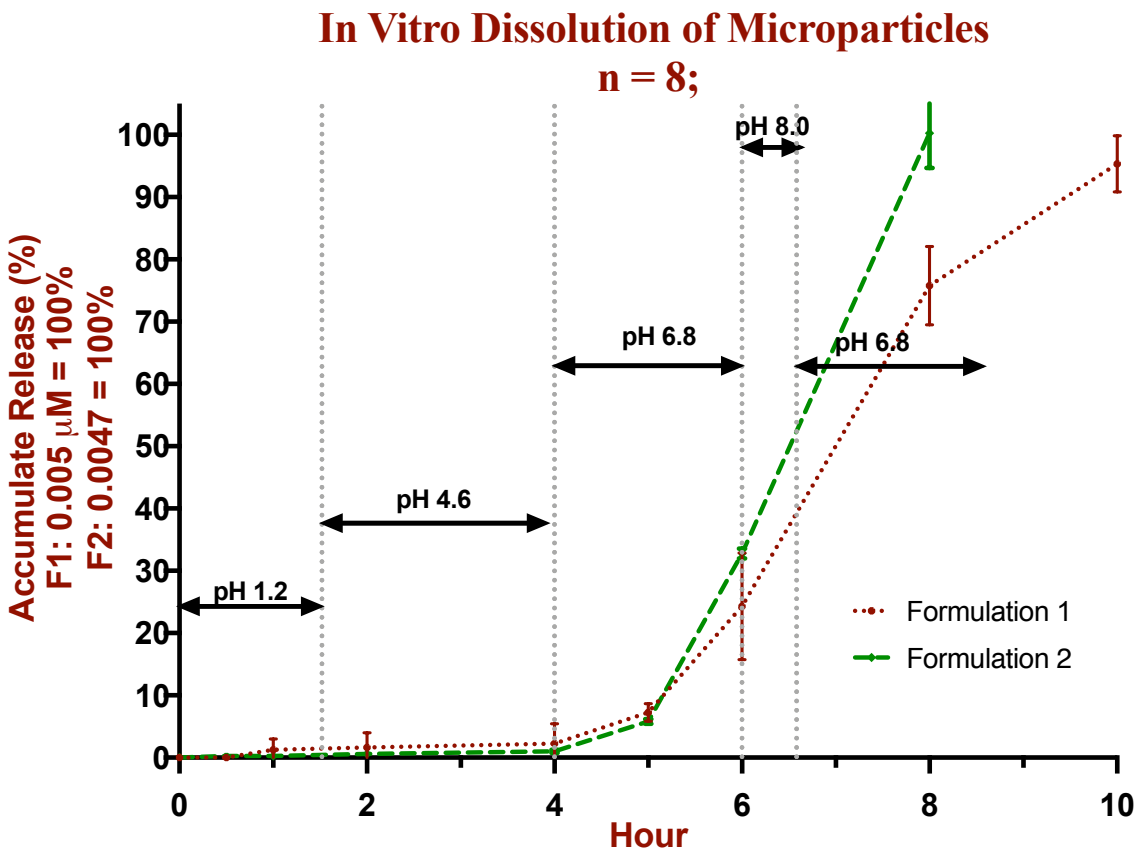

Figure 26: In vitro dissolution results of two 6A1 enteric coated microparticle formulations (F1 and F2 with each n=8) using simulated intestinal pH (1.2, 4.6, 6.8, 8, and 6.8 using 2.5 µmol/L of HCl or NaOH from the 2.5 µmol/L to adjust the 2.5 µmol/L phosphate buffer. 1.0mL of sample was collected at every half hour until a complete disappearance of the particle (approximately 10 hour).

5.4.3. In vivo pharmacokinetic study food effect on the $AUC_{\_systemic}$ of 6A1 and time of capsule release (C_{max}/T_{max})

A noncompartmental analysis of the blood concentration-time profile for food effect study was analyzed. The $AUC_{\_Ave24hour}$ of seven rats during fed and fasted states were calculated

using the trapezoidal rule. Fed animals had an $AUC_{\_Ave24hour}$ of 6.5 ± 1.02 µg/mL compared to 10.6 ± 1.5 µg/mL during a fasted state. The T_{max} of fasted animals was delayed by an hour compared to that of fasted animals, two hours post-dose (Figure 27). Statistical student t test with Welch's correction indicated that the $AUC_{\_Ave24hour}$ between the two group are insignificant (P-value = 0.6445). When compared with the T_{max} between groups, the result was different from the conventional understanding of gastric emptying of food in rats, which was influenced by the amount and type of food given. A study showed that a fatty meal delays the gastric emptying of liquids in awake rats, whereas fasting sped up the emptying process (188-190). However, capsule emptying was likely independent of the food effect. The result of fasted animals emptying capsules slower than a fed animal was also confirmed by a study done by Saphier et al., 2010 (171). However, the Hodges–Lehmann nonparametric population's parameter indicated that there was a significant difference in the T_{max} value (p = 0.0253). Simulation of prophylactic treatment in humans required that further pharmacokinetic studies be done with fed ad libitum animals. Multiple t test analyses indicated significant C_{max}/T_{max} differences between the first 2 hours; understandably, because absorption in the upper GI was influenced by the acidity and food content of the stomach.

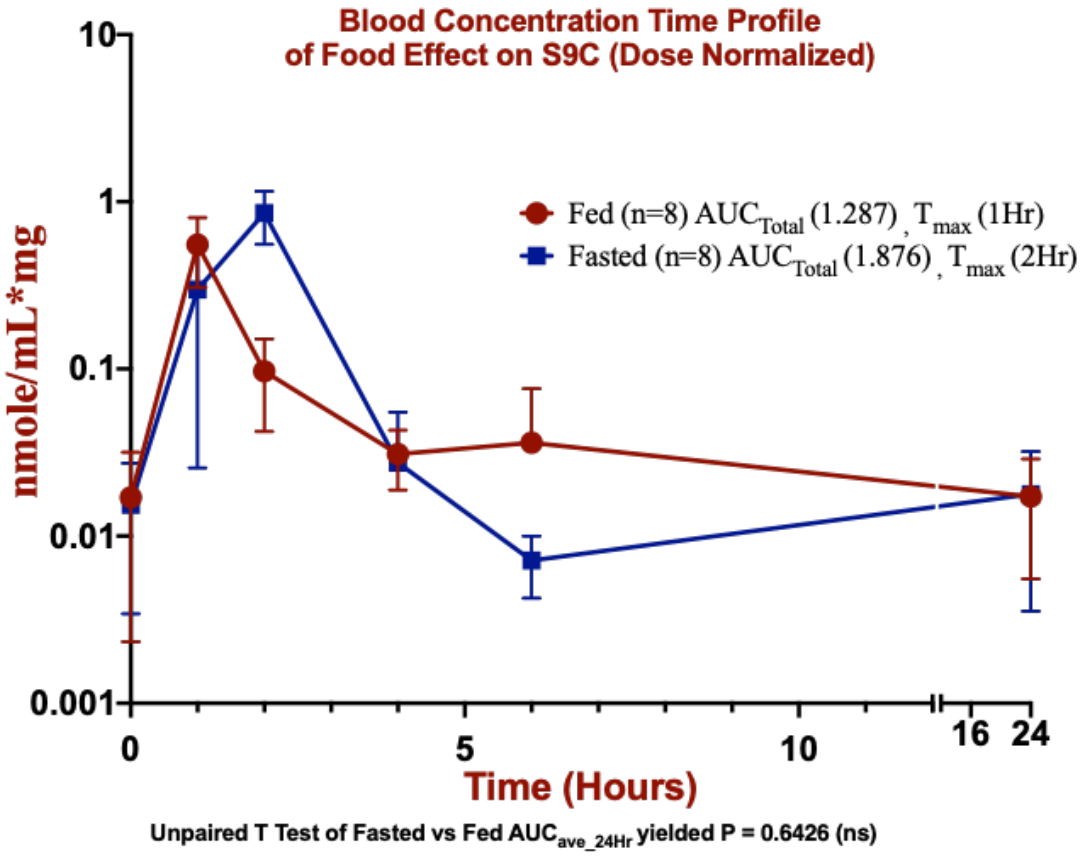

Figure 27: Blood concentration time profile of food effect was performed for coated sized 9 hard gelatin capsules (S9C). The dose normalized total area under the concentration curve of fasted animal (dose= 20mg/Kg with n=8 per group) was 45% higher compared to the fed group (n=8). Interestingly, unpaired T Test between two group yield insignificant difference (P=0.6426); however, the nonparametric 95% CI analysis of T_{max} shown significant different between fasted (T_{max} = 2 hours) and fed state (T_{max} = 1 hour).

5.4.4. Pharmacokinetic Study of Each Coating's Effect on the Total Systemic Exposure of 6A1

The dose normalized $AUC_{\_Ave24hour}$ of eight subjects of uncoated, enteric coated, and enteric and delayed release coated capsules were calculated using the trapezoidal rule. The uncoated capsule has $AUC_{\_Ave24hour}$ of 3.388 ± 0.6967 µg. The results are consistent with

the previous pharmacokinetic study of food effect in uncoated capsules. The $AUC_{\_Ave24hour}$ of enteric-coated capsules was 2.567 ± 0.48 µg. The enteric coating layer reduced total systemic exposure to 60.6% of uncoated capsules. The $AUC_{\_Ave24hour}$ of enteric and delayed release coated capsules had the smallest amount, 1.009 ± 0.1317 µg (Figure 28). The results indicated that the total systemic drug exposure had been reduced by 5.25 folds via the capsule's enteric and delayed release mechanism compared to uncoated capsules ($P < 0.0212$). The uncoated capsule had a T_{max} at one-hour post-dose, with the enteric coat, the capsules' T_{max} shifted to two hours post-dose. Compared to the two previous, the enteric delayed release coated capsules' T_{max} shifted noticeably to five hours post-dose ($P< 0.0001$).

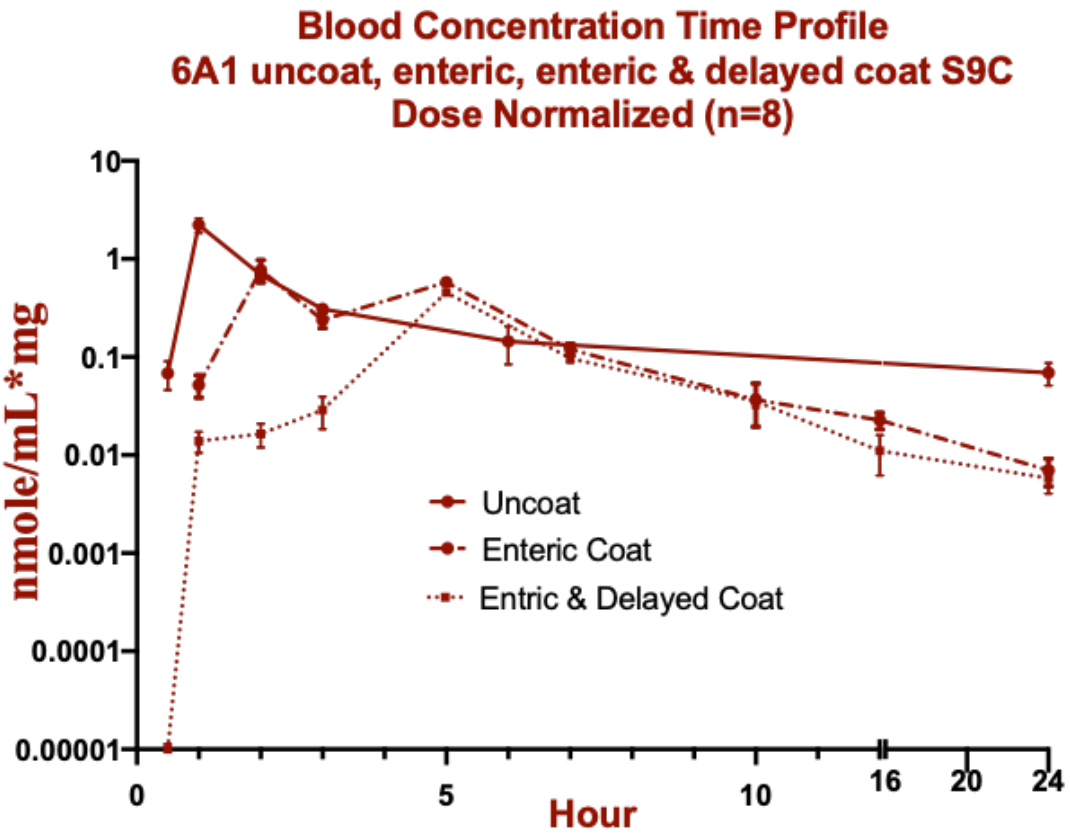

Figure 28: Blood concentration time profile of each successive coating was performed for uncoated and coated size 9 hard gelatin capsules (S9C). The dose normalized of $AUC_{\_total}$ (n=8) was highest in the uncoated (twice the enteric coats and three times the enteric& delayed coated). The uncoated size 9 capsules (S9C) contained raw drug powder packed inside the S9C. The enteric coat S9C contained raw drug powder packed inside S9C and a layer of ES100 of approximately 50nm in thickness. The enteric coat and delayed coat contained raw drug powder packed inside S9C, with a middle layer of approximately 150nm of PLGA8515, and an oute layer of ES100 of approximately 50nm in thickness. All animals were fed ad libitum. One-way ANOVA Sidak's multiple comparison test of $AUC_{\_total}$ between groups yield insignificant difference (P = 0.6617); however, the 2way ANOVA analysis of T_{max} (Row Factor P value) shown significant different between groups (P<0.001).

5.4.5. Single dose pharmacokinetic study of 6A1 microparticles formulated for sustained release using two leading microparticle Formulation 1 (F1) and Formulation 2 (F2)

Again, the $AUC_{\_Ave24hour}$ of the twelve subjects in the microparticles at the dose of 5 mg/kg was calculated using the trapezoidal rule. The $AUC_{\_Ave24hour}$ of 6A1, 6A1 glucuronide, and 6A1 sulfate were 1.43 ± 0.04 µg/ml, 0.84 ± 0.25 µg/mL, and 0.137 ± .06 µg/mL. The above pharmacokinetic parameters equaled to a dose normalized $AUC_{\_Ave24hour}$ of 0.7130 µM/Hr for F1 and 0.6649 µM/Hr for F2. The $AUC_{\_Ave24hour}$ exhibited the characteristics of a sustained release with the onset of both formulation at around three hours and the C_{max} 0.1854 for F1 and 0.1404 for F2. Noticeably, the C_{max}/T_{max} of 6A1 glucuronide (green curve) differed significantly from that of 6A1 (red curve) – 198 ng/mL at six hours versus 305.5 ng/mL at four hours. The pharmacokinetic parameters above suggested microparticles were absorbed, metabolized, and entered the EHR (Figure 29). Interestingly, in a dose normalized analysis using the unpaired student t test, the results indicated that there was no significant difference between the two formulation F1 and F2 (P = 0.8061).

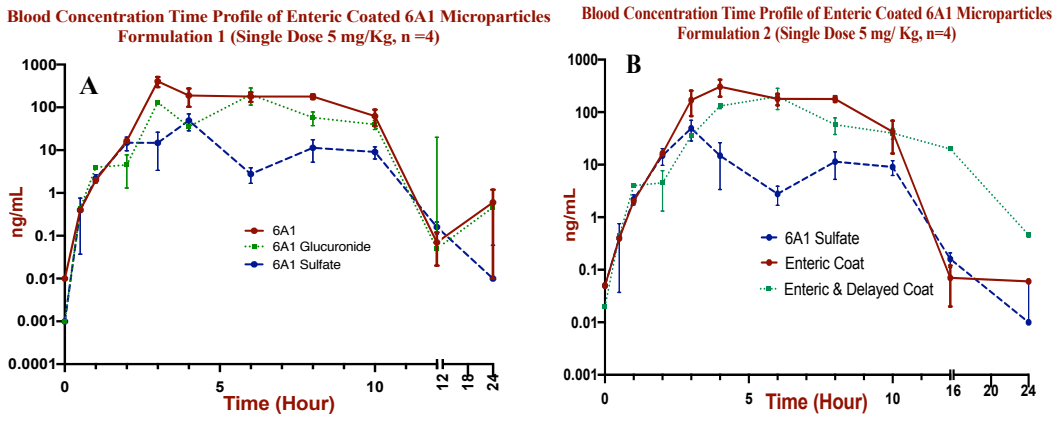

Figure 29: Blood concentration time profile pharmacokinetic study of microparticles: Formulation 1 and Formulation 2. Rats were fed ad libitum and given gavage of 5mg/Kg dose. Statistical analysis via student t test suggest there are insignificant differences between the two formulation with p = .8063

5.4.6. Multiple-Oral-Dose Regimen pharmacokinetic study of 6A1 microparticles formulated for sustained released packed inside the enteric and delayed release coated S9C

Familial adenomatous polyposis (FAP) is a chronic disease; multiple dosage regimens with appropriate drug concentration assist with regressing the onset of inflammation and polyposis formation. A short term (4 day) efficacy study of enterically coated microparticulates packed inside coated S9C attempted to assess the therapeutic drug concentration in the colon and ability to deliver a constant, sustained amount of drug (C_{max_ss}) to the colon while reducing the total systemic exposure ($AUC_{\_average\_ss}$). The mean plasma concentration-time profiles after a q12h oral administration of 20 mg/kg of 6A1 and of its metabolite, 6A1 glucuronide and sulfates, were displayed in Figure 30. Other

pharmacokinetic parameters can also be deduced from the experiment, such as 6A1 concentration at a steady state. NCA of Phoenix WinNonlin® 6.1 software (Pharsight Corporation, Mountain View, CA, USA) was used to determine the clearance rate of 6A1 at a steady state was (CL_{ss_F}) 107,222.7 mL/hr/kg. There was no significant difference in clearance rate between the two formulations ($P > 0.1$). Interestingly, Formulation 1 has a C_{ss} of 1,536.65 ng/mL compared to the 2,444.07 ng/mL for Formulation 2; thus, the colon tissue-specific of 6A1 in Formulation 1 was 37% less than that of Formulation 2 (1,536.6 ng/g compared to 2,444.7 ng/g, $P < 0.012$). The P values of 6A1 metabolites (glucuronide and sulfate) in the colonic tissue between groups was insignificant (Figure 31). It was unclear whether the size differences of the particles in Formulation 2 or the larger number of capsules given contributed to such differences. The colon tissue concentration further confirmed that the capsules delivered a sufficient amount of drug to the colon.

There was a significant difference between the amount of 6A1 and 6A1 sulfates accumulated in the liver tissues between the two groups (Figure 31). No appreciable accumulation was detected for either 6A1 or its metabolites when comparing between the single dose and multiple dosing assuming C_{ss} at 4 days in the F1 microparticles ($AUC\_{Dose\ Normalized}$: 0.5531 vs 0.5232 μM). However, for 6A1 single dose and multiple dosing of F2 microparticle, there was a significant increase in the steady stage concentration ($AUC\_{Dose\ Normalized}$: 0.6868 vs 0.9532 μM).

Table 8: Pharmacokinetic dosing schedule of multiple dosing of Formulation 1 and Formulation 2 microparticles packed inside S9C (20 mg/Kg Dose). Group 1 (n=6) were given formulation

Group 1		Rat Weight (grm)	265.3	267.1	276	253.3	242	237.5
Hours	**Time**		**Rat 1**	**Rat 2**	**Rat 3**	**Rat 4**	**Rat 5**	**Rat 6**
0	MON 9PM	Dose 1	9, 17	10, 18	11, 19	13, 21	14, 22	15, 23
12	TUE 9AM	Dose 2	16, 24	25, 33	26, 34	29, 12	27, 35	28, 36
24	TUE 9PM	Dose 3	30, 38	31,41	40, 42	49,50	43, 51	44, 52
36	WED 9AM	Dose 4	45, 57	46, 85	47,59	48, 61	53,62	54, 63
48	WED 9PM	Dose 5	69,77	68,76	76,75	66,74	65,73	64,56
60	THU 9AM	Dose 6	78, 92	71,79	72,80	81,89	90,82	83,91
72	THU 9PM	Dose 7	84,92	98,99	97,93	95,87	100,86	85,88
84	FRIDAY 9AM	Dose 8	32,108	101,104	102,103	105,106	108,107	109,40

Group 2		Rat Weight (grm)	252.1	245.5	262	244.5	243.7	257.5
Hours	**Time**		**Rat 7**	**Rat 8**	**Rat 9**	**Rat 10**	**Rat 11**	**Rat 12**
0	MON 9PM	Dose 1	153-6	157-9	160-2	163-5	4, 164, 165	129,137,145
12	TUE 9AM	Dose 2	1,9,17	2,10,18	3,11,19	5,13,21	6,14,22	7,15,23
24	TUE 9PM	Dose 3	8, 16, 24	4,12,64	25,33,41	27,35,43	27,35,43	28,36,44
36	WED 9AM	Dose 4	30,38,46	31,39,47	40,43,48	49,57,65	50,66,58	51,67,59
48	WED 9PM	Dose 5	88,80,72	71,63,55	75,79,54	69,19,53	68,45,52	62,92,82
60	THR 9AM	Dose 6	73,89,99	74,96,151	84,96,75	77,98,95	98,78,90	97,94,79
72	THR 9PM	Dose 7	127,126,125	122,123,124	117,119,120	114,115,116	111,112,113	81,91,101
84	FRIDAY 9AM	Dose 8	141,128,152	130,142,102	132,143,149	133,144,150	134,147,140	135,148,136

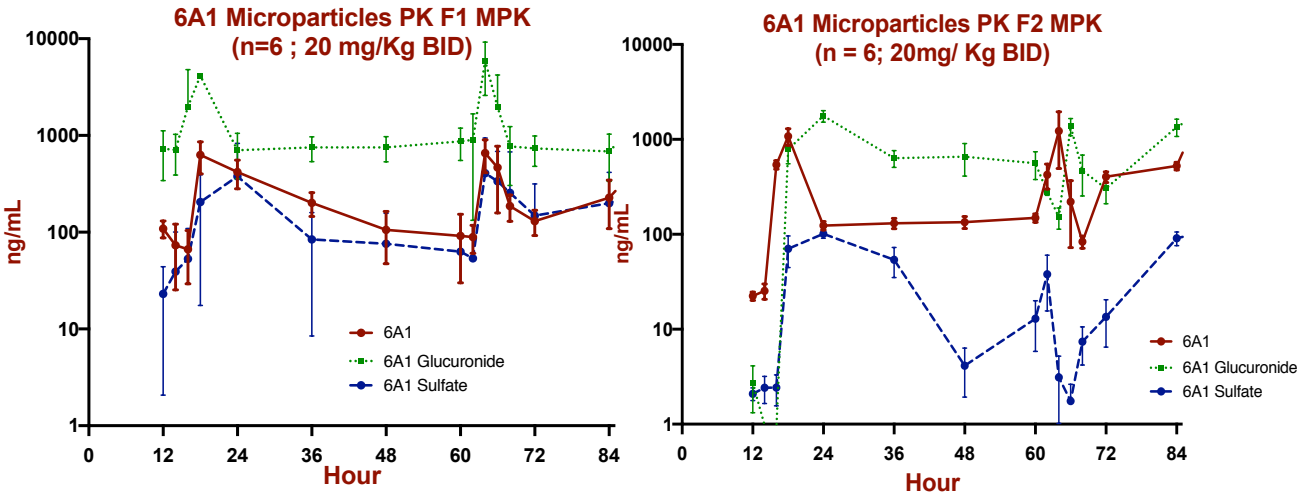

Figure 30: Multiple-Oral-Dose Regimen pharmacokinetic study of 6A1 microparticles formulated for sustained released packed inside the enteric and delayed release coated size 9 hard gelatin capsules (S9C). Blood concentration time profile of F344 rats (n=6 per group) dosed with 20mg/Kg BID for four days were collected at 12, 14, 16, 18, 24, 36, 48, 60, 62, 64, 66, 68, 72, 84, and 89 hours after gavage.

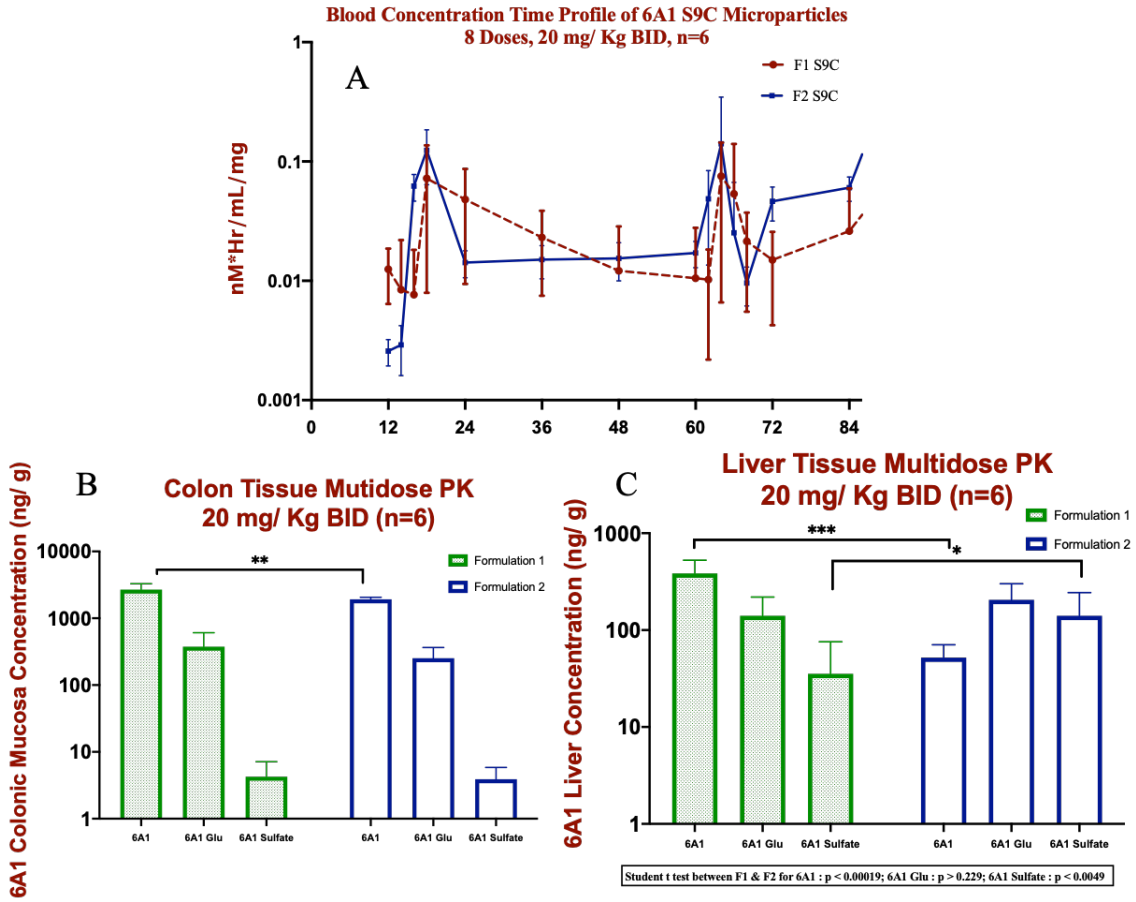

Figure 31: Ex vivo liver and colon tissues accumulation of 6A, 6A1 glucuronide, and 6A1 sulfate collected 6 hours post 8th dose for F1 and F2 (n=6). Tissues concentration of 6A1 extracted as descripted in section 3.3.5.2.

5.6. Conclusion

We achieved the project's objective. A de novo design of capsule coatings and formulations delivered a higher concentration of drug to the colon and reduced the systemic drug concentration multifold. Additionally, the long-term efficacy study using the above approach to compare the 6A1 concentration systemically versus the colon targeted at steady state was in progress to elucidate the pharmacodynamics of 6A1. Glucuronidation

was the main driving force for of 6A1 entering into EHR (); sulfation has little involvement in the phase two metabolism of 6A1. The completion of these studies using the F344 model will help establish the pharmacokinetic mechanism of such a drug delivery system. Further investigation of the 6A1 pharmacodynamic mechanism is needed to successfully translate the application into clinical care for FAP patients as preventive care.

Regardless, there is still no commercial drug for the treatment and prevention of polyposis (FAP) and CRC. Reformulation is crucial to lower systemic toxicity using hard gelatin-coated capsules for the treatment and prevention of FAP and CRC. Therefore, research for the targeted delivery of 6A1 and new delivery strategies will provide a therapeutic benefit to many chronically suffering patients.

The in vivo data suggested that these innovative approaches are the most promising. A combined approach of both pH dependent and time-dependent particulate systems is highly desirable for use in a true colon-specific drug delivery system. The combined approach may reduce the side effects of the drug caused by absorption from the stomach when given in the form of raw drugs. There are still several challenges, which need further input from the committee's cumulative experience. The ultimate goal of this research is to apply the knowledge discovered herein to bring comfort to patients.

All analyses were conducted using actual sampling times. The blood plasma concentration (C_{max}) and time at C_{max} (T_{max}) were determined from the observed values and confirmed with GraphPad Prism software. The trapezoidal rule was used to calculate the AUC_{total}

from time 0 to the last measurable time. Unfortunately, lack of a powerful model to address the recycling of 6A1, resulted in the analysis not yielding reliable pharmacokinetic parameters and the need for more empirical data. Overall, the pharmacokinetic studies revealed that the relative bioavailability of 6A1 was lower and the colonic tissue exposure higher when administered in the microparticles packed inside the S9C compared to the conventional oral suspension and/or intravenous route. Further analyses also revealed that relative bioavailability and exposure of 6A1 is higher when administered to subjects in the fast condition than subjects in the fed condition.

CHAPTER 6: DISCUSSION AND FUTURE DIRECTION

6.1. Novel Coating Technique

Hard gelatin capsules were packed with raw drug or microparticles; the capsules were then coated with PLGA 8515 to a thickness of 115 ± 35 nm thickness and an outer pH-sensitive Eudragit S100 coat of 50 ± 15 nm thickness to achieve colonic delivery. The new vacuum spin coating technique achieved an 88% success rate (410 of 450 capsules made passed the quality assurance tests). 6A1's pharmacokinetic behaviors in F344 rats were extensively studied.

We have completed the objectives of this study. A combination of formulated microparticles and coated capsules delivered 6A1 to the colon. The novel spin coating technique was able to coat high viscosity polymers, PLGA8515 and ES100, with a high mass loading of 10% w/w formulation and sufficiently covered the entire three dimensional nine millimeters hard gelatin capsules (S9C). The novel spin coating technique is an innovative coating approach that had not been accomplished prior to this research. The vacuum applied to the bottom of the capsules placed inside its respective slot within the coater plate creates a shear force that thinned out the polymers, which are behaving as non-Newtonian fluids. The thinning is due to the entanglement of polymer collapsing in the direction that vacuum is applied (bottom of the plate). The angle at which the capsule sits causes it to spin around as the centrifugal force resulting from the spinning of the coater plate. The centrifugal force is large enough to spin out the large undissolved polymers and

creates a vortex of air that facilitates further evaporation. The combination of vacuum and spinning creates a micro-environment that has a conical vortex within each capsule pod.

6.2. Novel Formulation

The formulation works via a successful blend of solvent mixtures. The solvent system is composed of acetone, IPA, and water; it provides for an optimal drying time without a lengthy drying period during processing between each successive coating. However, the solvent system did not evaporate as abruptly compared to 100% acetone, which has caused the film formation to be uneven and blister. Most importantly, the high mass loading of the polymer (10%) prevents the solution from having a running effect. Frequently, a high ratio of material to solvent and large molecular weight in a formula contributes to a high-viscosity. High viscosity (a thick formulation) yields better coat quality as compared to a low viscosity formulation. The intermolecular force of a higher viscosity formulation prevents the solution from forming a film that is not subjected to shrinking stress during drying and the resulting breakage. In a manufacturing setting, a thinner solution with low viscosity is used often used as it enhances adhesion to the substrate; however, the downside is the need for multiple coatings. The basic water spray applied to the capsule surface after sealing and before coating neutralizes the capsule's surface lysine, destabilizing their surface chemistry, thus promotes better adherent for the polymer and preventing peel-off.

A robust, sensitive, and validated UPLC-MS/MS method was also developed and successfully used to quantify 6A1, 6A1 glucuronide, and 6A1 sulfate in pharmacokinetic

blood, colonic mucosa, and liver tissue samples. The method has a multitude of advantages, such as high sensitivity (LLOQ 2 ng/mL), short analysis time (6 minutes), small sample size (10 μL), functional recovery with negligible matrix effect, and simplistic sample preparation. With all the above-mentioned advantages, this method was applied to preclinical pharmacokinetic/pharmacodynamic modeling studies of 6A1.

Fifteen pilot formulations with the help of JMP DoE software were able to produce a leading polymeric pH-sensitive PLGA 8515/ES100 particle loaded with the 6A1 formulation. The microparticle formulation has a theoretical EE of 30-45% after redissolving the polymer in DMC to extract the 6A1. The in vitro pH-dependent release profile of 6A1 microparticles showed a rapid release of drug in a neutral pH environment and the in vivo pharmacokinetic study showed an extended release profile, with the T_{max} at 3 hours. The formulation was successfully scaled-up, after synthesis, via collaboration and later used in the four days multiple dosing regimens.

6.3. Pharmacokinetic Studies of 6A1 in F344 Rats

Rats were fed ad libitum and given the drug via oral gavage. Different study conditions were investigated, such as food effect, real-time imaging agent mixed with 6A1 (supplemental), and uncoated capsule versus enteric or erosion coated capsules. Food is a confounding factor of capsules emptying from the stomach. Fasted animal has a higher T_{max}/C_{max} and $AUC_{Average24hourtotal}$ compared to their fed cohort.

Each additional coating applied to the capsules reduced the total systemic exposure of 6A1. Calculated using the trapezoidal rule, the uncoated, enteric coated, and enteric and delayed release coated capsules had an $AUC_{\_Ave24hour}$ of 6.55 ± 1.02 µg/mL. 3.97 ± 0.48 µg/mL, and 1.24 ± .50 µg/ml. Uncoated capsules $AUC_{\_total}$ was comparable to the fed stage of the food study experiment. The results also indicated a 5.25 fold reduction of AUC via capsule enteric and delayed release mechanism ($P < 0.0212$). The T_{max} was also significant between the three groups. Uncoated capsules had a T_{max} at one-hour post-dose. The enteric coated capsules delayed the T_{max} to two hours post-dose. The combination of PLGA8515 and ES100 coating delayed the T_{max} to five hours post-dose compared to uncoated capsules ($P< 0.0001$).

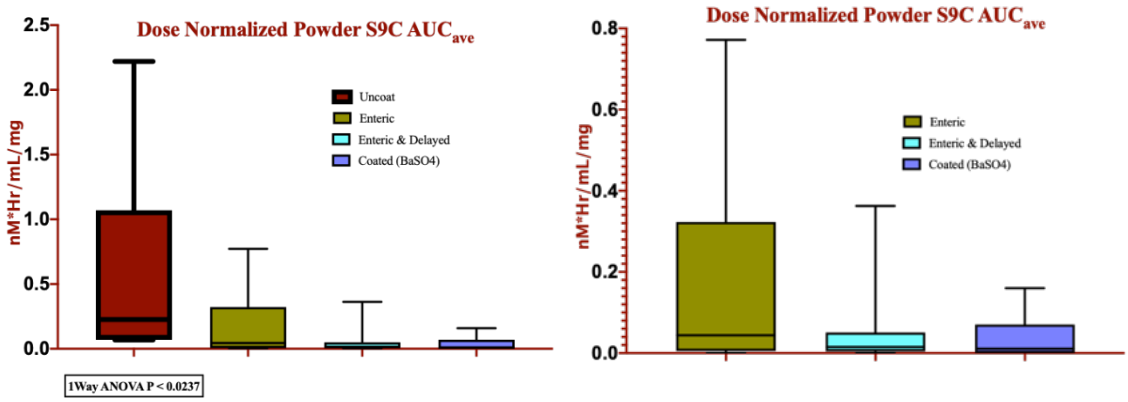

Figure 32: Blood concentration time profile of 6A1 across three different size 9 hard gelatin capsule coatings showed the enteric and delayed release coating has the lowest systemic drug circulations (Teal color block, AUC_{total}).

The enteric and delayed release formulation administered via oral gavage seems to closely simulate a prophylactic treatment with the highest colon tissue accumulation. In a parallel study done within our group, Yun's data indicated blood level C_{ss} could be reached after

four days of medication at 40 mg/Kg twice a day (180). As such, this research included a short term (four days) efficacy study with coated capsules housed the leading microparticles. The colonic concentration of 6A1 was comparable between Yun's study of 40 mg/Kg twice daily (3300 ± 300 ng/g) to that of the four-day multiple dosing of coated capsules at 20 mg/Kg (2,682 ng/g for Formulation 1 and 1,916 ng/g for Formulation 2). Since the coated capsule's dosage was reduced by half, the result strongly suggested that lowering the dose could achieve similar colonic concentration.

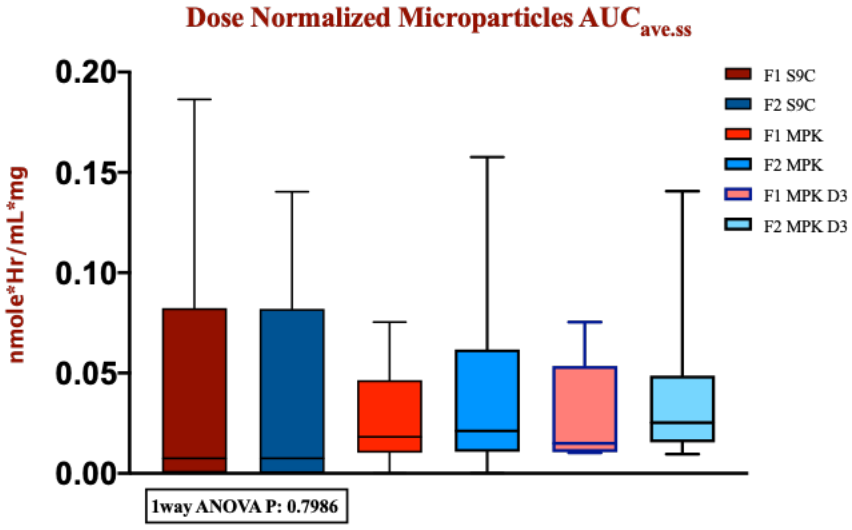

Figure 33: Blood concentration time profile of 6A1 of enteric and delayed release coated size 9 hard gelatin capsule packed with microparticle F1 and F2. The single dose and the via twice daily for four day at 20mg/Kg has similar.

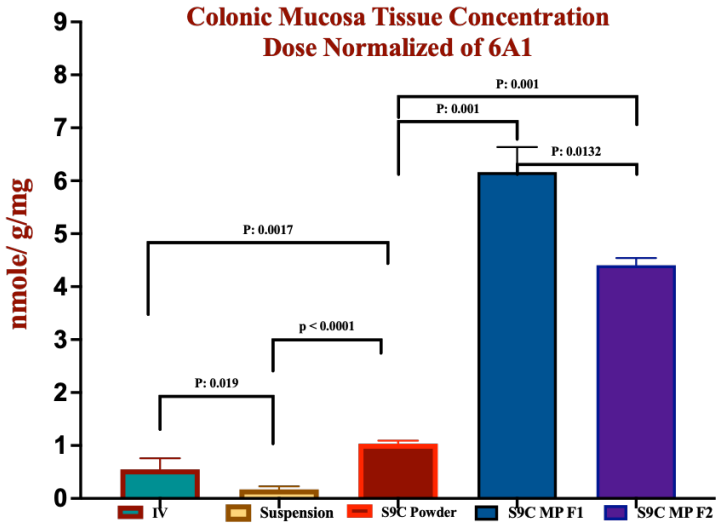

Figure 34: Colonic tissue drug concentration of 6A1 with normalized dosage across IV, oral suspension, size 9 coated capsules with raw powder, and size 9 capsule with microparticle formulations. The microparticles formulation 1 has the highest colon tissue accumulation of 6A1.

Table 9: A dose normalized comparison of colonic tissue concentration of 6A1 across IV, oral suspension, size 9 capsule (SC9) packing with powder, and microparticles.

	Colonic Tissue Concen. nmole/g/mg	Times IV Concen.
IV	0.55	-
Suspension	0.17	0.31
S9C Powder	1.03	1.88
S9C F1 MPss	6.16	11.21
S9C F2 MPss	4.41	8.01

Interestingly, glucuronidation levels in the multidose four-day study are the main driving force for of 6A1 entering EHR; sulfation has little involvement in the phase two metabolism of 6A1. This conclusion was evidence that when compared with the

glucuronide and sulfate concentrations in liver tissues, between the two groups, there is no significant difference ($P > 0.05$). For colonic mucosa tissues, the amount of 6A1 accumulation in Formulation 1, which has smaller microparticulate, was significantly higher than that of Formulation 2. The particle size difference might have contributed to the observed data. The P value of glucuronide concentration between the two groups was insignificant ($P > 0.05$). One can infer that the differences between the two groups were due to the particle sizes and not the activity of microbiomes or the delivery method. Microbiomes can be ruled out as the causative factor since the glucuronide generated in the liver was secular and the rat groups are cage mates given the opportunity to practice coprophagy, as rats are known to want. Also, the delivery system could not have been the causative factor for the P value variance since the AUC are similar between two groups.

6.2.1. Advantages of Vacuum Spin Coating Technique

Currently, no commercially available coating machine exists for gelatin capsules smaller than size five. Compared with conventional coating, we propose an adaptor that could sidestep the standard low mass loading of 3% and instead use a 10% mass loading. The adaptor was sized to fit any conventional magnetic spinner and vacuum. The adaptor can be used to coat both the aqueous and organic solvent based systems because it does not require a spraying nozzle to apply the solvent to the substrate. Furthermore, the spin vacuum adaptor does not need high heat as a curing process since the spinning creates an air vortex within each pod that facilitates solvent evaporation. The vacuum spin coater was

also designed to produce individualized small-scale batches consisting of 8 or 16 capsules. Currently, the coating success rate is around 80%, meaning that for every quantity of eight capsules, one will fail the visual, weight, or in vitro dissolution test. Most noticeably, this reduced the amount of processing time and the total waste associated with unused material to practically zero. The spin vacuum design resolves the shortfalls of the conventional coating techniques mentioned above, which does not have the capability to run pilot testing of a drug or produce individually tailored medicines where the pharmacokinetics of the drugs can be controlled and modified. We have discovered that the thickness of the coating layers was controllable by adjusting two parameters of the spin vacuum coater. First, the total suction applied by the vacuum facilitates the surface creeping of 10% of the material. The force exerted onto the capsule by the vacuum also spreads the formulation evenly to the gap and covers the junction between the cap and body of the capsule. Secondly, the spinning rate of the machine creates a centrifugal shearing force that facilitates the expulsion of chunky or undissolved polymer and also thins out the coating material. Together, the total suction of the vacuum and spinning rate precisely control the optimal thickness of the PLGA and ES100.

The method of coating capsules according to the invention is novel compared to conventional coating methods. The conventional method is for a large quantity of hard capsules filled with a drug to be charged into an apparatus which is then heated and rotated either under vacuum or atmospheric pressure. The invention uniquely allows for small batch production as is desired in research and development labs. Small batches are

desirable for the production of personalized medications. When compared to conventional capsule coating equipment, the cost of the invention is significantly less. The quality of the capsule coating is superior in enteric and acid-resistant characteristics and the delayed release mechanism compared to conventional coatings rapidly disintegrated in intestinal fluid. Furthermore, the quantities of the coating agent, active ingredients, and fillers can be reduced; the products obtained are of higher quality, and the production cost for both researching laboratory and clinical setting are reduced. The invention allows for the delayed burst release of the capsule to specific region in the GI track is tunable through the controlling the coating thickness and the formulation of polymers.(191)

6.3 Future Direction

Polyposis in the rat colon (Pirc) and Kyoto Apc Delta (KAD) are two rat models that carry different mutations in the adenomatous polyposis coli gene (Apc). The Pirc and KAD models are both susceptible to inflammation derived colon cancer; the Pirc model is more sporadic in its colonic cancer development. Pirc and KAD models are more likely to develop colon cancer in the male cohort versus the female cohort. The KAD model more appropriate for inflammation induced colorectal cancer longitudinal etiology studies. In contrast to Pirc, the KAD model rats do not spontaneously develop tumors and are homozygously afflicted because of mutation across both sexes. Azoxymethane-dextran sodium sulfate (AOM-DSS) introduced into the KAD model rats (across both sexes) results

in chemically induced inflammation leading to colonic tumor formation in 100% of subjects.

Many studies have found that selective COX-2 inhibitors (particularly Celebrex) regresses polyposis formation in Pirc animals. However, the modification of the 6A1 compound to facilitate its active phase 2 metabolism and enter enterohepatic recirculation, might potentially reduce its efficacy against COX-2. For instance, PGE_2's level is reduced in half by 6A1 with an effective inhibition concentration of around 70 μM, which is seventy times higher than Celebrex's inhibition concentration of 1 μM (unpublished data acquired through intestinal acute TNBS inflammation and perfusion study). In vitro data reveals that 6A1's IC_{50} (μm) requires 8.4 times more concentration than Celebrex (0.1178 vs 0.041) in recombinant human COX-2 enzyme anti-inflammatory activity assay, 21 times in HCA-7 cells line (0.064 +/- 0.005 vs 0.003 +/- 0.0001), and 462 times in Raw264.7 cells (113). In vivo data from a four day dosing study showed a slight decrease in the PGE_2 level within the mucosa (-19%); however, the endoscopic data accessing the tumor burden and statistical results were insignificant (180).

Multiple methods are available to improve the efficacy data of 6A1; enhancing the solubility of 6A1 and conducting further tests using the KAD disease model are the best methods to improve the efficacy data. Compound 6A1 belongs to the Class II of the biopharmaceutical classification system in which the compound is highly permeable but has very low solubility. An in vitro PBS buffer test shows that at pH 7.4, 6A1 is about ten

times lower in solubility than Celebrex (1 μM vs 12.5 μM). Low drug concentration was also observed in the mucosa tissue, where 6A1 is about four times lower than Celebrex. Enhancing the compound solubility might help improve the current efficacy status of the compound. It is suspected that compound 6A1 might be highly protein bound thus leading to its low activity in the colon. A simple membrane dialysis after incubating 6A1 with human serum albumin or blood will help elucidate the amount of unbound drug available to reach target.

Currently, it is hypothesized that the ability of 6A1 to regress colonic polyps is via the inhibition of the COX-2 enzyme that leads to production of the PGE_2. However, emerging data and publications suggest that the COX-2 dependent inhibition pathway is one of many antineoplastic mechanisms observed in NSAIDs. Also, the accumulation of systemic PGE_2 in the colon could also contribute to the progression of tumors. If there are other mechanisms and systemic PGE_2 significantly contributes to tumor progression, delivery of 6A1 to the colon and its enterohepatic recirculation pathway may be less effective than theorized towards the regression of polyposis. Further studies therefore are crucial to differentiating the origin of PGE_2 in the colon.

Another issue that may have contributed to the underperformance of 6A1 compared to Celebrex is the COX independent pathway (192). Numerous preclinical and clinical data indicated at a high NSAIDs drug exposure concentration, some other COX-independent pathways dominate the antineoplastic and antiproliferation (193). Perhaps COX-dependent

pathway is one of the contributing factors for polyposis formation in FAP but it is not the only one (194). By targeting COX-2 dependent pathway, we might have omitted other mechanisms leading to the underperformance observed in 6A1.

In vivo studies are in progress with the aim of achieving a higher success rate using better, more potent COX-2 inhibitors. The completion of these studies using the F344 model will help establish the pharmacokinetic mechanism of such a drug delivery system. Further, investigation of the 6A1 pharmacodynamic mechanism is needed for a successful translational study. The in vivo data suggested that these innovative approaches are the most promising. A combined approach of both pH dependent and time-dependent particulate systems is highly desirable for use in a true colon-specific drug delivery system. The combined approach may reduce the side effects of the drug caused by absorption from the stomach when given in the form of raw drugs. There are still several challenges, which need further input from the committee's cumulative experience. The ultimate goal of this research is to apply the knowledge discovered herein to bring comfort to patients.

BIBLIOGRAPHY

1. Half E, Bercovich D, Rozen P. Familial adenomatous polyposis. Orphanet J Rare Dis. 2009;4:22. Epub 2009/10/14. doi: 10.1186/1750-1172-4-22. PubMed PMID: 19822006; PMCID: PMC2772987.
2. Attard TM, Cuffari C, Tajouri T, Stoner JA, Eisenberg MT, Yardley JH, Abraham SC, Perry D, Vanderhoof J, Lynch H. Multicenter experience with upper gastrointestinal polyps in pediatric patients with familial adenomatous polyposis. Am J Gastroenterol. 2004;99(4):681-6. Epub 2004/04/20. doi: 10.1111/j.1572-0241.2004.04115.x. PubMed PMID: 15089902.
3. Baglioni S, Genuardi M. Simple and complex genetics of colorectal cancer susceptibility. Am J Med Genet C Semin Med Genet. 2004;129C(1):35-43. Epub 2004/07/21. doi: 10.1002/ajmg.c.30023. PubMed PMID: 15264271.
4. Ashburn JH, Kalady MF. Adenomatous Polyposis Syndromes: Familial Adenomatous Polyposis and MutYH-Associated Polyposis. Current Colorectal Cancer Reports. 2017;13(4):302-9. doi: 10.1007/s11888-017-0379-0.
5. Kinney AY, Hicken B, Simonsen SE, Venne V, Lowstuter K, Balzotti J, Burt RW. Colorectal cancer surveillance behaviors among members of typical and attenuated FAP families. Am J Gastroenterol. 2007;102(1):153-62. Epub 2007/02/03. doi: 10.1111/j.1572-0241.2006.00860.x. PubMed PMID: 17266693.
6. Arber N, Lieberman D, Wang TC, Zhang R, Sands GH, Bertagnolli MM, Hawk ET, Eagle C, Coindreau J, Zauber A, Lanas A, Levin B. The APC and PreSAP trials: a post hoc noninferiority analysis using a comprehensive new measure for gastrointestinal tract injury in 2 randomized, double-blind studies comparing celecoxib and placebo. Clin Ther. 2012;34(3):569-79. doi: 10.1016/j.clinthera.2012.02.001. PubMed PMID: 22386831.
7. James AS, Chisholm P, Wolin KY, Baxter M, Kaphingst K, Davidson NO. Screening and Health Behaviors among Persons Diagnosed with Familial Adenomatous Polyposis and Their Relatives. J Cancer Epidemiol. 2012;2012:506410. Epub 2012/08/18. doi: 10.1155/2012/506410. PubMed PMID: 22899922; PMCID: PMC3414059.
8. Tudyka VNC, S.K. Surgical treatment in familial adenomatous polyposis. Annals of Gastroenerology. 2012;25:201-6.
9. Archive USFaDAF. COX-2 Selective (includes Bextra, Celebrex, and Vioxx) and Non-Selective Non-Steroidal Anti-Inflammatory Drugs (NSAIDs) 10903 New Hampshire Avenue
Silver Spring, MD 20993: US FDA; 01/09/2015 [updated 01/09/2015; cited 2017 10/09]Cox-2 selective Drugs]. Available from: https://www.fda.gov/drugs/drugsafety/postmarketdrugsafetyinformationforpatientsandproviders/ucm429364.htm.

10. Cheng Y, et.al.; . Role of prostacyclin in the cardiovascular response to thromboxane A2. Science Direct. 2002;6087:1386-7.
11. Varga Z, Sabzwari SRA, Vargova V. Cardiovascular Risk of Nonsteroidal Anti-Inflammatory Drugs: An Under-Recognized Public Health Issue. Cureus. 2017;9(4):e1144. Epub 2017/05/12. doi: 10.7759/cureus.1144. PubMed PMID: 28491485; PMCID: PMC5422108.
12. Subbaramaiah KD, A.J. Cyclooxygenase 2: a molecular target for cancer prevention and treatment. Pharmacological Sciences. 2003;24(2):7.
13. Simmons DL, Botting RM, Hla T. Cyclooxygenase isozymes: the biology of prostaglandin synthesis and inhibition. Pharmacol Rev. 2004;56(3):387-437. doi: 10.1124/pr.56.3.3. PubMed PMID: 15317910.
14. FitzGerald GA. Coxibs and Cardiovascular Disease. N Engl J Med. 2004;351(17).
15. Patrono C. Cardiovascular Effects of Nonsteroidal Anti-inflammatory Drugs. Curr Cardiol Rep. 2016;18(3).
16. Baron JA, Sandler RS, Bresalier RS, Lanas A, Morton DG, Riddell R, Iverson ER, Demets DL. Cardiovascular events associated with rofecoxib: final analysis of the APPROVe trial. Lancet. 2008;372(9651):1756-64. Epub 2008/10/17. doi: 10.1016/s0140-6736(08)61490-7. PubMed PMID: 18922570.
17. Bertagnolli MM, Eagle CJ, Zauber AG, Redston M, Solomon SD, Kim K, Tang J, Rosenstein RB, Wittes J, Corle D, Hess TM, Woloj GM, Boisserie F, Anderson WF, Viner JL, Bagheri D, Burn J, Chung DC, Dewar T, Foley TR, Hoffman N, Macrae F, Pruitt RE, Saltzman JR, Salzberg B, Sylwestrowicz T, Gordon GB, Hawk ET. Celecoxib for the prevention of sporadic colorectal adenomas. N Engl J Med. 2006;355(9):873-84. Epub 2006/09/01. doi: 10.1056/NEJMoa061355. PubMed PMID: 16943400.
18. Bresalier RS, Et. Al., . Cardiovascular events associated with rofecoxib in colorectal adenoma chemoprevention trial. N Engl J Med. 2005;352(11):1092-9.
19. Nikam VKK, K.B.; Gaware, V.M.; Dolas, T.R.; Dhamak, K.B.; Somwanshi, K.B; Khadse, A.N.; Kashid, V.A. Eudragit a versatile polymer: a review. Pharmacologyonline. 2011;1:12.
20. Antman EMD, D; Loscalzo, J. Cyclooxygenase inhibition and cardiovascular risk. Circulation. 2005;112(5):759-70.
21. McAdam BFea. Systemic biosynthesis of prostacyclin by cocloogenenase (COX)-2: the human pharcology of a selective inhibitor of COX-2. Proceedings of the National Academy of Sciences of the United States of America. 1999;96(1):272-7.
22. Steinbach G, M.D., PhD., Lynch, Patrick M,M.D., J.D., Phillips, Robin KS,M.B., B.S., Wallace, Marina H,M.B., B.S., Hawk, Ernest,M.D., M.P.H., Gordon, Gary B,M.D., PhD., . . . Kelloff, G. The effect of celecoxib, a cyclooxygenase-2 inhibitor, in familial adenomatous polyposis. The New England Journal of Medicine. 2000;342(26), 1946-52.
23. Steinbach G, Lynch PM, Phillips RK, Wallace MH, Hawk E, Gordon GB, Wakabayashi N, Saunders B, Shen Y, Fujimura T, Su LK, Levin B, Godio L, Patterson S, Rodriguez-Bigas MA, Jester SL, King KL, Schumacher M, Abbruzzese J, DuBois RN,

Hittelman WN, Zimmerman S, Sherman JW, Kelloff G. The effect of celecoxib, a cyclooxygenase-2 inhibitor, in familial adenomatous polyposis. N Engl J Med. 2000;342(26):1946-52. Epub 2000/06/30. doi: 10.1056/NEJM200006293422603. PubMed PMID: 10874062.
24. Su LK, Barnes CJ, Yao W, Qi Y, Lynch PM, Steinbach G. Inactivation of germline mutant APC alleles by attenuated somatic mutations: a molecular genetic mechanism for attenuated familial adenomatous polyposis. Am J Hum Genet. 2000;67(3):582-90. Epub 2000/08/05. doi: 10.1086/303058. PubMed PMID: 10924409; PMCID: PMC1287518.
25. Su LK, Steinbach G, Sawyer JC, Hindi M, Ward PA, Lynch PM. Genomic rearrangements of the APC tumor-suppressor gene in familial adenomatous polyposis. Hum Genet. 2000;106(1):101-7. Epub 2000/09/12. PubMed PMID: 10982189.
26. Sheng JQ, Li SR, Yang XY, Zhang YH, Su H, Yu DL, Yan W, Geng HG. Clinical management of adenomatous polyposis in patients with hereditary non-polyposis colorectal cancer and familial adenomatous polyposis. Zhonghua Yi Xue Za Zhi. 2006;86(8):526-9. Epub 2006/05/10. PubMed PMID: 16681880.
27. Phillips RK, Wallace MH, Lynch PM, Hawk E, Gordon GB, Saunders BP, Wakabayashi N, Shen Y, Zimmerman S, Godio L, Rodrigues-Bigas M, Su LK, Sherman J, Kelloff G, Levin B, Steinbach G. A randomised, double blind, placebo controlled study of celecoxib, a selective cyclooxygenase 2 inhibitor, on duodenal polyposis in familial adenomatous polyposis. Gut. 2002;50(6):857-60. Epub 2002/05/16. doi: 10.1136/gut.50.6.857. PubMed PMID: 12010890; PMCID: PMC1773237.
28. Katz JA. COX-2 inhibition: what we learned--a controversial update on safety data. Pain Med. 2013;14 Suppl 1:S29-34. Epub 2014/01/01. doi: 10.1111/pme.12252. PubMed PMID: 24373107.
29. Higuchi T, Iwama T, Yoshinaga K, Toyooka M, Taketo MM, Sugihara K. A randomized, double-blind, placebo-controlled trial of the effects of rofecoxib, a selective cyclooxygenase-2 inhibitor, on rectal polyps in familial adenomatous polyposis patients. Clin Cancer Res. 2003;9(13):4756-60. Epub 2003/10/29. PubMed PMID: 14581346.
30. Kerr DJ, Dunn JA, Langman MJ, Smith JL, Midgley RS, Stanley A, Stokes JC, Julier P, Iveson C, Duvvuri R, McConkey CC. Rofecoxib and cardiovascular adverse events in adjuvant treatment of colorectal cancer. N Engl J Med. 2007;357(4):360-9. Epub 2007/07/27. doi: 10.1056/NEJMoa071841. PubMed PMID: 17652651.
31. FitzGerald GA. Coxibs and Cardiovascular Disease. The New England Journal of Medicine. 2004;351(17):1709-11. doi: 10.1056/NEJMp048288.
32. Lynch PM, Ayers GD, Hawk E, Richmond E, Eagle C, Woloj M, Church J, Hasson H, Patterson S, Half E, Burke CA. The safety and efficacy of celecoxib in children with familial adenomatous polyposis. Am J Gastroenterol. 2010;105(6):1437-43. Epub 2010/03/18. doi: 10.1038/ajg.2009.758. PubMed PMID: 20234350.
33. Chandrasekharan NVS, D.L. The Cyclooxygenase. Genome Biology. 2004;5(9):241.

34. Rouzer CA, Marnett LJ. Cyclooxygenases: structural and functional insights. J Lipid Res. 2009;50 Suppl:S29-34. Epub 2008/10/28. doi: 10.1194/jlr.R800042-JLR200. PubMed PMID: 18952571; PMCID: PMC2674713.
35. Arico S, Pattingre S, Bauvy C, Gane P, Barbat A, Codogno P, Ogier-Denis E. Celecoxib induces apoptosis by inhibiting 3-phosphoinositide-dependent protein kinase-1 activity in the human colon cancer HT-29 cell line. The Journal of biological chemistry. 2002;277(31):27613-21. Epub 2002/05/10. doi: 10.1074/jbc.M201119200. PubMed PMID: 12000750.
36. Sobolewski C, Cerella C, Dicato M, Ghibelli L, Diederich M. The role of cyclooxygenase-2 in cell proliferation and cell death in human malignancies. Int J Cell Biol. 2010;2010:215158. Epub 2010/03/27. doi: 10.1155/2010/215158. PubMed PMID: 20339581; PMCID: PMC2841246.
37. Araki YSO, S.; Hussain, P.; Nagashima, M.; He, P.; Shiseki, M.; Miura, K.; Harris, C.;. Regulation of Cyclooxygenase-2 Expression by the Wnt and Ras Pathway. Cancer research. 2003;63:728-34.
38. Kolligs FT, Bommer G, Goke B. Wnt/beta-catenin/tcf signaling: a critical pathway in gastrointestinal tumorigenesis. Digestion. 2002;66(3):131-44. Epub 2002/12/14. doi: 10.1159/000066755. PubMed PMID: 12481159.
39. Carlson MW, E.T.; Prescott, S.M.;. Regulation of COX-2 transcription in colon cancer cell line by Pontin52:TIP49a. Molecular Cancer. 2003;2(42).
40. Amidon S, Brown JE, Dave VS. Colon-targeted oral drug delivery systems: design trends and approaches. AAPS PharmSciTech. 2015;16(4):731-41. doi: 10.1208/s12249-015-0350-9. PubMed PMID: 26070545; PMCID: PMC4508299.
41. Sharma S, Sinha VR. Current pharmaceutical strategies for efficient site specific delivery in inflamed distal intestinal mucosa. Journal of controlled release : official journal of the Controlled Release Society. 2018;272:97-106. Epub 2018/01/11. doi: 10.1016/j.jconrel.2018.01.003. PubMed PMID: 29317245.
42. Zhang M, Merlin D. Nanoparticle-Based Oral Drug Delivery Systems Targeting the Colon for Treatment of Ulcerative Colitis. Inflamm Bowel Dis. 2018;24(7):1401-15. Epub 2018/05/23. doi: 10.1093/ibd/izy123. PubMed PMID: 29788186; PMCID: PMC6085987.
43. McConnell EL, Fadda HM, Basit AW. Gut instincts: explorations in intestinal physiology and drug delivery. International journal of pharmaceutics. 2008;364(2):213-26. Epub 2008/07/08. doi: 10.1016/j.ijpharm.2008.05.012. PubMed PMID: 18602774.
44. Guo Y, Zong S, Pu Y, Xu B, Zhang T, Wang B. Advances in Pharmaceutical Strategies Enhancing the Efficiencies of Oral Colon-Targeted Delivery Systems in Inflammatory Bowel Disease. Molecules. 2018;23(7). Epub 2018/07/06. doi: 10.3390/molecules23071622. PubMed PMID: 29973488; PMCID: PMC6099616.
45. Patel SK, Zhang Y, Pollock JA, Janjic JM. Cyclooxgenase-2 inhibiting perfluoropoly (ethylene glycol) ether theranostic nanoemulsions-in vitro study. PLoS

One. 2013;8(2):e55802. Epub 2013/02/15. doi: 10.1371/journal.pone.0055802. PubMed PMID: 23409048; PMCID: PMC3567136.
46. Rao J, McClements DJ. Formation of flavor oil microemulsions, nanoemulsions and emulsions: influence of composition and preparation method. J Agric Food Chem. 2011;59(9):5026-35. Epub 2011/03/18. doi: 10.1021/jf200094m. PubMed PMID: 21410259.
47. Authors M. Nanoemulsions-Nanoarchitectonics for smart delivery and drug targeting2016-2017.
48. McConnell EL, Liu F, Basit AW. Colonic treatments and targets: issues and opportunities. J Drug Target. 2009;17(5):335-63. Epub 2009/06/27. doi: 10.1080/10611860902839502. PubMed PMID: 19555265.
49. Cisterna BAK, N.; Choi, W.II.; Tavakkoli, A.; Farokhazad, O.C.; Vilos, C. Targeting NP for CRC. Nanomedicine. 2016;11(18):2443.
50. Kraft JC, Freeling JP, Wang Z, Ho RJ. Emerging research and clinical development trends of liposome and lipid nanoparticle drug delivery systems. J Pharm Sci. 2014;103(1):29-52. Epub 2013/12/18. doi: 10.1002/jps.23773. PubMed PMID: 24338748; PMCID: PMC4074410.
51. Authors C. Liposome: Nano and microscale drug delivery system. Science Direct. 2017.
52. Pileri P, Campagnoli S, Grandi A, Parri M, De Camilli E, Song C, Ganfini L, Lacombe A, Naldi I, Sarmientos P, Cinti C, Jin B, Grandi G, Viale G, Terracciano L, Grifantini R. FAT1: a potential target for monoclonal antibody therapy in colon cancer. Br J Cancer. 2016;115(1):40-51. Epub 2016/06/22. doi: 10.1038/bjc.2016.145. PubMed PMID: 27328312; PMCID: PMC4931367.
53. Feng T, Wei Y, Lee RJ, Zhao L. Liposomal curcumin and its application in cancer. Int J Nanomedicine. 2017;12:6027-44. Epub 2017/09/02. doi: 10.2147/IJN.S132434. PubMed PMID: 28860764; PMCID: PMC5573051.
54. Krajewska JBB, A.; Fichna, J. New Trends in Liposome-based Drug Delivery In Colorectal Cancer. Mini-Reviews in Medicinal Chemistry. 2019;19(1). doi: 10.2174/1389557518666180903150928.
55. Nguyen TXH, L; Gauthier, M; Yang, G; Wang, Q.;. Recent advances in liposomes surface modification for oral drug delivery. Nanomedicine. 2016;11(9). doi: 1748-6963.
56. Grifantini R, Taranta M, Gherardini L, Naldi I, Parri M, Grandi A, Giannetti A, Tombelli S, Lucarini G, Ricotti L, Campagnoli S, De Camilli E, Pelosi G, Baldini F, Menciassi A, Viale G, Pileri P, Cinti C. Magnetically driven drug delivery systems improving targeted immunotherapy for colon-rectal cancer. Journal of controlled release : official journal of the Controlled Release Society. 2018;280:76-86. Epub 2018/05/08. doi: 10.1016/j.jconrel.2018.04.052. PubMed PMID: 29733876.

57. Evans DFP, G.; Bramley, R.; Clark, A.G; Dyson, T.J.; Hardcastle, J.D Measurement of gastrointesinal pH profiles in normal ambulant human subjects. Gut. 1988;29:1035-41.
58. Fallingborg JC, L.A.; Ingeman-Neilsen, M.; Jacobsen, B.A.; Abildgaard, K.; Rasmussen, H.H. pH-profile and regional transit times of the normal gut measured by a radiotelemetry device. Ailment Pharmacol Ther. 1989;3(6).
59. Lamprecht AS, Ulrich ; Lehr, Claus-Michael Size dependent bioadhesion of micro and nanoparticulate carrier to the inflammed colonic mucosa. Pharmaceutical Research. 2001;18(6):6.
60. Fadda HM, McConnell EL, Short MD, Basit AW. Meal-induced acceleration of tablet transit through the human small intestine. Pharm Res. 2009;26(2):356-60. Epub 2008/11/05. doi: 10.1007/s11095-008-9749-2. PubMed PMID: 18982248.
61. Ibekwe VC, Fadda HM, McConnell EL, Khela MK, Evans DF, Basit AW. Interplay between intestinal pH, transit time and feed status on the in vivo performance of pH responsive ileo-colonic release systems. Pharmaceutical Research. 2008;25:1828-35.
62. Nugent SK, D.; Rampton, D.; Evans, D. Intestinal luminal pH in inflammatory bowel disease: possible determinants and implications for therapu with aminosalicylates and other drugs. Gut. 2001;48:571-7.
63. Basit AW, & McConnell E. I. . Drug Delivery to the Colon. In: Delivery CRiOD, editor. Oral Drug Delivery: New York: Springer.
; 2001. p. 386
.
64. Ibekwe VC, Liu F, Fadda HM, Khela MK, Evans DF, Parsons GE, Basit AW. An investigation into the in vivo performance variability of pH responsive polymers for ileo-colonic drug delivery using gamma scintigraphy in humans. J Pharmaceutical Sci. 2006;95:2760-76.
65. Hardy JGL, S.W.; Clark, A.G. Enema volume and spreading. International journal of pharmaceutics. 1986;31:151-5.
66. Pang X, Jiang Y, Xiao Q, Leung AW, Hua H, Xu C. pH-responsive polymer-drug conjugates: Design and progress. Journal of controlled release : official journal of the Controlled Release Society. 2016;222:116-29. Epub 2015/12/26. doi: 10.1016/j.jconrel.2015.12.024. PubMed PMID: 26704934.
67. Maurer AH. Gastrointestinal Motility, Part 2: Small-Bowel and Colon Transit. Journal of Nuclear Medicine Technology. 2016;44(1):12-8. doi: 10.2967/jnumed.113.134551.
68. Weitschies W, Wilson CG. In vivo imaging of drug delivery systems in the gastrointestinal tract. International journal of pharmaceutics. 2011;417(1-2):216-26. doi: 10.1016/j.ijpharm.2011.07.031. PubMed PMID: 21820499.
69. Davis SSH, J.G; Fara, J.W. Transit of pharmaceutical dosage forms through the small intestine. Gut. 1986;27:886-92.

70. Hebden JM, Gilchrist PJ, Blackshaw EF, M.E.; Perkins, A.C., Wilson CG, Spiller RC. Night-time quiescence and morning activation in the human colon: effect on transit of dispersed and large single unit fomulations. Eur J Gastroenterol Hepatol. 1999;11(12):1379-85.
71. Gorbach S, Nahas L, Weinstein L, Levitan R, Patterson J. Studies of intestinal microflora. IV. The microflora of ileostomy effluent: a unique microbial ecology. Gastroenterology. 1967(6).
72. Hill M, Drasar BS. The normal colonic bacterial flora. From the bacterial metabolism research lab. 1975.
73. Sinha VR, Kumria R. Polysaccharide matrices for microbially triggered drug delivery to the colon. Drug Dev Ind Pharm. 2004;30(2):143-50. Epub 2004/04/20. doi: 10.1081/DDC-120028709. PubMed PMID: 15089048.
74. Jain A, Gupta Y, Jain SK. Potential of calcium pectinate beads for target specific drug release to colon. J Drug Target. 2007;15(4):285-94. Epub 2007/05/10. doi: 10.1080/10611860601146134. PubMed PMID: 17487697.
75. Vandamme F, Lenourry A, Charrueau C, Chaumeil JC. The use of polysaccharides to target drugs to the colon. J Carbohydrate Polymers. 2002:219-31.
76. Bliss DZ, Weimer PJ, Jung HJ, Savik K. In vitro degradation and fermentation of three dietary fiber sources by human colonic bacteria. J Agric Food Chem. 2013;61(19):4614-21. Epub 2013/04/06. doi: 10.1021/jf3054017. PubMed PMID: 23556460; PMCID: PMC3668776.
77. Siew LF, Man SM, Newton JM, Basit AW. Amylose formulations for drug delivery to the colon: a comparison of two fermentation models to assess colonic targeting performance in vitro,. International Journal of Pharmaceutics,. 2004;273(1-2):129-34.
78. Larsen EM, Johnson RJ. Microbial esterases and ester prodrugs: An unlikely marriage for combating antibiotic resistance. Drug Dev Res. 2019;80(1):33-47. Epub 2018/10/12. doi: 10.1002/ddr.21468. PubMed PMID: 30302779; PMCID: PMC6377847.
79. Katsuma MW, S.; Takemura, S. et.al.; . Scintigraphic Evaluation of a Novel Colon-Targeted Deliery System (CODES) in Healthy Volunteers. J of Pharmaceutical Science. 2003;93(5).
80. Kim DJ, YH. Intestinal bacterial Beta-glucuronidase activity of patients wiht colon cancer. Arch Pharm Res. 2001;24(6):3.
81. Ibekwe VC, Khela MK, Evans DF, Basit AW. A new concept in colonic drug targeting: a combined pH-responsive and bacterially-triggered drug delivery technology. Aliment Pharmacol Ther. 2008;28(7):911-6. Epub 2008/07/24. doi: 10.1111/j.1365-2036.2008.03810.x. PubMed PMID: 18647282.
82. Pastorelli L, Saibeni S, Spina L, Signorelli C, Celasco G, de Franchis R, Vecchi M. Oral, colonic-release low-molecular-weight heparin: an initial open study of Parnaparin-MMX for the treatment of mild-to-moderate left-sided ulcerative colitis.

Aliment Pharmacol Ther. 2008;28(5):581-8. Epub 2008/08/15. doi: 10.1111/j.1365-2036.2008.03757.x. PubMed PMID: 18700898.
83. Brunner MG, R. et. al.;. <Brunner 2003.pdf>. Alimen Pharmacol Ther. 2003;17:1163-69. doi: 10.1046/j.0269-2813.2003.01564.x.
84. Brunner M, Ziegler S, Di Stefano AF, Dehghanyar P, Kletter K, Tschurlovits M, Villa R, Bozzella R, Celasco G, Moro L, Rusca A, Dudczak R, Muller M. Gastrointestinal transit, release and plasma pharmacokinetics of a new oral budesonide formulation. Br J Clin Pharmacol. 2006;61(1):31-8. Epub 2006/01/05. doi: 10.1111/j.1365-2125.2005.02517.x. PubMed PMID: 16390349; PMCID: PMC1884991.
85. SaintyCo IPPP. Classification & Types of Tablet Coating Machine (Learn How to Choose the Right Tablet Coater). In: Dr. M. Gohel; Kiranmai; A. Basu AD, S. Dey, editor. p. https://www.saintytec.com/types-of-tablet-coating-machine/.
86. Qiao M, Zhang L, Ma Y, Zhu J, Chow K. A novel electrostatic dry powder coating process for pharmaceutical dosage forms: immediate release coatings for tablets. Eur J Pharm Biopharm. 2010;76(2):304-10. Epub 2010/07/06. doi: 10.1016/j.ejpb.2010.06.009. PubMed PMID: 20600889.
87. Patil H, Tiwari RV, Repka MA. Hot-Melt Extrusion: from Theory to Application in Pharmaceutical Formulation. AAPS PharmSciTech. 2016;17(1):20-42. doi: 10.1208/s12249-015-0360-7.
88. Castaneda-Hernandez G, Caille G, du Souich P. Influence of drug formulation on drug concentration-effect relationships. Clinical pharmacokinetics. 1994;26(2):135-43. Epub 1994/02/01. doi: 10.2165/00003088-199426020-00006. PubMed PMID: 8162657.
89. Leucuta SE. Selecting oral bioavailability enhancing formulations during drug discovery and development. Expert opinion on drug discovery. 2014;9(2):139-50. Epub 2014/01/07. doi: 10.1517/17460441.2014.877881. PubMed PMID: 24387781.
90. Stuurman FE, Nuijen B, Beijnen JH, Schellens JH. Oral anticancer drugs: mechanisms of low bioavailability and strategies for improvement. Clinical pharmacokinetics. 2013;52(6):399-414. Epub 2013/02/20. doi: 10.1007/s40262-013-0040-2. PubMed PMID: 23420518.
91. Maddaford SP. A medicinal chemistry perspective on structure-based drug design and development. Methods Mol Biol. 2012;841:351-81. Epub 2012/01/10. doi: 10.1007/978-1-61779-520-6_15. PubMed PMID: 22222460.
92. Tang W, Lu AY. Drug metabolism and pharmacokinetics in support of drug design. Current pharmaceutical design. 2009;15(19):2170-83. Epub 2009/07/16. PubMed PMID: 19601821.
93. Lalka D, Griffith RK, Cronenberger CL. The hepatic first-pass metabolism of problematic drugs. Journal of clinical pharmacology. 1993;33(7):657-69. Epub 1993/07/01. PubMed PMID: 8366191.
94. Yang Z, Zhu W, Gao S, Yin T, Jiang W, Hu M. Breast cancer resistance protein (ABCG2) determines distribution of genistein phase II metabolites: reevaluation of the roles of ABCG2 in the disposition of genistein. Drug metabolism and disposition: the

biological fate of chemicals. 2012;40(10):1883-93. Epub 2012/06/28. doi: 10.1124/dmd.111.043901. PubMed PMID: 22736306; PMCID: 3463821.
95. Alvarez AI, Vallejo F, Barrera B, Merino G, Prieto JG, Tomas-Barberan F, Espin JC. Bioavailability of the glucuronide and sulfate conjugates of genistein and daidzein in breast cancer resistance protein 1 knockout mice. Drug metabolism and disposition: the biological fate of chemicals. 2011;39(11):2008-12. Epub 2011/08/11. doi: 10.1124/dmd.111.040881. PubMed PMID: 21828252.
96. Gu L, House SE, Prior RL, Fang N, Ronis MJ, Clarkson TB, Wilson ME, Badger TM. Metabolic phenotype of isoflavones differ among female rats, pigs, monkeys, and women. The Journal of nutrition. 2006;136(5):1215-21. Epub 2006/04/15. PubMed PMID: 16614407.
97. Iyanagi T. Molecular mechanism of phase I and phase II drug-metabolizing enzymes: implications for detoxification. International review of cytology. 2007;260:35-112. Epub 2007/05/08. doi: 10.1016/s0074-7696(06)60002-8. PubMed PMID: 17482904.
98. Tukey RH, Strassburg CP. Human UDP-glucuronosyltransferases: metabolism, expression, and disease. Annu Rev Pharmacol Toxicol. 2000;40:581-616. doi: 10.1146/annurev.pharmtox.40.1.581. PubMed PMID: 10836148.
99. Gamage N, Barnett A, Hempel N, Duggleby RG, Windmill KF, Martin JL, McManus ME. Human sulfotransferases and their role in chemical metabolism. Toxicol Sci. 2006;90(1):5-22. PubMed PMID: 16322073.
100. Wu B, Kulkarni K, Basu S, Zhang S, Hu M. First-pass metabolism via UDP-glucuronosyltransferase: a barrier to oral bioavailability of phenolics. J Pharm Sci. 2011;100(9):3655-81. doi: 10.1002/jps.22568. PubMed PMID: 21484808; PMCID: PMC3409645.
101. Beyerle J, Frei E, Stiborova M, Habermann N, Ulrich CM. Biotransformation of xenobiotics in the human colon and rectum and its association with colorectal cancer. Drug metabolism reviews. 2015;47(2):199-221. Epub 2015/02/18. doi: 10.3109/03602532.2014.996649. PubMed PMID: 25686853.
102. Chen J, Wang S, Jia X, Bajimaya S, Lin H, Tam VH, Hu M. Disposition of flavonoids via recycling: comparison of intestinal versus hepatic disposition. Drug metabolism and disposition: the biological fate of chemicals. 2005;33(12):1777-84. Epub 2005/08/27. doi: 10.1124/dmd.105.003673. PubMed PMID: 16120792.
103. Watanabe Y, Nakajima M, Yokoi T. Troglitazone glucuronidation in human liver and intestine microsomes: high catalytic activity of UGT1A8 and UGT1A10. Drug metabolism and disposition: the biological fate of chemicals. 2002;30(12):1462-9. Epub 2002/11/16. PubMed PMID: 12433820.
104. Roberts MS, Magnusson BM, Burczynski FJ, Weiss M. Enterohepatic circulation: physiological, pharmacokinetic and clinical implications. Clinical pharmacokinetics. 2002;41(10):751-90. Epub 2002/08/07. doi: 10.2165/00003088-200241100-00005. PubMed PMID: 12162761.

105. Gao Y, Shao J, Jiang Z, Chen J, Gu S, Yu S, Zheng K, Jia L. Drug enterohepatic circulation and disposition: constituents of systems pharmacokinetics. Drug Discov Today. 2014;19(3):326-40. doi: 10.1016/j.drudis.2013.11.020. PubMed PMID: 24295642.
106. LaRusso NF, Korman MG, Hoffman NE, Hofmann AF. Dynamics of the enterohepatic circulation of bile acids. Postprandial serum concentrations of conjugates of cholic acid in health, cholecystectomized patients, and patients with bile acid malabsorption. The New England journal of medicine. 1974;291(14):689-92. Epub 1974/10/03. doi: 10.1056/NEJM197410032911401. PubMed PMID: 4851463.
107. Lucas C, Barnich N, Nguyen HTT. Microbiota, Inflammation and Colorectal Cancer. Int J Mol Sci. 2017;18(6). doi: 10.3390/ijms18061310. PubMed PMID: 28632155; PMCID: PMC5486131.
108. Sheil BS, F.; O'Mahony, L. Probiotic Effects on IBD 2007. The Journal of Nutrition. 2007;137(3):5.
109. Zhang X, Dong D, Wang H, Ma Z, Wang Y, Wu B. Stable knock-down of efflux transporters leads to reduced glucuronidation in UGT1A1-overexpressing HeLa cells: the evidence for glucuronidation-transport interplay. Molecular pharmaceutics. 2015;12(4):1268-78. doi: 10.1021/mp5008019. PubMed PMID: 25741749.
110. Zhang J, Lacroix C, Wortmann E, Ruscheweyh HJ, Sunagawa S, Sturla SJ, Schwab C. Gut microbial beta-glucuronidase and glycerol/diol dehydratase activity contribute to dietary heterocyclic amine biotransformation. BMC Microbiol. 2019;19(1):99. Epub 2019/05/18. doi: 10.1186/s12866-019-1483-x. PubMed PMID: 31096909; PMCID: PMC6524314.
111. Kirkby NS LM, Harrington LS, Leadbeater PD, Milne GL, Al-Yamani M, Adeyemi O, Warner TD, Mitchell JA. Cyclooxygenase-1, not cyclooxygenase-2, is responsible for physiological production of prostacyclin in the cardiovascular system. Proceedings of the National Academy of Sciences of the United States of America. 2012;109(43):7. Epub 2012 Oct 23. doi: 10.1073/pnas.1209192109; PMCID: PMC3491520.
112. Laine L, Connors LG, Reicin A, Hawkey CJ, Burgos-Vargas R, Schnitzer TJ, Yu Q, Bombardier C. Serious lower gastrointestinal clinical events with nonselective NSAID or coxib use. Gastroenterology. 2003;124(2):288-92. doi: 10.1053/gast.2003.50054. PubMed PMID: 12557133.
113. Hu M, Ma Y, Gao S, inventorsLocally Bioavailable Drugs. USA2016.
114. Wang D, Dubois RN. The role of COX-2 in intestinal inflammation and colorectal cancer. Oncogene. 2010;29(6):781-8. Epub 2009/12/01. doi: 10.1038/onc.2009.421. PubMed PMID: 19946329; PMCID: PMC3181054.
115. Brandao RD, Veeck J, Van de Vijver KK, Lindsey P, de Vries B, van Elssen CH, Blok MJ, Keymeulen K, Ayoubi T, Smeets HJ, Tjan-Heijnen VC, Hupperets PS. A randomised controlled phase II trial of pre-operative celecoxib treatment reveals anti-tumour transcriptional response in primary breast cancer. Breast Cancer Res.

2013;15(2):R29. doi: 10.1186/bcr3409. PubMed PMID: 23566419; PMCID: PMC3672758.
116. Sano H, Kawahito Y, Hashiramoto A, Mukai S, Asai K, Kimura S, Kato H, Kondo M, Hla T. Expression of Cox 1 and cox 2 in Human colorectal cancer. Cancer research. 1995;55(17):4.
117. Ogino S, Kirkner GJ, Nosho K, Irahara N, Kure S, Shima K, Hazra A, Chan AT, Dehari R, Giovannucci EL, Fuchs CS. Cyclooxygenase-2 expression is an independent predictor of poor prognosis in colon cancer. Clin Cancer Res. 2008;14(24):8221-7. Epub 2008/12/18. doi: 10.1158/1078-0432.CCR-08-1841. PubMed PMID: 19088039; PMCID: PMC2679582.
118. Ricciotti E, Yu Y, Grosser T, Fitzgerald GA. COX-2, the dominant source of prostacyclin. Proceedings of the National Academy of Sciences of the United States of America. 2013;110(3):E183. doi: 10.1073/pnas.1219073110. PubMed PMID: 23292931; PMCID: PMC3549068.
119. Staff NCI. Drug combination shrinks duodnal polyps in people with familial adenomatous polyposis: National Cancer Institute 2016 [cited 2017 October 9]. Available from: https://www.cancer.gov/news-events/cancer-currents-blog/2016/erlotinib-sulindac-fap.
120. Gong L, Thorn CF, Bertagnolli MM, Grosser T, Altman RB, Klein TE. Celecoxib pathways: pharmacokinetics and pharmacodynamics. Pharmacogenetics and genomics. 2012;22(4):310-8. Epub 2012/02/18. doi: 10.1097/FPC.0b013e32834f94cb. PubMed PMID: 22336956; PMCID: Pmc3303994.
121. Zamek-Gliszczynski MJ, Hoffmaster KA, Nezasa K, Tallman MN, Brouwer KL. Integration of hepatic drug transporters and phase II metabolizing enzymes: mechanisms of hepatic excretion of sulfate, glucuronide, and glutathione metabolites. European journal of pharmaceutical sciences : official journal of the European Federation for Pharmaceutical Sciences. 2006;27(5):447-86. doi: 10.1016/j.ejps.2005.12.007. PubMed PMID: 16472997.
122. Paulson SKV, M.B.; Jessen, S.M.; Lawal, Y.; Gresk, C.J.; Yan, B.; Maziasz, T.J.; Cook, C.S.; Karim, A. Pharmacokinetics of Celecoxib after Oral Administration in Dogs and Humans: Effect of Food and Site of Absorption. The Journal of pharmacology and experimental therapeutics. 2001;297(2):7. Epub January 22, 2001.
123. Paulson SKH, J. D.; Liu, K.W.N.; Hajdu, E.; Bible, R.H.JR.; Piergies, A.; Karim, A. Metabolism and Excretion of [14C] Celebrex in Healthy male volunteers. Drug Metabolism and Disposition. 1999;28(3):7.
124. Chan LMS, Lowes S, Hirst BH. The ABCs of drug transport in intestine and liver: efflux proteins limiting drug absorption and bioavailability. European Journal of Pharmaceutical Sciences. 2004;21(1):25-51. doi: 10.1016/j.ejps.2003.07.003.
125. Mazerska Z, Mroz A, Pawlowska M, Augustin E. The role of glucuronidation in drug resistance. Pharmacol Ther. 2016;159:35-55. doi: 10.1016/j.pharmthera.2016.01.009. PubMed PMID: 26808161.

126. Rowland A, Miners JO, Mackenzie PI. The UDP-glucuronosyltransferases: their role in drug metabolism and detoxification. Int J Biochem Cell Biol. 2013;45(6):1121-32. doi: 10.1016/j.biocel.2013.02.019. PubMed PMID: 23500526.
127. Wu BB, S.; Meng, S.; Wang, X.; Hu, M. Regioselective Sulfation and Glucuronidation of Phenolics: Insights into the stuctural Basis. Curr Drug Metab. 2011;12:16.
128. Ning J, Hou J, Wang P, Wu JJ, Dai ZR, Zou LW, Li W, Ge GB, Ma XC, Yang L. Interspecies variation in phase I metabolism of bufalin in hepatic microsomes from mouse, rat, dog, minipig, monkey, and human. Xenobiotica. 2015;45(11):954-60. Epub 2015/06/09. doi: 10.3109/00498254.2015.1035359. PubMed PMID: 26053559.
129. Xu H, Kulkarni KH, Singh R, Yang Z, Wang SW, Tam VH, Hu M. Disposition of naringenin via glucuronidation pathway is affected by compensating efflux transporters of hydrophilic glucuronides. Molecular pharmaceutics. 2009;6(6):1703-15. Epub 2009/09/10. doi: 10.1021/mp900013d. PubMed PMID: 19736994; PMCID: Pmc2941777.
130. An G, Morris ME. The sulfated conjugate of biochanin A is a substrate of breast cancer resistant protein (ABCG2). Biopharmaceutics & drug disposition. 2011;32(8):446-57. doi: 10.1002/bdd.772. PubMed PMID: 21910126.
131. Wang M, Yang G, He Y, Xu B, Zeng M, Ge S, Yin T, Gao S, Hu M. Establishment and use of new MDCK II cells overexpressing both UGT1A1 and MRP2 to characterize flavonoid metabolism via the glucuronidation pathway. Mol Nutr Food Res. 2016;60(9):1967-83. Epub 2016/02/03. doi: 10.1002/mnfr.201500321. PubMed PMID: 26833852; PMCID: PMC5358013.
132. Giacomini KMH, S. M.; Tweedie, D. J. ;Benet, L. Z.;Brouwer, K. L. ;Chu, X. ;Dahlin, A. ;Evers, R. ;Fischer, V.;Hillgren, K. M.;Hoffmaster, K. A.;Ishikawa, T.;Keppler, D.;Kim, R. B.;Lee, C. A.;Niemi, M.;Polli, J. W.;Sugiyama, Y.;Swaan, P. W.;. Ware, J. A.; Wright, S. H.; Yee, S. W. ;Zamek-Gliszczynski, M. J. ; Zhang, L. Membrane transporters in drug development. Nature reviews Drug discovery. 2010;9(3):215-36. doi: 10.1038/nrd3028. PubMed PMID: 20190787; PMCID: 3326076.
133. Roberts MSM, B.M.; Burczynski, F.J.; Weiss, M. Enterohepatic Circulation: Physiological, Pharmacokinetic and Clinical Implications. Clin Pharmacokinet 2002;41(10):39.
134. Fukuyama T, ; Yamaoka, K.; Ohata, Y.; Nakagawa, T. A New analysis method fo redispostion Kinetics of enterohepatic circulation of Diclofenac in Rats. Drug metabolism and disposition: the biological fate of chemicals. 1994;22(3):7.
135. Pellock SJ, Redinbo MR. Glucuronides in the gut: Sugar-driven symbioses between microbe and host. The Journal of biological chemistry. 2017;292(21):8569-76. doi: 10.1074/jbc.R116.767434. PubMed PMID: 28389557; PMCID: PMC5448086.
136. Yang GG, S.; Singh, R.; Basu, S.; Shatzer, K.; Zen, M.; Liu, J.; Tu, Y.; Zhang, C.; Wei, J.; Shi, J.; Zhu, L.; Liu, L.; Wang, Y.; Gao, S.; Hu, M. Glucuronidation: driving

factors and their impact on glucuronide disposition. Drug Metabolism Reviews. 2017;49(2):33.
137. Chan AT. Aspirin and familial adenomatous polyposis: coming full circle. Cancer Prev Res (Phila). 2011;4(5):623-7. doi: 10.1158/1940-6207.CAPR-11-0157. PubMed PMID: 21543340; PMCID: PMC3097995.
138. Pfiser CiNSP. PreSap NIH Web2001-2007. Available from: https://clinicaltrials.gov/ct2/show/study/NCT00141193.
139. CVM FC. Bioanalytical Method Validation-Guidance for Industry. 2018.
140. New LC, E.C.Y Evaluation of BEH C18, BEH HILIC, and HSS T3 (C18) column chemistries for the UPLC-MS-MS analysis of glutathione, glutathione disulfide, and opthalimic acid in mouse liver and human plasma. Journal of Chromatographic science. 2008;46:209-13.
141. Chang JHY, P.; Lee, T.; Klopf, W.; Takao, D. The Role of pH in the Glucuronidation of Raloxifene, Mycophenolic Acid and Ezetimibe. Molecular pharmaceutics. 2009;6(4):1216-27.
142. Romand S, Rudaz S, Guillarme D. Separation of substrates and closely related glucuronide metabolites using various chromatographic modes. J Chromatogr A. 2016;1435:54-65. Epub 2016/01/29. doi: 10.1016/j.chroma.2016.01.033. PubMed PMID: 26818236.
143. Chambers E, Wagrowski-Diehl DM, Lu Z, Mazzeo JR. Systematic and comprehensive strategy for reducing matrix effects in LC/MS/MS analyses. J Chromatogr B Analyt Technol Biomed Life Sci. 2007;852(1-2):22-34. Epub 2007/01/24. doi: 10.1016/j.jchromb.2006.12.030. PubMed PMID: 17236825.
144. Guo HXL, E. Phospholipid-based matrix effect in LC-MS bioanalysis. Bioanalysis. 2011;3(4):349-52.
145. Ma Y, Gao S, Hu M. Quantitation of celecoxib and four of its metabolites in rat blood by UPLC-MS/MS clarifies their blood distribution patterns and provides more accurate pharmacokinetics profiles. J Chromatogr B Analyt Technol Biomed Life Sci. 2015;1001:202-11. Epub 2015/08/19. doi: 10.1016/j.jchromb.2015.07.026. PubMed PMID: 26281772; PMCID: PMC4659650.
146. Loidolt P, Madlmeir S, Khinast JG. Mechanistic modeling of a capsule filling process. International journal of pharmaceutics. 2017;532(1):47-54. Epub 2017/09/06. doi: 10.1016/j.ijpharm.2017.08.125. PubMed PMID: 28870766.
147. Marques MR. Enzymes in the dissolution testing of gelatin capsules. AAPS PharmSciTech. 2014;15(6):1410-6. Epub 2014/06/20. doi: 10.1208/s12249-014-0162-3. PubMed PMID: 24942315; PMCID: PMC4245433.
148. Skov K, Oxfeldt M, Thogersen R, Hansen M, Bertram HC. Enzymatic Hydrolysis of a Collagen Hydrolysate Enhances Postprandial Absorption Rate-A Randomized Controlled Trial. Nutrients. 2019;11(5). Epub 2019/05/16. doi: 10.3390/nu11051064. PubMed PMID: 31086034; PMCID: PMC6566347.

149. Thoma KB, K. Enteric coated hard gelatin capsules. Capsulgel Tech Bull. 1986:1-17.
150. Gullapalli RP, Mazzitelli CL. Gelatin and Non-Gelatin Capsule Dosage Forms. J Pharm Sci. 2017;106(6):1453-65. doi: 10.1016/j.xphs.2017.02.006. PubMed PMID: 28209365.
151. Astete CES, C.M. PLGA nanoparticle DSC characterization. J Biomater Sci Polymer Edn 2006;17(3):247-489.
152. Malaekeh-Nikouei B, Sajadi Tabassi SA, Jaafari MR, Davies NM. The effect of complexation on characteristics and drug release from PLGA microspheres loaded by cyclosporine-cyclodextrin complex. Journal of Drug Delivery Science and Technology. 2006;16(5):345-50. doi: 10.1016/s1773-2247(06)50063-2.
153. Makadia HK, Siegel SJ. Poly Lactic-co-Glycolic Acid (PLGA) as Biodegradable Controlled Drug Delivery Carrier. Polymers (Basel). 2011;3(3):1377-97. Epub 2012/05/12. doi: 10.3390/polym3031377. PubMed PMID: 22577513; PMCID: PMC3347861.
154. Gopferich A. Mechanism of polymer degradation and erosion. Biometerials. 1994;17:103-14.
155. Gorrasi G, Pantani R. Effect of PLA grades and morphologies on hydrolytic degradation at composting temperature: Assessment of structural modification and kinetic parameters. Polymer Degradation and Stability. 2013;98(5):1006-14. doi: 10.1016/j.polymdegradstab.2013.02.005.
156. Gleadall A, Pan J, Kruft MA, Kellomaki M. Degradation mechanisms of bioresorbable polyesters. Part 2. Effects of initial molecular weight and residual monomer. Acta Biomater. 2014;10(5):2233-40. Epub 2014/01/30. doi: 10.1016/j.actbio.2014.01.017. PubMed PMID: 24473239.
157. Paakinaho K, Heino H, Vaisanen J, Tormala P, Kellomaki M. Effects of lactide monomer on the hydrolytic degradation of poly(lactide-co-glycolide) 85L/15G. J Mech Behav Biomed Mater. 2011;4(7):1283-90. Epub 2011/07/26. doi: 10.1016/j.jmbbm.2011.04.015. PubMed PMID: 21783137.
158. Codari F, Lazzari S, Soos M, Storti G, Morbidelli M, Moscatelli D. Kinetics of the hydrolytic degradation of poly(lactic acid). Polymer Degradation and Stability. 2012;97(11):2460-6. doi: 10.1016/j.polymdegradstab.2012.06.026.
159. Barbanti SHZ, C.C.A.; Duek, E.A.D.R.; . Effect of Salt Leaching on PCL and PLGA (50/50) Resorbable Scaffolds. Materials Research. 2008;11(1):75-8-.
160. Dong WY, Korber M, Lopez Esguerra V, Bodmeier R. Stability of poly(D,L-lactide-co-glycolide) and leuprolide acetate in in-situ forming drug delivery systems. Journal of controlled release : official journal of the Controlled Release Society. 2006;115(2):158-67. doi: 10.1016/j.jconrel.2006.07.013. PubMed PMID: 16963145.
161. Silva ATCR, Cardoso BCO, Silva MESRe, Freitas RFS, Sousa RG. Synthesis, Characterization, and Study of PLGA Copolymer in Vitro Degradation. Journal of Biomaterials and Nanobiotechnology. 2015;06(01):8-19. doi: 10.4236/jbnb.2015.61002.

162. Obeidat WM, Price JC. Preparation and evaluation of Eudragit S 100 microspheres as pH-sensitive release preparations for piroxicam and theophylline using the emulsion-solvent evaporation method. J Microencapsul. 2006;23(2):195-202. Epub 2006/06/07. doi: 10.1080/02652040500435337. PubMed PMID: 16754375.
163. Makhlof A, Tozuka Y, Takeuchi H. pH-Sensitive nanospheres for colon-specific drug delivery in experimentally induced colitis rat model. European Journal of Pharmaceutics and Biopharmaceutics. 2009;72(1):1-8. doi: 10.1016/j.ejpb.2008.12.013.
164. McGinity JW, Felton L. Aqueous Polymeric coatings for Pharmaceutical Dosage Forms 3rd ed. New York, NY: Informa Healthcare USA, Inc; 2008.
165. Yang Y, Shen L, Yuan F, Fu H, Shan W. Preparation of sustained release capsules by electrostatic dry powder coating, using traditional dip coating as reference. International journal of pharmaceutics. 2018;543(1-2):345-51. Epub 2018/03/31. doi: 10.1016/j.ijpharm.2018.03.047. PubMed PMID: 29601974.
166. Sahu NP, B.; Panigrahi, S. Fundamental understanding and modeling of spin coating process: A review. Indian J Physiic. 2009;83(4):493-502.
167. Bruce CR. DSC technology: and enhanced tool for coatings analysis. Paint and Coating Industry2002. p. 70.
168. Liu P, De Wulf O, Laru J, Heikkila T, van Veen B, Kiesvaara J, Hirvonen J, Peltonen L, Laaksonen T. Dissolution studies of poorly soluble drug nanosuspensions in non-sink conditions. AAPS PharmSciTech. 2013;14(2):748-56. Epub 2013/04/26. doi: 10.1208/s12249-013-9960-2. PubMed PMID: 23615772; PMCID: PMC3666001.
169. Durig TaF, Resa. Evaluation of floating and sticking extended release delivery system- an unconventional dissolution test. Journal of Controlled Release. 2000;67:7. Epub December 18 1999.
170. Peterson JD. In: Systems PIVIGaTCuII, editor. PerkinElmer, Inc Hopkinton, MA, USA. p. 1-15.
171. Saphier S, Rosner A, Brandeis R, Karton Y. Gastro intestinal tracking and gastric emptying of solid dosage forms in rats using X-ray imaging. International journal of pharmaceutics. 2010;388(1-2):190-5. doi: 10.1016/j.ijpharm.2010.01.001. PubMed PMID: 20079410.
172. Parikh TG, S.S; Meena, A; Serajuddin, A. T.M. Investigation of thermal and viscoelastic properties of polymers relevant to hot-melt-extrusion III: polymethacrylates and polymethacrylic-acid based-polymers. J Excipients and Food CHem. 2014;5(1):56-64.
173. Danley RL. New heat flux DSC measurement technique. THermochimica Acta. 2002;395:201-8.
174. Shatzer K, Xie L, Wang W, Distefano J, Yun C, Gao S, Singh R, Hu M. A sensitive and validated UPLC-MS/MS method for quantifying a newly synthesized COX-2 inhibitor (6A1) and its metabolites in blood, liver, and colonic mucosa of F344 rats . 2019.

175. Meagher MJ, Leone B, Turnbull TL, Ross RD, Zhang Z, Roeder RK. Dextran-encapsulated barium sulfate nanoparticles prepared for aqueous dispersion as an X-ray contrast agent. Journal of Nanoparticle Research. 2013;15(12). doi: 10.1007/s11051-013-2146-8.
176. Yeh BM, FitzGerald PF, Edic PM, Lambert JW, Colborn RE, Marino ME, Evans PM, Roberts JC, Wang ZJ, Wong MJ, Bonitatibus PJ, Jr. Opportunities for new CT contrast agents to maximize the diagnostic potential of emerging spectral CT technologies. Advanced drug delivery reviews. 2017;113:201-22. doi: 10.1016/j.addr.2016.09.001. PubMed PMID: 27620496; PMCID: PMC5344792.
177. Mattsson O. A Simple Method of Ensuring Correct Concentration of Barium Contrast Media. Acta Radiologica. 2010;39(6):501-6. doi: 10.3109/00016925309136736.
178. Cheheltani R, Ezzibdeh RM, Chhour P, Pulaparthi K, Kim J, Jurcova M, Hsu JC, Blundell C, Litt HI, Ferrari VA, Allcock HR, Sehgal CM, Cormode DP. Tunable, biodegradable gold nanoparticles as contrast agents for computed tomography and photoacoustic imaging. Biomaterials. 2016;102:87-97. doi: 10.1016/j.biomaterials.2016.06.015. PubMed PMID: 27322961; PMCID: PMC4941627.
179. Ashton JR, West JL, Badea CT. In vivo small animal micro-CT using nanoparticle contrast agents. Front Pharmacol. 2015;6:256. doi: 10.3389/fphar.2015.00256. PubMed PMID: 26581654; PMCID: PMC4631946.
180. Yun C. Efficacy Evaluation of COX-2 Inhibitors on Colorectal Adenoma Prevention by Using the Pirc Rat Model. Houston, Texas USA: University of Houston; 2018.
181. Nardelli S, Pisani LF, Tontini GE, Vecchi M, Pastorelli L. MMX((R)) technology and its applications in gastrointestinal diseases. Therap Adv Gastroenterol. 2017;10(7):545-52. Epub 2017/08/15. doi: 10.1177/1756283X17709974. PubMed PMID: 28804515; PMCID: PMC5484438.
182. Fiorino G, Fries S, De La Rue SA, Malesci AC, Repici A, Danese S. New Drug Delivery Systems in Inflammatory Bowel Disease: MMX™ and Tailored Delivery to the Gut. Curr Med Chem. 2017;17(17):7.
183. Simovic S, Song Y, Nann T, Desai TA. Intestinal absorption of fluorescently labeled nanoparticles. Nanomedicine. 2015;11(5):1169-78. Epub 2015/03/21. doi: 10.1016/j.nano.2015.02.016. PubMed PMID: 25791810; PMCID: PMC4476919.
184. Rinkenauer AC, Press AT, Raasch M, Pietsch C, Schweizer S, Schworer S, Rudolph KL, Mosig A, Bauer M, Traeger A, Schubert US. Comparison of the uptake of methacrylate-based nanoparticles in static and dynamic in vitro systems as well as in vivo. Journal of controlled release : official journal of the Controlled Release Society. 2015;216:158-68. Epub 2015/08/19. doi: 10.1016/j.jconrel.2015.08.008. PubMed PMID: 26277064.
185. Kusonwiriyawong C, van de Wetering P, Hubbell JA, Merkle HP, Walter E. Evaluation of pH-dependent membrane-disruptive properties of poly(acrylic acid)

derived polymers. European Journal of Pharmaceutics and Biopharmaceutics. 2003;56(2):237-46. doi: 10.1016/s0939-6411(03)00093-6.
186. Timin AS, Gao H, Voronin DV, Gorin DA, Sukhorukov GB. Inorganic/Organic Multilayer Capsule Composition for Improved Functionality and External Triggering. Advanced Materials Interfaces. 2017;4(1). doi: 10.1002/admi.201600338.
187. Wang J, Flanagan DR. Developing solid oral dosage forms: Pharmaceutical Theory and Practice-Fundamental of Dissolution2009.
188. Qualls-Creekmore E, Tong M, Holmes GM. Time-course of recovery of gastric emptying and motility in rats with experimental spinal cord injury. Neurogastroenterol Motil. 2010;22(1):62-9, e27-8. Epub 2009/07/02. doi: 10.1111/j.1365-2982.2009.01347.x. PubMed PMID: 19566592; PMCID: PMC2805043.
189. Keshavarzi Z, Khaksari M, Shahrokhi N. The effect of COXIBs on the gastric emptying in male rats. IJBMS. 2013.
190. Santos CL, Medeiros BA, Palheta-Junior RC, Macedo GM, Nobre-e-Souza MA, Troncon LE, Santos AA, Souza MH. Cyclooxygenase-2 inhibition increases gastric tone and delays gastric emptying in rats. Neurogastroenterol Motil. 2007;19(3):225-32. Epub 2007/02/16. doi: 10.1111/j.1365-2982.2007.00913.x. PubMed PMID: 17300293.
191. Han FY, Thurecht KJ, Whittaker AK, Smith MT. Bioerodable PLGA-Based Microparticles for Producing Sustained-Release Drug Formulations and Strategies for Improving Drug Loading. Front Pharmacol. 2016;7:185. doi: 10.3389/fphar.2016.00185. PubMed PMID: 27445821; PMCID: PMC4923250.
192. Gurpinar E, Grizzle WE, Piazza GA. COX-Independent Mechanisms of Cancer Chemoprevention by Anti-Inflammatory Drugs. Front Oncol. 2013;3:181. Epub 2013/07/23. doi: 10.3389/fonc.2013.00181. PubMed PMID: 23875171; PMCID: PMC3708159.
193. Tinsley HN, Grizzle WE, Abadi A, Keeton A, Zhu B, Xi Y, Piazza GA. New NSAID targets and derivatives for colorectal cancer chemoprevention. Recent Results Cancer Res. 2013;191:105-20. Epub 2012/08/16. doi: 10.1007/978-3-642-30331-9_6. PubMed PMID: 22893202; PMCID: PMC3703626.
194. He TCC, T.A.; Bogelstein, B.; Kinzler, K.W.;. PPARdelta is an APC-regulated target of NSAIDs. Cell. 1999;29(3):335-45.

SUPPLEMENTAL

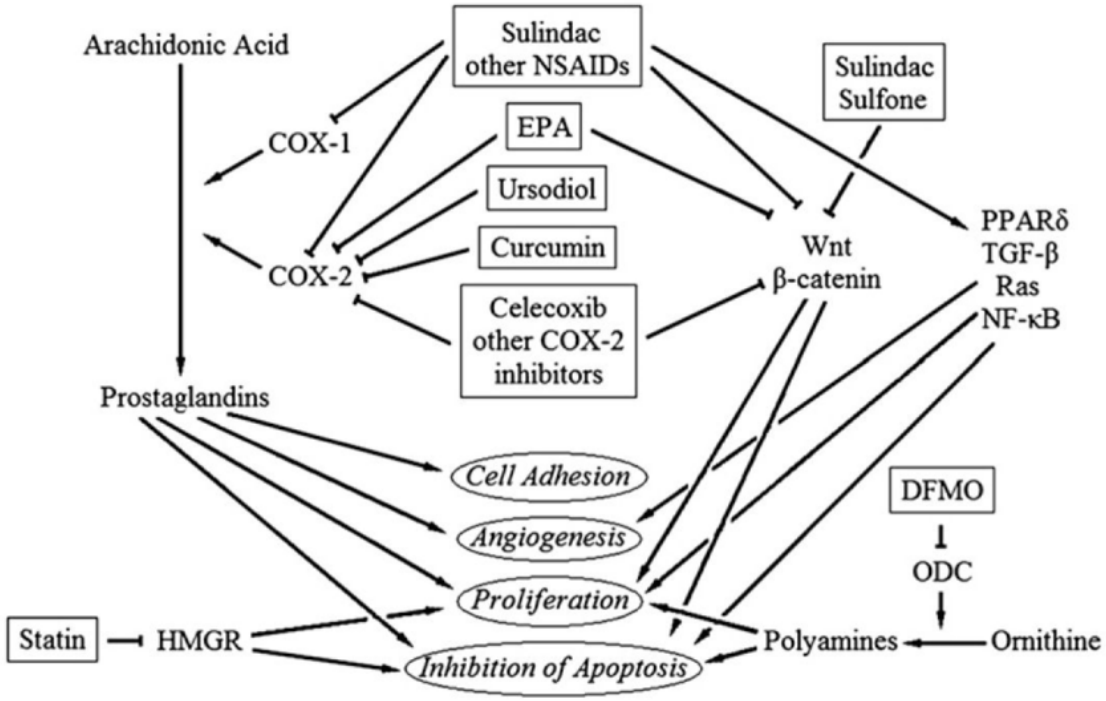

S1. Mechanism of Chemoprevention via Cox-2 Inhibition (Chapter 1, Page 32)

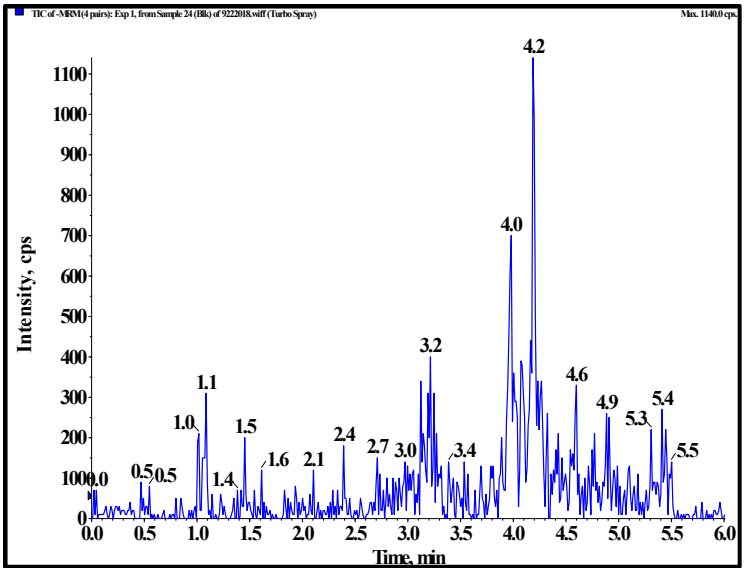

S2: Blank matrix sample injection after 6 ULOQ injections shown negligible internal standard peak at 4.2 minutes (Chapter 3.4.2 page 76)

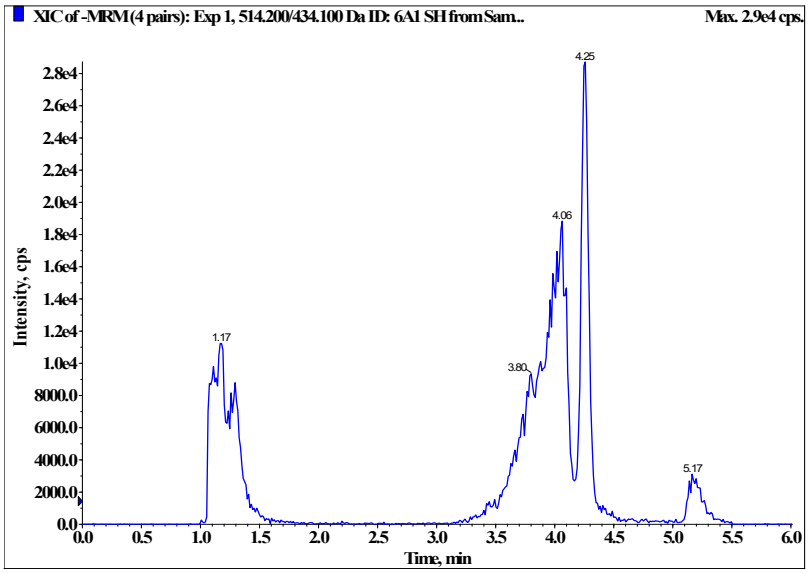

S3: LLOQ injection using Raptor Restek Biphenyl column (Chapter 3.4.2 page 79)

Plasticizer
Films of EUDRAGIT® tend to become brittle (cracking) below 10%. To improve the elasticity up to 25% can be added. EUDRAGIT® L 100 and EUDRAGIT® S 100 in aqueous formulations require a much higher proportion of plasticizer (40 - 50%). In all formulations, triethyl citrate has proved its worth as a plasticizer.

Solvents
Acetone and alcohols are preferentially used for manufacturing polymer solutions. An overview of the average dissolution time in minutes for the most common solvents or solvent / water mixture shows the following table.

Solvent	EUDRAGIT® L 100-55	EUDRAGIT® L 100	EUDRAGIT® S 100
Methanol	10	15	30
Methanol / water 97:3	10	15	25
Ethanol	20	10	10
Ethanol/water 97:3	20	10	25
Ethanol/water 6:4	20	20	40
Isopropyl alcohol	30	40	35
Isopropyl alcohol / water 97:3	20	15	20
Isopropyl alcohol / water 6:4	20	25	45
n-Butanol	30	70	swelled
Acetone	35	15	10
Acetone / water 97:3	15	25	10
Acetone / water 6:4	15	15	swelled
Acetone / isopropyl alcohol 4:6	-	30	5

S4: Rohm Evonik recommendation of solvents and plasticizer for ES100 (Chapter 4.2)

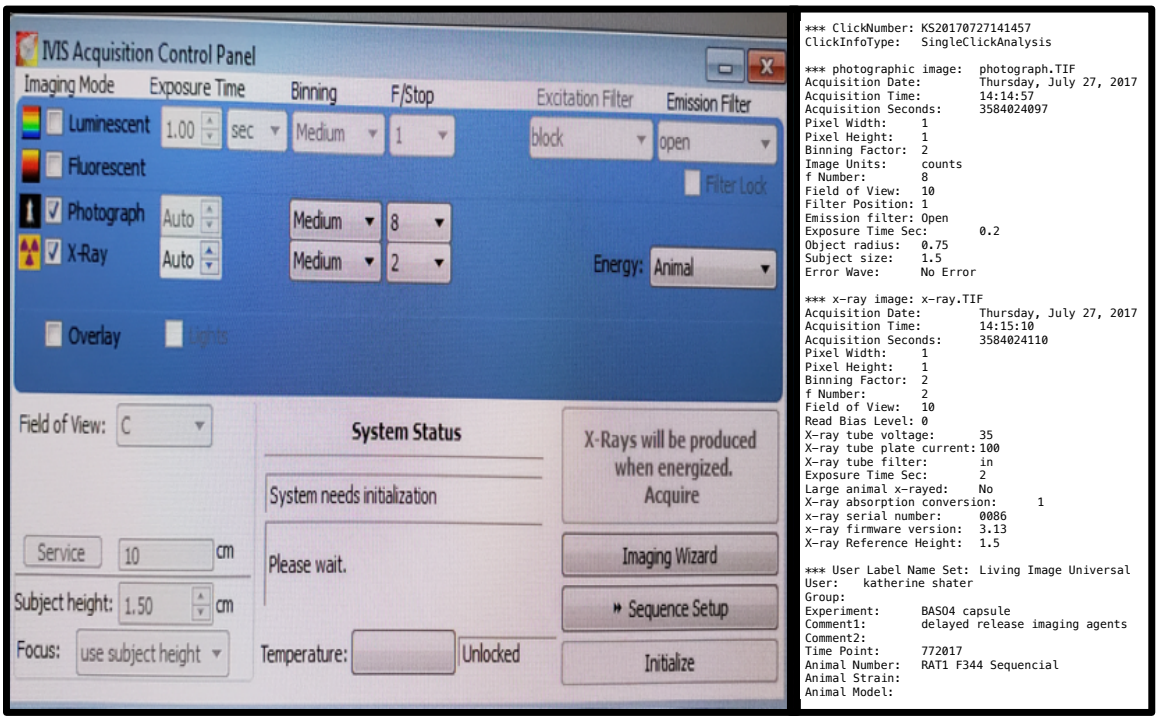

S5: IVIS imaging parameters and special data analysis (Chapter 4

S6: Blue stained fecal droppings were observed 10 hours post dosed as well as polymer residuals.

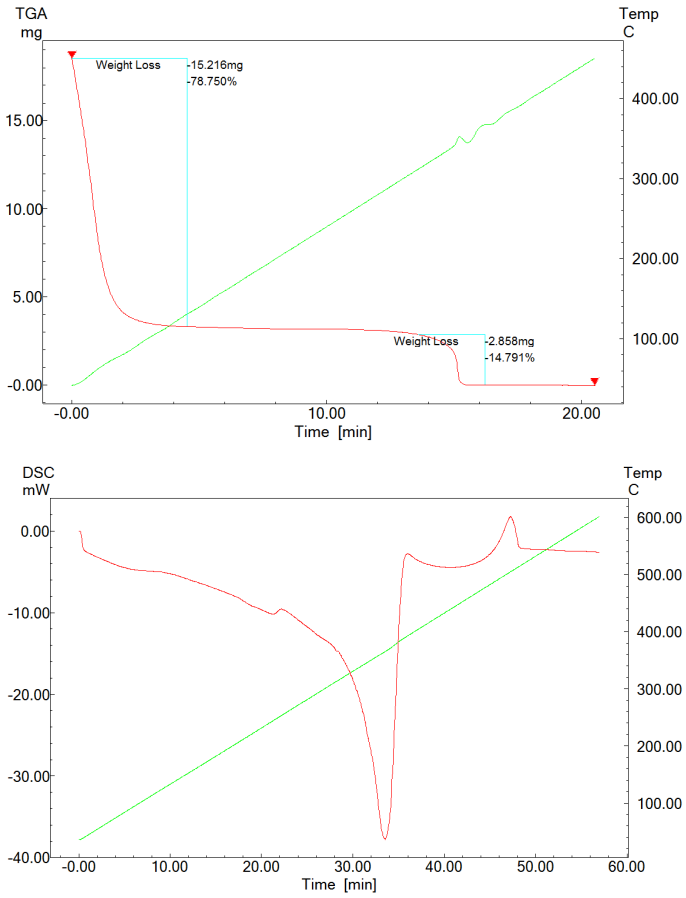

S7: Consistent ratio of solvent (first weight loss) to total solid mass (second weight loss) with respect to temperature.Glass transition, endothermic peak , and exothermic temperatures are consistent with historical data